RAVIKANTH KONA

RAVIKANTH.KONA@GMAIL.COM

EDUCATION

Doctor of Philosophy (PhD) – Pharmaceutical Sciences

UNIVERSITY OF MARYLAND, SCHOOL OF PHARMACY – DEPARTMENT OF PHARMACEUTICAL SCIENCES 2007-2012

Master of Science (MS) – Analytical Chemistry

MISSOURI STATE UNIVERSITY – DEPARTMENT OF CHEMISTRY 2005-2007

Honors Bachelor of Science (BS) – Pharmacy

OSMANIA UNIVERSITY – SCHOOL OF PHARMACY 2000-2004

PROFESSIONAL EXPERIENCE

UNIVERSITY OF MARYLAND DEPARTMENT OF PHARMACEUTICAL SCIENCES Baltimore, MD

Graduate Research Assistant

Under the direction of **Stephen W. Hoag**, PhD, conducted research to develop more effective methods of formulation development, process monitoring, and process control. Technical processes:

Projects – **Funded and scientifically guided by FDA**:

- Developed immediate release dosage form using fluid bed granulation/drying. Established real-time *In-line* monitoring system to determine moisture levels and granulation end-point using NIR and chemometrics
- Applied Quality by Design (QbD) principles in formulation development of immediate release tablets manufactured via roller compaction

GMP Experience UMB, MD

- Written SOPs, batch records, and product specifications
- Performed identification tests on raw materials and responsible for equipment maintenance/cleaning validation
- Performed manufacturing of various solid dosage forms in GMP facility for contracted project

ABBOTT LABORATORIES Abbott Park, IL

Formulation Intern, Summer 2010

Project – Tablet Formulation Development of Spray Dried Dispersions (SDD) Based on Assessment of Powder Manufacturability

- Performed flow characterization of SDD blends using **Schulze®** ring shear cell tester
- Integrated flow and mechanical properties of sprayed dried formulation blends to systematically identify and develop scalable SDD platform compositions and processing options to streamline the development of SDD tablet formulations

MALVERN INSTRUMENTS Columbia, MD

Chemical Imaging Intern, Summer 2008

- Utilized NIR (SyNIRgi) chemical imaging tool to monitor component distribution and determine its concentration in pharmaceutical tablets

MISSOURI STATE UNIVERSITY DEPARTMENT OF CHEMISTRY Springfield, MO

Research Assistant, 2006 – 2007

Project – Monitoring the Transport of Ions across Modified Alumina Nanomembranes

- Modified alumina nanomembrane using trialkoxysilanes and characterized using Infrared spectroscopy and Scanning Electron Microscopy (SEM)
- Examined transport of analytes across modified membrane using UV-Visible and fluorescence spectroscopy
- Used sol-gel chemistry to synthesize nanotubes

UNIVERSITY OF MARYLAND DEPARTMENT OF PHARMACEUTICAL SCIENCES and **MISSOURI STATE UNIVERSITY DEPARTMENT OF CHEMISTRY**

Teaching Assistant, 2005 and 2007

- Conducted pharmaceutical and compounding labs for PharmD courses
- Taught and led organic chemistry and chemistry labs for undergraduates
- Administered exams and evaluated student performance

HONORS & ACHIEVEMENTS

Rho Chi Honor Society Inductee, 2011

American Association of Pharmaceutical Scientists (**AAPS) Formulation Design and Development (FDD) Section Leadership Committee** – Graduate Student Representative, 2009 - 2011

American Association of Pharmaceutical Scientists (**AAPS) Formulation Design and Development (FDD) Leadership Mentoring Program-** Development Team, 2009 - 2011

AstraZeneca Travel Award – American Association of Pharmaceutical Scientists (AAPS), November 14-18, 2010, New Orleans, LA

University Indian Association Secretary, 2009 - 2010

AstraZeneca Travel Award – American Association of Pharmaceutical Scientists (AAPS), November 7-11, 2009, Los Angeles, CA

American Association of Pharmaceutical Scientists (**AAPS) UMB Student Chapter Secretary**, 2008 - 2009

University Indian Association Treasurer, 2008 - 2009

UMB AAPS Travel Award – American Association of Pharmaceutical Scientists (AAPS), November 16-20, 2008, Atlanta, GA

Graduate Interdisciplinary Forum Outstanding Poster Presentation Award, Missouri State University, April 8, 2006, Springfield, MO

Honors Bachelor of Pharmacy, 2004

PUBLICATIONS

R. Kona, Robert Mattes, Bela Jancsi, R. Fahmy, J. Polli, S. Hoag. Application of in-line near infrared spectroscopy and multivariate batch modeling for process monitoring in fluid bed granulation**.** (in preparation)

R. Kona, R. Fahmy, J. Polli, Marilyn Martinez, S. Hoag. Quality-by-Design III: Application of Near-Infrared Spectroscopy to monitor roller compaction in-process and product quality attributes in formulation development of immediate release tablets. (in preparation)

R. Fahmy, **R. Kona**, R. Dandu, W. Xie, G. Claycamp, L. Torbeck, S. Hoag. Quality-by-Design I: Application of Failure Mode Effect Analysis (FMEA) and Plackett-Burman design of experiments in the identification of "main factors" in the formulation and process design space for roller compacted Ciprofloxacin Hydrochloride immediate release tablets. AAPS PharmSciTech, 2012.

S. Penumetcha, **R. Kona,** J. Hardin, A. Molder, E. Steinle. Monitoring Transport across Modified Nanoporous Alumina Membranes. *Sensors*, 2007, 7, 2942-2952.

PRESENTATIONS

R. Kona, R. Mattes, R. Fahmy, and S. Hoag. Real-time on-line monitoring system in a fluid bed to determine moisture levels and granulation end-point: Using near-infrared spectroscopy (NIR) and chemometrics. AAPS, October 23-27, 2011, Washington, DC

R. Kona, R. Dandu, R. Fahmy, J. Polli, and S. Hoag. Hydroxypropyl cellulose (HPC) as dry binder in the formulation development of Ciprofloxacin hydrochloride immediate release tablets: Influence of binder source, lubricant type and their levels on the critical quality attributes (CQAs). Excipient Fest, May 10-11, 2011, Baltimore.

R. Kona, R. Dandu, R. Fahmy, and S. Hoag. Quality by Design (QbD): Application of Near Infrared Spectroscopy (NIRS) as a control strategy tool for measuring in-process and product quality attributes of Ciprofloxacin immediate release tablets produced via roller compaction. AAPS, November 14-18, 2010, New Orleans

R. Kona, R. Dandu, R. Fahmy, V. Lancaster, W. Xie, D. Bensley, J. Polli, and S. Hoag. Correlation Study between Disintegration and Dissolution Tests for Ciprofloxacin Immediate Release Tablets. AAPS, November 14-18, 2010, New Orleans

V. Moolchandani, **R. Kona**, X. Fuo, T. Freeman, and S. Hoag. Dynamic and static powder analysis of formulations and its application in capsule filling. AAPS, November 14-18, 2010, New Orleans

R. Kona, R. Dandu, R. Fahmy, D. Bensley, and S. Hoag. Investigation of Formulation and Manufacturing process variables on roller compacted Ciprofloxacin tablets. AAPS, November 7-11, 2009, Los Angeles

R. Dandu, **R. Kona**, R. Fahmy, D. Bensley, and S. Hoag. Application of Plackett-Burman design of experiments (DOE) to describe product design space: Identification of critical formulation and process variables. AAPS, November 7-11, 2009, Los Angeles

R. Kona, R. Fahmy, D. Bensley, and S. Hoag. Application of Near-Infrared spectroscopy to predict different strengths of Acetaminophen in different formulations.AAPS, November 16-20, 2008, Los Angeles

V. Moolchandani, **R. Kona**, J. Langridge, L. L. Augusburger, S. Hoag. Comparative Powder Flow Analysis of Lactose as an Excipient and its Formulations for Capsule Filling. AAPS, November 16-20, 2008, Los Angeles

V. Moolchandani, **R. Kona**, S. Hoag. Flow Property Characterization of Different Grades of Lactose by Shear Cell Analysis. University of Maryland Baltimore, Pharmacy Research Day, 2007, Baltimore

R. Kona and E. Steinle. Modifying Alumina Nanochannel Membranes with Trimethoxy Silane 232nd National ACS Meeting, September 2006, San Francisco

R. Kona and E. Steinle. Monitoring Transport of Ions across Modified Alumina Nanomembrane. Graduate Interdisciplinary forum, Missouri State University, April 8, 2006, Springfield

PROFESSIONAL AFFILIATIONS

American Association of Pharmaceutical Scientists (AAPS)

UMB Pharmacy Graduate Student Association (PGSA)

American Chemical Society (ACS)

Abstract

Title of Dissertation: Application of near-infrared spectroscopy to monitor in-process and product quality attributes for granulation and immediate release tablet production.

Ravikanth Kona, Ph.D., 2012

Dissertation Directed By: Stephen W. Hoag, Ph.D.

Professor

Department of Pharmaceutical Sciences

School of Pharmacy

University of Maryland, Baltimore, USA

The purpose of this study was to investigate the application of NIR spectroscopy to monitor critical in-process and excipient variables in the manufacturing of immediate release tablets. In this study, roller compaction and fluid bed granulation were used for the granulation of Ciprofloxacin hydrochloride and Fexofenadine hydrochloride, respectively. In roller compaction, prior knowledge was systematically incorporated into the risk assessment using failure mode and effect analysis (FMEA). The factors identified using FMEA were quantitatively assessed using a Placket-Burman screening design. Results indicated that roll pressure (RP) was the most critical roller compaction process factor affecting the granule size and flow. Binder grade, Klucel® EXF vs JF and tablet compression force (Pmax) were found to be critical to the release characteristics of Ciprofloxacin. This study demonstrated that the scientific rationale and quality risk

management analysis were used to successfully and efficiently determine the Critical quality attributes. Four factors, RP, Pmax, binder source (Klucel® EXF vs Nisso®-L), and lubricant type (monohydrate vs dihydrate), were further investigated using high resolution experimental design. The results showed that binder and lubricant replacement was insignificant. In addition, NIR was used at various stages of the product development, and the partial least square (PLS) regression models developed have successfully predicted blend uniformity, particle size, crushing force, and disintegration time of the batches manufactured in the same location. However, the models yielded higher prediction errors for batches manufactured at a different location. In fluid bed granulation, a PLS model was developed to successfully predict the moisture levels in real time using in-line NIR probe specially designed for this application. This combined with humidity and temperature data from a novel PyroButton® in conjunction with multivariate data analysis techniques was used to develop multivariate statistical process control charts (MSPC) such as scores, distance to model (DModX), and Hotelling T^2. The application of these charts for process monitoring and fault detection was further evaluated. In summary, these findings demonstrate the application of NIR in conjunction with multivariate chemometric models as a potential Process Analytical Technology (PAT) tool for effective process monitoring and process control in pharmaceutical manufacturing.

APPLICATION OF NEAR-INFRARED SPECTROSCOPY TO MONITOR IN-PROCESS AND PRODUCT QUALITY ATTRIBUTES FOR GRANULATION AND IMMEDIATE RELEASE TABLET PRODUCTION

By

Ravikanth Kona

Dissertation submitted to the faculty of the Graduate School
of the University of Maryland, Baltimore in partial fulfillment
of the requirements for the degree of
Doctor of Philosophy
2012

This Thesis is dedicated to

my mother, Rekha Kona

and

my father, Murali Krishna Kishore Kona

Thank you for everything!

Acknowledgements

My graduate studies here at the University of Maryland are filled with people who inspired, mentored, and supported me to grow both professionally and personally. I would like to thank all those people who helped me make this journey an enriching one. Particularly, I would like to thank the following people:

My mentor, Dr. Stephen W. Hoag, for giving me this opportunity to pursue doctoral studies under his supervision, and for his support and commitment towards my education and scientific growth. The professionalism and work ethic he brings to this profession are great models for excellence and made a lasting impression on me. I am forever indebted for his guidance.

I would also like to thank my thesis committee members, Dr. James Polli, Dr. Raafat Fahmy, Dr. Richard Dalby and Dr. Anjan Nan for their guidance and insight. I would like to especially thank Dr. James Polli and Dr. Anjan Nan for serving as readers for my dissertation. I also wish to thank Dr. Richard Dalby for agreeing to serve on my committee under short notice.

I would like to thank Dr. Marilyn Martinez and Dr. Gregg Claycamp from the Food and Drug Administration for providing regulatory insights into biopharmaceutical and quantitative risk assessment, respectively.

I owe my deepest gratitude to Dr. Ramesh Dandu for his scientific assistance with various aspects of formulation developments and his guidance with scientific writing, resulting in several coauthored publications.

I am grateful for US Food and Drug Administration (FDA) and Consortium for Industrial Pharmaceutics Education and Training (CIPET) for the financial support of my research, without their support this research wouldn't have been possible. I would also like to extend my gratitude to my scientific collaborators outside the university, Robert Mattes and Dr. Denise Root of Foss NIRSystems, for providing XDS process analyzer and Dr. Bela Janisk for Pyrobutton®, which are important PAT tools in my research for process monitoring.

I would like to thank my current lab mates, Hanpin Lim, Ting Wang, Dr. Seon Hepburn, Bhavesh Kothari, Jacky Lin, Sophie Peng, and Heather Boyce, for their scientific assistance and for all the laughs and good times we shared. Special thanks to Dr. Ahmed Abdelwahab for his assistance with chemometric modeling. Our discussions helped me gain a better understanding of the fundamental in chemometrics. I would also like to thank my past lab mates, Drs. Vikas Moolchandani, Vivek Dave, and Harris Howland for sharing their knowledge not just with formulation sciences but other aspects of graduate life as well. Special thanks to my friends, Rahul Deshmukh, Chandra Khantwal, Pankdeep Chhabra, Vicky Hsu, and Tatiana Silva for making this journey a pleasurable one.

I would like to express my gratitude to the rest of the faculty and staff of Pharmaceutical Sciences, special thanks to Colleen Day, Ruth McLean, Nicole Derr, and Abby Ratcliff, their assistance with the graduate school paperwork and deadlines made my graduate life much more pleasurable.

Above all I like to express by deepest gratitude to by brother, Raghavendra Kona, and sister-in-law, Shirisha Kona, and the rest of my family and friends for supporting me throughout my graduate studies. Last but not the least, I would like to thank my parents, Murali Krishna Kishore Kona and Rekha Kona, for their unconditional love and support and standing by me through the challenges of graduate school and most importantly having faith in me, and for that I will ever be grateful.

Table of Contents

List of Tables

List of Figures

List of Abbreviations

API	Active pharmaceutical ingredient
BC	Baseline correction
CF	Crushing force
CI	Carr's compressibility index
CIP	Ciprofloxacin hydrochloride monohydrate
CPP	Critical process parameters
CQA	Critical quality attributes
D	Derivative
Db	Bulk density
DModX	Distance to model
DOE	Design of experiments
DSC	Differential scanning calorimetry
Dt	Tapped density
FDA	Food and drug administration
FMEA	Failure mode and effect analysis
FMECA	Failure mode, effects and criticality analysis
FSS	Feed screw speed
FTA	Fault tree analysis
GMP	Good manufacturing practices

HACCP	Hazard analysis and critical control points
HAZOP	Hazard operability analysis
HPC	Hydroxypropyl cellulose
HPLC	High performance liquid chromatography
ICH	International conference on harmonization
InGaAs	Indium gallium arsenide
IR	Infrared
KBr	Potassium bromide
kN	Kilonewton
kp	Kilopond
MgSt-D	Magnesium stearate dihydrate
MgSt-M	Magnesium stearate monohydrate
MSC	Multiplicative scatter correction
MLR	Multi linear regression
NIRS	Near-infrared spectroscopy
NPS	N-Point Smoothing
PAT	Process analytical technology
PB	Plackett-Burman
PbS	Lead sulfide
PbSe	Lead selenide
PCA	Principle component analysis
PCR	Principle component regression

PHA	Preliminary hazard analysis
PLS	Partial least square
Pmax	Maximum compression pressure
PXRD	Power X-ray crystallography
QbD	Quality by design
QTPP	Quality target product profile
RC	roller compaction
RG	Roll gap
RH	Relative humidity
RP	Roll pressure
RPN	Risk priority numbers
RS	Roll speed
RSD	Relative standard deviation
SEC	Standard error of calibration
SECV	Standard error of cross validation
SEL	Standard error of lab
SEP	Standard error of prediction
SG	Savitzky-Golay
SNV	Standard normal variant
SPE	Squared prediction error
Std.Dev	Standard deviation
USP	United states pharmacopeia

UV	Ultra-violet
WV	Weight variation
X	Particle size

Chapter 1 Introduction and Background

1.1 Introduction

Pharmaceutical manufacturing processes consist of series of unit operations, which are intended to impart desirable properties to materials.(1) In order to ensure acceptable and reproducible change each time, both in-process attributes of the unit operations and the product quality attributes of the materials needs to be constantly monitored and controlled. Over last several decades, chemical attributes such as identity, assay, purity etc., have been monitored with the help of several analytical techniques such as High Performance Liquid Chromatography (HPLC), Ultraviolet Spectroscopy (UV), Powder X-ray Crystallography (PXRD), and Differential Scanning Calorimetry (DSC). However, certain physical and chemical attributes of the materials are not well understood.(1) Failure to identify and detect minor differences in the material quality could manifest in the final product and impact its performance. Tests to identify the product quality and the process end point are often performed using several offline techniques, where samples are drawn during the process or at the end of manufacturing and tested for its quality. This conventional method of quality testing and process control is time consuming and could delay the end point determination. In addition, different tests are required for each attributes as it only addresses one quality attribute of the active ingredient and other information related to the formulation matrix is lost or not accounted for. In 2004, FDA issued Process Analytical Technology (PAT) guidance for the pharmaceutical industries

to voluntarily implement PAT during manufacturing and quality control for real time monitoring of in-process and product quality attributes, in an effort to build quality in to the system through timely measurement, rather than merely measuring the quality at the end of the product.(1)

In the following sections, a brief discussion is provided on the PAT initiative and its importance on the product quality. Also discussed are the theory, principles, application of near-infrared spectroscopy (NIRS) as the PAT tool, and reasons for applying chemometrics for multivariate data analysis. In addition, two unit operations commonly used in pharmaceutical industry, (i) dry granulation technique performed by roller compaction and (ii) wet granulation technique using fluid bed are briefly discussed. Here, in addition to its principle and theory, process factors affecting critical attributes are outlined. Finally in this chapter, hypothesis, specific aims, and scope of this dissertation are detailed.

1.1.1 Process Analytical Technology (PAT)

In August 2002, the Food and Drug Administration (FDA) announced a new initiative, "Pharmaceutical Current Good Manufacturing Practices (CGMPs) for the 21st Century—a Risk Based Approach" in an effort to improve and modernize pharmaceutical manufacturing.(2) One key element of this initiative is the implementation of the PAT during pharmaceutical manufacturing. The goal of PAT as described in the guidance document is to enhance process understanding and maintain control of manufacturing

processes through proper design, analysis, and control of critical in-process and material attributes that influence the quality of a dosage form.(1) A process is considered well understood when all critical sources of variability have been identified and the process continuously and reliability meets the product quality attributes over the design space established for materials and process conditions.(3) There are several process analyzers such as Near-Infrared Spectroscopy (NIRS), Raman, Infrared Spectroscopy, Near-Infrared Chemical Imaging, and UV-Vis Spectroscopy currently available for identifying and monitoring critical in-process and product variables.(4) They can be used at-line where the samples are removed and analyzed close to the process, on-line where the samples are removed from the process stream and analyzed and placed back to the process, in-line technique where the analyzed is installed inside the process stream, or off-line where the samples are removed and analyzed away from the process.

The more recently launched "Quality by Design" initiative is intended to improve product quality and provide regulatory flexibility for the industry to improve manufacturing processes.(5-7) The ICH (Q8) defines QbD as "a systematic approach to development that begins with predefined objectives and emphasizes product and process understanding and process control, based on sound science and quality risk management". Figure 1-1 show the various steps involved in the drug development using QbD paradigm. The initial step is to identify and define the Quality Target Product Profiles (QTPP). According to ICHQ8 (R2) guidance document, QTTP is defined as a "prospective summary of the quality characteristics of a drug product that ideally will be achieved to ensure the desired quality, taking into account safety and efficacy of the drug

product."(5) To define QTPP for a product, performance attributes such as therapeutic dose, type of dosage form, route of administration, and product release characteristics which could influence the pharmacokinetic profile of the drug need to be identified. Once defined, the next step is to understand the material input and in-process process parameters to determine the CQA that affect the QTPP. Once all the sources of variability are identified, a process design space can be established. ICH Q8 (R2) defines design space as "The multidimensional combination and interaction of input variables (e.g. material attributes) and process parameters that have been demonstrated to provide assurance of quality".(5) In short, working within the design space is not considered change but movement outside the space is considered a change and would require regulatory post approval changes.(5,8) Once the design space is established, the CQA need to be continuously monitored and controlled, which is achieved with the help of statistical and PAT tools for real time process monitoring.(3,9)

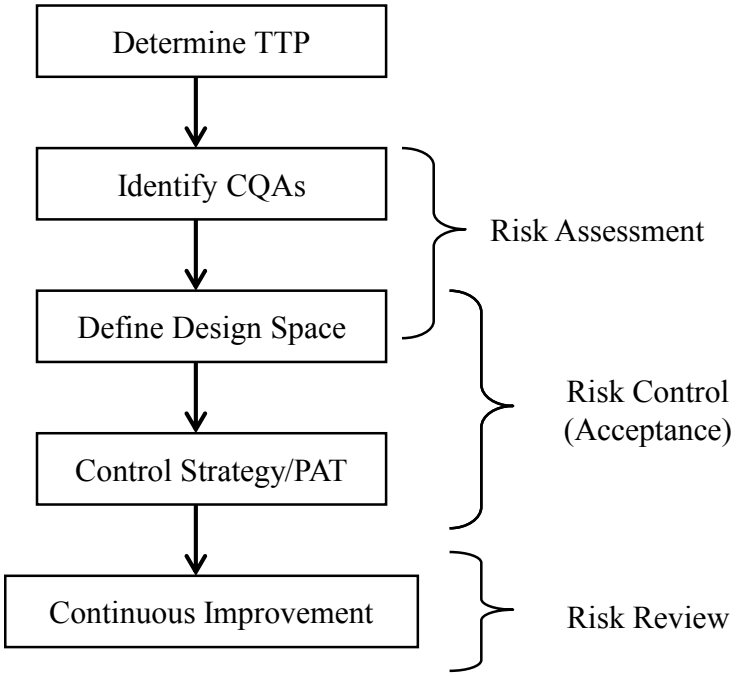

Figure 1-1. QbD drug product development flow chart.

1.1.2 Near-Infrared Spectroscopy (NIRS)

The NIRS uses regions between 800 nm to 2500 nm of the electromagnetic spectra which corresponds to a frequency range of 4000 cm^{-1} to 12,500 cm^{-1}.(10) When molecules absorb energy at a certain wavelength, they get excited from the ground state to a higher energy state, resulting in a change in the fundamental vibrating frequency. In NIR molecules can vibrate at two fundamental modes, stretching and bending.(11,12) In stretching, there is change in the length of the bond between two atoms, whereas in bending vibration there is a change in the inter-atomic bond angle. The NIR spectrum is mainly composed of overtones and combination bands arising from the fundamental vibration of -OH, -CH, and -NH. The intensity of these absorption bands is 10 to 100

times weaker than the fundamental IR bands, which results in broad overlapping regions.(11) In the Mid-Infrared regions, due to strong absorption, the thickness of the sample was limited to thin sections (e.g. KBr pellets) to limit the amount of material interacting with the light. In the NIR regions, the low absorption coefficient permits deeper penetration into a sample, which is of analytical advantage, as the samples such a turbid solutions or tablets can be scanned without sample preparation. The major limitation of using NIRS is assigning spectral features due to overlapping peaks. However, due to recent advances in statistical techniques the interpretation of large number of NIR spectra was made easier and the limitation associated with overlapping peaks has been reduced. The use of NIR was first introduced by Karl Norris (13) who demonstrated the use of NIRS in the evaluating biological substrates.

1.1.3 Near-Infrared Spectrometer

A typical NIR spectrophotometer consists of a light source, a monochromator, a sample holder, and a detector; see Figure 1-2. The light source usually consists of tungsten-halogen lamp with peak spectral radiance at approximately 1000 nm when operated at filament temperature of 2000 K.(14)

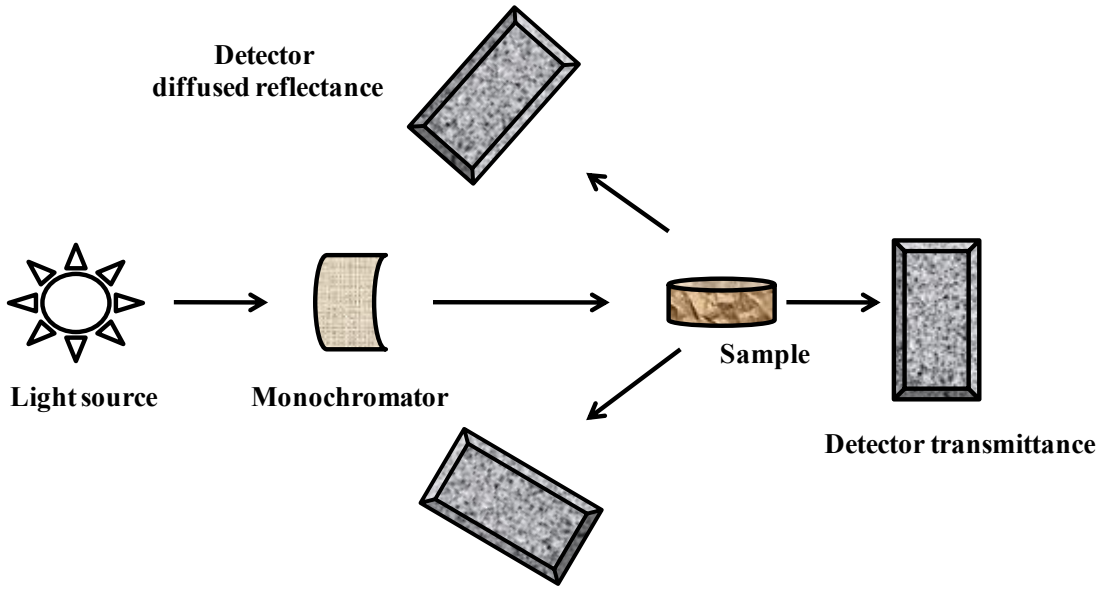

Figure 1-2. Basic configuration of the NIR spectrophotometer. Adapted from Reich *et al.*(15)

The type of detector depends on the sample to be measured. Figure 1-3 shows different modes of measurement. Transparent materials are measured in transmittance mode, whereas, semi-solid and turbid solutions are either measured in diffuse transmittance or diffuse reflectance depending on the absorption and scattering characteristics of the material. The earlier detectors commonly used in the NIR are lead sulphide and lead selenide (Pbs and PbSe), they are highly sensitive and inexpensive, but they suffered from linearity, saturation and speed or response.(4) Photodiode devices such as the Indium-Gallium-Arsenide (InGaAs) and extended-InGaAs detectors are very linear, very fast and very sensitive making them a popular choice.(4)

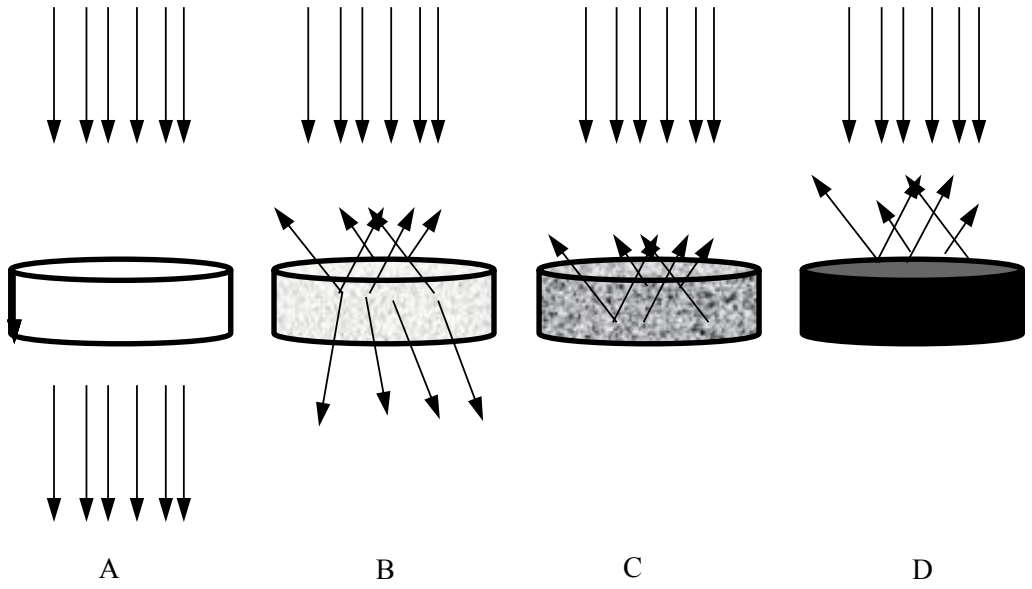

Figure 1-3. Different NIR measuring modes.(A) Reflectance, (B) Transflectance, (C) Diffuse reflectance, (D) Reflectance. Adapted from Reich *et al*.(15)

1.1.4 NIR Spectral Data

As discussed earlier, NIR spectra consist of complex, broad, and overlapping bands comprising both physical and chemical information, making them difficult to interpret. Thus, a data processing technique which extracts the relevant information is required. Chemometric methods are often used for this purpose. The International Chemometric Society has defined chemometrics as the "Science of relating measurements made of a chemical system or process to the state of the system via application of mathematical or statistical analysis".(14) In other words, chemometrics is the application of mathematics and statistics to extract useful chemical/physical information from complex data. Qualitative and quantitative analysis are the two types of data analysis in the

chemometrics.(10) Unsupervised learning is used to find patterns and explore groupings in the data set using clustering techniques such as Hierarchical Cluster Analysis (HCA) and Principle Component Analysis (PCA). Quantitative technique constructs models using NIR spectra and the constituent value of interest and uses the calibrated model to predict future samples.(4,10) Partial Least Squares (PLS) and Multiple Linear Regressions (MLR) are the examples of supervised learning techniques.

1.1.5 Multivariate Chemometric Modeling

To develop a robust and stable calibration model, two things are essential (i) the samples should include all the sources of variability that the model will see in application and (ii) representative samples should span the entire range of constituent values of interest. This section briefly describes the steps involved in the multivariate model development and model validation. The details of each could be found elsewhere in several books and research papers.(10)(12)

1.1.6 Sample Collection and Scanning

The number of samples required to build a robust calibration model depends on the complexity of the data set. If the sample matrix is simple (e.g. pure raw material where water is the analyte of interest), ten data points spanning the entire concentration range may be sufficient. For complex matrices (e.g. fermentation broths), 30 – 50 or more samples may be required to cover all the variations.(12,16) The temperature of the

samples is extremely critical as the NIR spectrum is sensitive to the temperature; this is particularly important for liquid samples. It is ideal to scan solid samples at room temperature when the analysis is performed in a laboratory. When the analysis is performed in a less controlled environment, it is recommended to include temperature variation in to the calibration set.(16)

1.1.7 Reference Method Analysis

In order to build a robust calibration model, it is essential to determine the measurement error of the reference extremely carefully.(17) Sampling errors and reference process errors will be carried over to the NIR method.(16) Reference method should be performed on the same sample scanned by the NIR.

1.1.8 Math-Pretreatments

The NIR raw spectra consist of both physical, chemical, and well as noise of the sample components being analyzed. The primary objective of math pretreatment is to minimize, eliminate or standardize non constituent variables and extract useful information during model development.(15) The most commonly used pretreatments are derivatives (1^{st} and 2^{nd}), Standard Normal Variant (SNV), Savitzky-Golay (SG), Mean Centering, Detrending, Normalization, N-Point Smoothing (NPS), and Auto-scaling.(10,15) In this section only few treatments are discussed, additional details can be found elsewhere in books on chemometric modeling.(4,10)

Normalization is carried out to remove systemic variations in the samples; this puts all the variables on the same scale by dividing each variable by a constant.(10) Sample weighting is similar to normalization which is accomplished by multiplying each variable by a constant.(10) Smoothing techniques reduce the random noise, which increase the signal-to-noise ratio. In auto-scaling, both mean center and scaling is used and could sometimes amplify the noise and needs to use carefully.(10) It can be applied to put the variables on a more equal footing before modeling is done.(4,10) Baseline corrections are used to remove systematic error in the samples. Derivatives on the other hand are used to reduce the baseline shifts and slopes and also help to improve the peak resolutions. First order derivatives reduce the baseline shifts and second order derivative mitigates the baseline slopes. Derivatives are most commonly used with smoothing techniques such as SG which uses a polynomial function.

1.1.9 Sample Selection

After the sample spectra are mathematically pretreated, they undergo a sample selection process to detect spectral outliers and remove redundant samples, failure to do so can result in less sensitive and less robust calibration models. During sample selection, the data set is divided into two, calibration set which is used to build the model and validation set which is used to test the robustness of the model. Three sample selection techniques commonly used are: (1) random, (2) selection based on NIR spectra only, and (3) selection based on the reference data only or the combination of spectral selection and reference method.(16) Here in this research, selection based on spectra using

Mahalanobis distance is used where, sample selection is based on the NIR spectra only and identifies spectra that are statistically different from the rest of the data set and redundant samples which do not add any new spectral features. The details of other methods could be found elsewhere in several books and research papers.(10,16)

1.1.10 Model Development

There are two types of calibration model development; univariate and multivariate. Univariate models are where a single response variable is regressed against the constituent value of interest. In multivariate model development, multiple responses are calibrated against a sample constituent value. MLR, PCR, and PLS are common used multivariate regression analysis techniques. In the section, only PCA and PLS are discussed.

Principal Component Analysis

The PCA is commonly used to reduce huge number of correlated or collinear variables to a few uncorrelated variables. The new variables are called the Principal Components (PC) or factors which explains the trends or the variability in the data set. The first PC explains the largest variation in the data set and each successive PC explains the remaining variability. Principal Component Regression is similar to and is simply an extension of PCA except there is a regression step involved on the compressed data.(10) This is graphically represented in Figure 1-4.

Partial Least Square

Like the PCR method, PLS uses similar mathematical models to reduce the rank based upon the maximum variance in the data matrix and capture the maximum covariance between X and Y. The main difference between PLS and PCR is the way X data is decomposed. In PCR, the X data is rank ordered based solely on the variance in the X data matrix followed by the regression of PC's using Y. In case of PLS, decomposition of X is such a way that the variables uncorrelated to Y are removed and most variance in the X and Y are explained and the variable are now referred as latent variables, see Figure 1-5.(10)

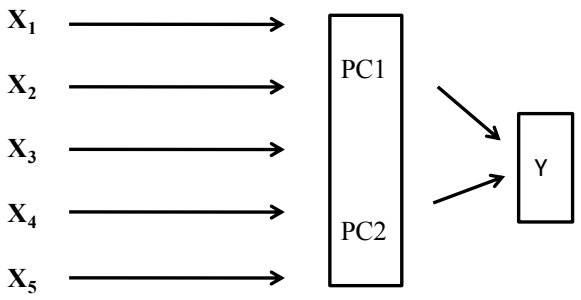

Figure 1-4. Graphical representation of PCA. Figure adapted from Martens and Naes "Multivariate Calibration" John Wiley & Sons, 1989.(18)

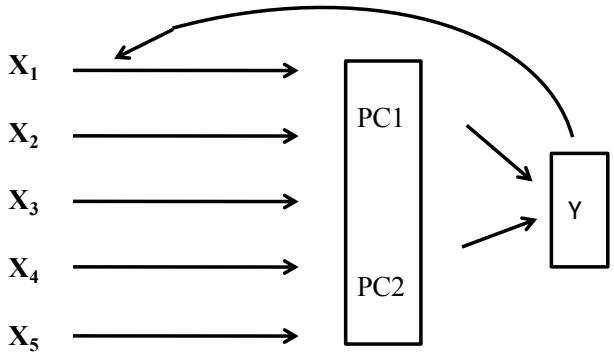

Figure 1-5. Graphical representation of PLS. Figure adapted from Martens and Naes "Multivariate Calibration" John Wiley & Sons, 1989.(18)

1.1.11 Model Calibration Validation

A calibrated model needs to be validated before it is use for prediction. Validation is typically performed using a separate data set and should cover the full range of constituent values used in the model development. The prediction errors assess the predictability and applicability of the model. Statistical parameters obtained during the model development such as standard error of calibration (SEC) and prediction (SEP), residuals and factor selected must be carefully evaluated.(17,19) The number of factors selected and the coefficient of fit (R^2) must be carefully considered. In PLS models, cross validation helps in identifying the optimum number of factors needed to build the model. SEC alone does not adequately assess the predictability of the model. Selecting too many factors would result in lower SEC values but when the model is tested with an external set would yield high prediction errors (SEP) when tested with external data set, which suggests that the model is over-fitted, i.e. factors not related to the actual constituents of

interest such as noise are used to construct the model. On the other hand if too few factors are used, this would result in an under-fitted model with a higher SEP.

1.1.12 Model Prediction and Evaluation

The next important step in the validation of the model is testing its predictability. Once the calibration model is built, it must be tested with an external dataset, from new batch or batches, not used in building the model. Then the SECV is evaluated to see if it yielded satisfactory SECV value.

1.1.13 Model Statistical Parameters

Standard Error of Calibration (SEC)

The SEC of the calibration set is the standard deviation of the NIR values from the reference value. SEC must not be used alone and the limit value is two to three times standard error of lab (SEL).

$$SEC = \sqrt{\frac{\sum_{i=1}^{n} (reference\ \ value_i - NIR\ \ value_i)^2}{n - p}} \qquad \text{Equation: 1.1}$$

where, n = samples and p = number of factors in the calibration

Standard Error of Cross Validation (SECV)

During calibration model development, parts of the samples are used to build the model and other part is used to validate the model.

$$SECV = \sqrt{\frac{\sum_{i=1}^{n}\left(reference\ value_i - NIR\ value_i\right)^2}{n}} \qquad \text{Equation: 1.2}$$

where, n = number of cross validation samples

Standard Error of Prediction (SEP)

SEP if the error estimate when the calibration model is tested with external data set.

$$SEP = \sqrt{\frac{\sum_{i=1}^{n}(reference\ value_i - NIR\ valueY_i)^2}{n}} \qquad \text{Equation: 1.3}$$

1.1.14 Roller Compaction Critical Variables

Roller Compaction

Roller compaction (RC) is a dry granulation technique mainly intended to improve the flow and compaction behavior of powders. Dry granulation using roller compaction has been used in pharmaceutical industry for more than 50 years but gained popularity recently due to the improvement in the instrumentation and process control.(20) Due to

greater production capacity and use of minimal lubricant made this a preferred technique over other dry granulation technique like slugging.(21,22) Other advantages of RC process are that it is simple, economical, continuous, easily automated and suitable for drugs that are sensitive to heat and moisture.(23,24)

Dry granulation is a particle bonding process; most of the particle deformation takes place as the material pass through the feeding zone. As the material passes through the compaction zone, the powder blend is compressed and compacted between two counter rotating rollers, as a result the particle deforms, fragments and bonds resulting in a ribbon.(20) These ribbons are further milled to achieve desired granule sizes. Figure 1-6 illustrates different regions/zones of the roller compactor.(25) Depending on the level of stress experienced by the material between the rollers, Kleinebudde *et al,* categorized this area is divided into three different zones, see Figure 1-6. First is the feeding region, where material experiences very little stress as the material pass through this region and the density increases due to the particles rearrangement. Second is the compaction region where the particles deform, breaks, and bonds due to the higher levels of stress. Depending on the nature of the material, plastic deformation and/or brittle facture occurs. The nip angle is the angle where the compacted material enters the nip region, and the nip angle depends on the coefficient of friction between the roller surface and the material. (26,27) Third is the extrusion region also called slip zone where the materials undergo elastic recovery and increase in porosity as the material is released.

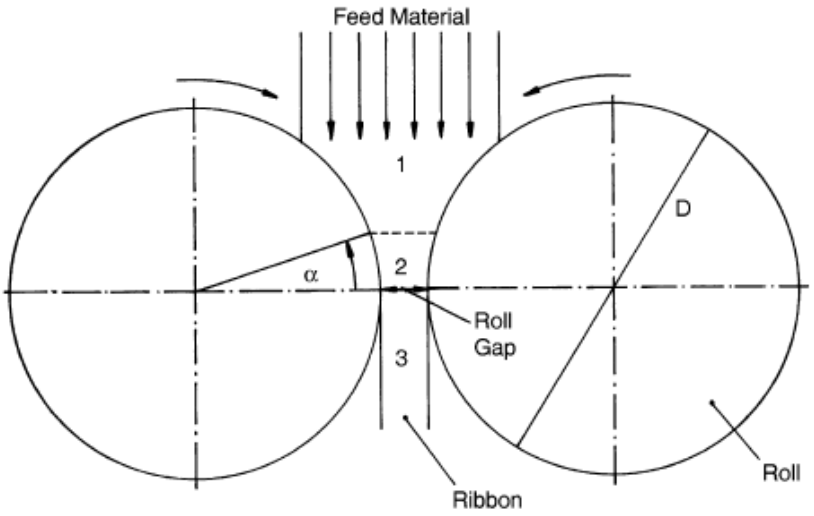

Figure 1-6. Different zones in a roller compactor. Feed zone (1), compaction zone (2), extrusion zone (3), nip-angle (α), and roller diameter (D) (taken from Kleinebudde *et. al*).(28)

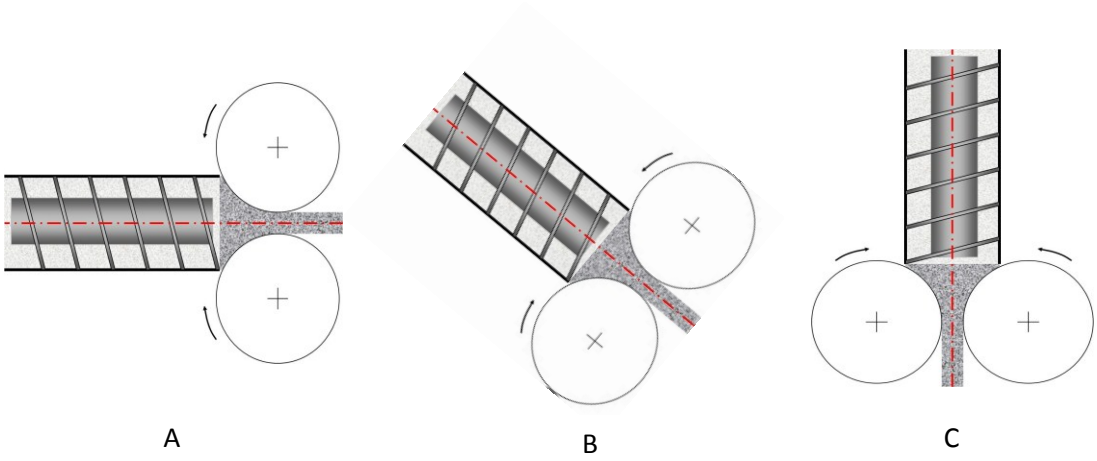

Figure 1-7. Different configurations of roller compactor. Horizontal (A), inclined (B), and vertical (C) (Adapted from Guigon and Simone).

Machine Variables

Feeder design and feeder mechanisms are critical machine variables that could impact material compaction.(29) Different suppliers have different feeder mechanisms. They can be gravity feeder or a forced feeder. Gravity feeder works well with material that has good flow characteristics and does not use any external feeding mechanism to feed the material into the rollers. In case of a forced feeder, a rotating screw or an auger is installed; this feeds the material into the rotating rollers. Figure 1-7 shows different roller compactor configurations commercially available. Rollers are mounted in vertical direction (Bepex, Freund, and Fitzpatrick), inclined (Gerteis), and horizontal or vertical (Alexanderwerk).(25) Roller surfaces can be smooth, fluted, or corrugated. Smooth surface are used when powder gripping is not an issue and can help reduce the sticking problem. On the other hand knurled/ corrugated surfaces provide additional sticking for material which has feeding issues. In addition, different roll width and roll diameters are available and can be customized depending on the user requirements.

Process Variables

Roll pressure (RP), roll speed (RP), feed screw speed (FSS), and roll gap (RG) are the four roll compaction critical processing parameters than need to be optimized to maintain the quality of the product.

Roll pressure/compaction force is the amount of force exerted by the rollers on the material. It was reported that high RP, produces strong compacts with less fines.(30-

32). On the other hand, over compaction may lead to poor quality granules due to loss of compactablity and these granules when compressed into tablets, which can lead to lower hardness and higher friability.(31,33,34) Inghelbrecht *et al*, have reported that this behavior is prominent when plastically deforming material like microcrystalline cellulose is used.(35) While Wu *et al*, have reported that brittle materials are less susceptible to compactablility loss. This is extremely critical as most pharmaceutical powders contain both plastic and brittle material so the roll pressure needs to be optimized to maintain product quality.

Feed screw speed dictates the rate at which the material is fed into the rollers. This parameter need to be optimized based on the material flow, roll speed, and aeration conditions. Low FSS operating conditions may cause insufficient material feeding in to nip region resulting in poor quality ribbons. At higher screw speed may lead to over feeding the material and could lead to caking of material and eventually interrupting the flow.(29)

Roll speed determine the dwell time the material under the rollers and is dependent on the flow properties and the nature of the material (plastic vs brittle). For a plastic material like microcrystalline cellulose low roll speeds increases the dwell time and result in loss of compactability of the material leading to tablets with low hardness and friable.(34,36) In case of materials that exhibit significant elastic recovery, high roll speed may lead to cracking or friable resulting in poor quality of the ribbon due to short dwell time.(37,38)

It was reported that granules of desired quality can be obtained by controlling the ratio of FSS to RP.(39) Gupta *et al,* reported that the density and strength of the ribbon was independent of the roll pressure when FSS to RS ration was maintained constant.(40) For plastically deforming materials, high RS to FSS ratio and low RP were found to be critical to produce tablets with desired hardness and dissolution rate. Similar observations were reported for partially deforming material such as lactose.(41)

1.1.15 PAT in Roller Compaction

Miller first reported the use of roller compaction and NIRS to map roller compaction unit operations on three different active ingredients by subjecting them to different compaction conditions.(42) Studies were conducted on ibuprofen/starch, aspirin/starch and acetaminophen/starch blends where he demonstrated that NIR is sensitive to the density differences between 10 and 20 bar roll pressures. Miller reported an increase in NIR absorbance at higher roller pressure and under vacuum deaeration in case of 50/50 Ibuprofen/Starch compacts. This was followed by series of papers by Gupta *et al*,(40,43-46) on noninvasive real-time application of NIRS on the properties of the roller compacted ribbons and granules. They monitored the influence of ribbon strength on the granules and granule size distribution. The upward shift in the NIR spectra resulting from density differences was used as a basis for quantifying the compact strength, granule size and granule size distribution. At a constant feed screw speed, an increase in the roll speed resulted in spectra shifting to a lower absorbance. It was also observed that with the increase in roll speed, the particle size distribution of the milled compacts decreased.

Later Kirsch *et al*, used the slope of best fit line and found a linear correlation between the slope and the tablet hardness.(47) Lim *et al*, studied the effect of various process parameters on the influence of ribbon porosity. It was reported that, increase in roll speed, increased the porosity of the ribbon due to decrease in the dwell times. It was also reported that the increase in the roll pressure, decreased the ribbon porosity due to high pressure on the powders. In addition, this paper also demonstrated the use of NIR chemical imaging as nondestructive tool to monitor the porosity of the ribbon at various roller compaction processing conditions.(48)

1.1.16 Fluid bed Granulation and Drying - Critical Variables and End Point

Fluid bed granulation is a wet granulation technique for producing granules by spraying solution (typically binder solution) on to a fluidized powder. The particles in the path of the spray get wetting and collide with each other to adhere and forms granules. Figure 1-8, is the schematic representation of the top spray fluid bed granulator set-up. Here, the particles are suspended in the air stream entering from the bottom of the granulator. Binder solution is sprayed from the top on to the powder at certain atomization pressure. There are two modes of granulation, dry stage, where the binder solution is prayed at a rate less than or equal to the evaporation rate. In wet stage, the binder solution is applied at a higher rate than the evaporation to build enough moisture for granulation, this results in high dense granules.

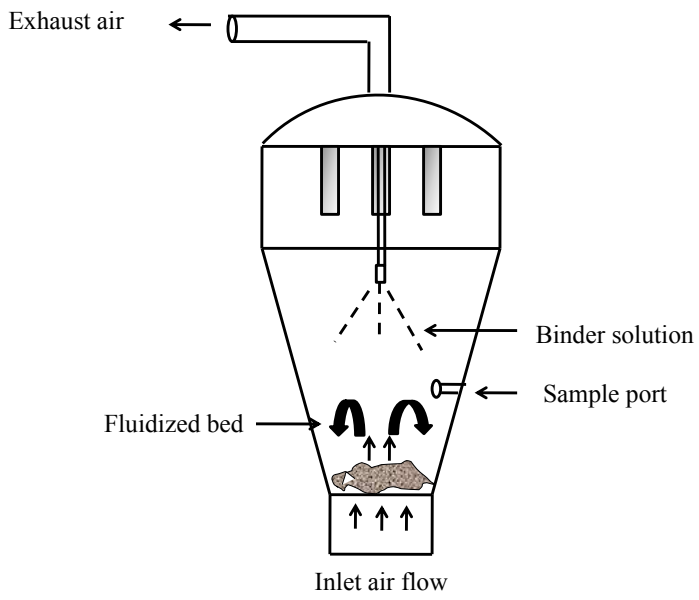

Figure 1-8. Schematic representation of top spray fluid-bed granulator.

The wet granulation of pharmaceutical powders are generally carried out to improve the flow characteristics, compression properties, increase the density, change the drug release characteristics, make uniform blends, i.e., minimize segregation, and reduce the dust. It offers significant advantages over multistage wet granulation techniques. The first pharmaceutical application of fluid bed granulation was reported by Wuster (49,50) for coating drug particle using air suspension technique, which was followed by Scott and his coworkers where much of the focus was on design and operation of the equipment based on the material and energy balance and heat and mass transfer relationships.(51,52) A comparative study between fluid bed granulation and conventional wet massing technique by Liske and Mobus (53) indicated that granules produced by FBG was finer, more flowing and homogenous granules which after compression produced stronger and

faster disintegrating tablets over wet granulation. In early days fluidized bed was mainly used for drying the pharmaceutical granules but currently it is used for granulation, pelletization, drying, and coating.

Particle Agglomeration and Growth

Agglomeration is a size enlargement process where fine particle are held together by spraying a binder solution. The final product is an aggregate in which the final particle can be identified. Three mechanisms of the granule growth have been suggested, and Parikh *et al*,(54)summarized three mechanism for granule growth. These are

- *Adhesion and cohesion bridges are formed due to immobile liquids. Thin adsorption layers can contribute to bonding of fine particles*
- *Mobile liquids due to interfacial and capillary forces*
- *Solid bridges are formed during the drying process when the dissolved substance crystallizes*

Iveson *et al*,(55) described the wet granulation as a combination of three rate processes. Figure 1-9 illustrates different stages of the granulation process.

- *Wetting and nucleation, where the liquid is brought in contact with the dry power and binder is distributed throughout the powder bed*
- *Consolidation and growth, where the granule compaction and growth occurs due to collision between the two granules, granules and powder, and granules and the walls of the equipment*

- *Attrition and breakage, occurs during the process when wet or dry granules impact, wear or compact or during the process handling*

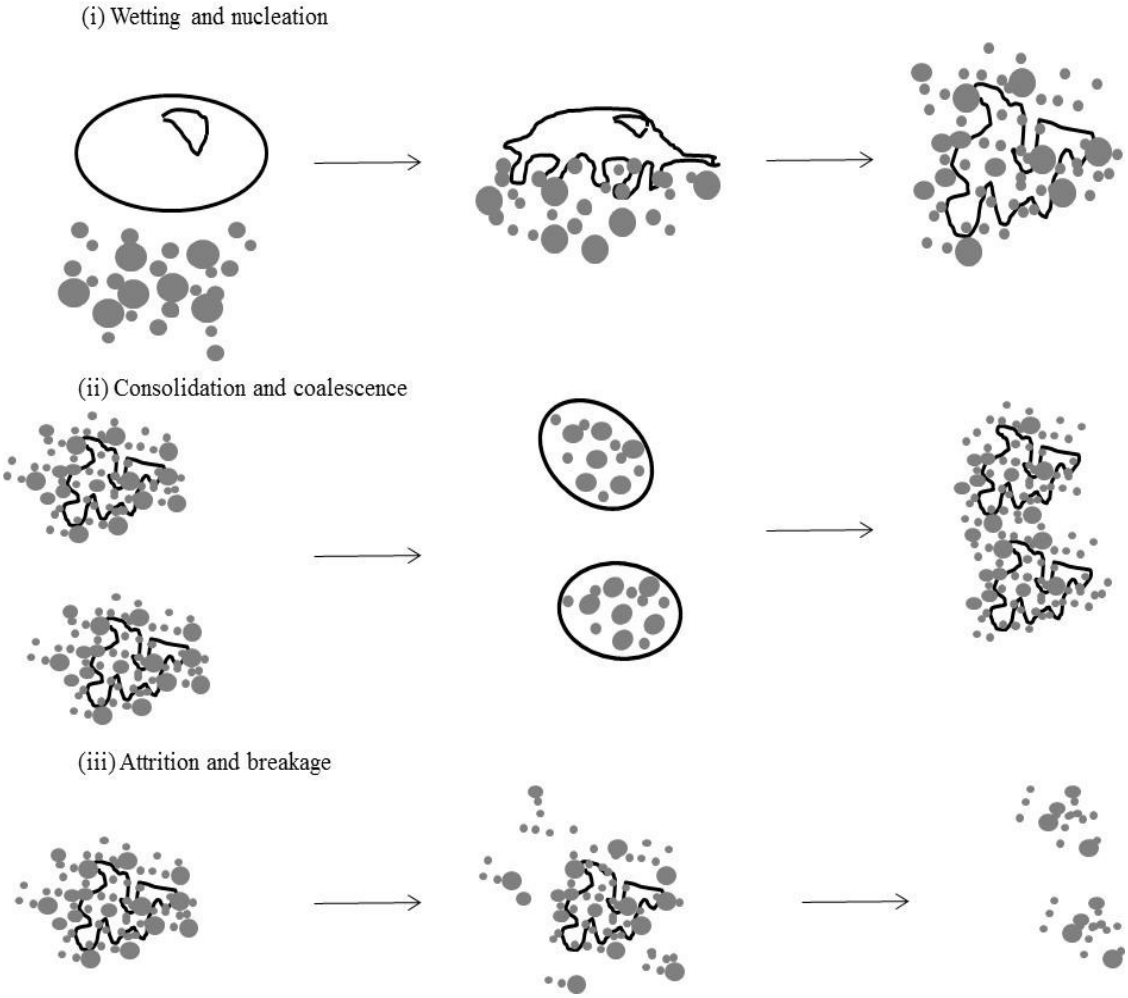

Figure 1-9. Different rate processes during the wet granulation. Figure modified from Iveson *et al* (55) and Cantor *et al*.(56)

Fluid bed drying

The purpose of drying in fluid bed is to remove excess moisture or solvent from the granules to desired levels for subsequent processing such as compression. Water in granules exists in bound or free form. These forms of water in the powder bed exist in pendular, funicular and capillary state (57) and it is the amount of water that can be removed from the material by drying at a specified temperature and humidity.

Drying involves heat and mass transfer. Water evaporates due to heat transfer from the surroundings by a process called convection. Convection involves movement of heat from one point to another by the mixing of one portion of fluid (gas, solid, liquid) with another, i.e., the bulk movement of material. Mass is transferred in the form of a vapor from the surface and in the form of liquid or vapor within surroundings, both these processes are interdependent.(58)(54) In addition to convection, heat transfer can also takes place due to conduction, where heat is transferred in the fluids by vibration and collision of molecules and free electrons and by transfer by electromagnetic waves or photons in case of radiation.(59) Figure 1-10 shows the different stages during drying where Figure 1-10b is obtained by plotting dW/dt obtained by differentiating the data from Figure 1-10a. Segment A-B represents the initial phase where the material is heated to the drying temperature. This is followed by segment B-C which is constant rate or steady state period, where the moisture moves from the saturated regions to the surface of the material either by convection by drying gas or by both convection and radiation. At

steady state, the drying rate per unit area is constant. Equation 1.4 describes the steady state condition when heat and mass transfer takes places simultaneously.

$$-\frac{dW}{dt} = \frac{h_t A(T - T_s)}{\lambda_s} = k_a A(p_s - p)\,(60) \qquad \text{Equation: 1.4}$$

Where: $\frac{dW}{dt}$ is the drying rate, h_t is the heat transfer coefficient, A is the surface area, $T$is the total heat, T_s is the temperature of the liquid surface, λ_s is the latent heat of vaporization, k_a is the mass transfer coefficient, p_s is the vapor pressure of the liquid.

The falling rate period starts when the system no longer maintains balance between mass and heat transfer. Prost *et al*, described the mechanisms of internal mass transfer as:(60)

- *Capillary movement within fine and porous granules*
- *Diffusion and surface tension of the liquid*
- *Pressure induced liquid and vapor flow where the vapor escapes from the opposite side of the heated surface*

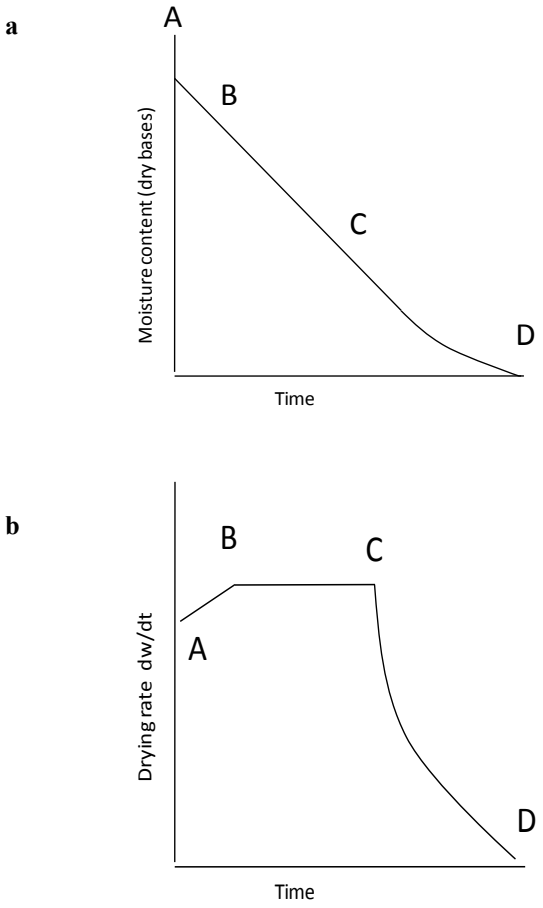

Figure 1-10. Different drying periods. Modified from Cooper *et al*. and Lipsanen *et al*.

1.1.17 Variables in Fluid bed Granulation and Drying

Factors influencing fluid bed granulation can be classified into three different categories.

- Product variables
- Instrument related variables
- Process variables

Product and formulation variables

Properties of starting material such as particle size distribution, cohesiveness, charge, wetting characteristics, and nature of material such a crystalline or amorphous were found to impact the properties of the granules. It was reported that low particle density, narrow size distribution, low cohesiveness, and spherical or nearly spherical area is ideal for processing (54). Aulton and Banks reported that particle size of the starting material is related to its wettability, and was related to the cosθ, where θ represents the contact angle (61). In addition to material properties, the dose of drug in the formulation was also found to be critical. Several authors have reported that the binder type, binder concentration, and the binder quantity play a critical role in the quality of the granules such as flow properties, friability, bulk density, and size distribution.(52,62-69) It was also reported that addition of binder in dry form and subsequent granulation with ethanol produced large mean size of granules compared to binder in solution form. However, binder in solution produced more free flowing and less friable granules.(70) Binder temperature was also found to play a critical role as it affects the viscosity of the solution which in turn affects the droplet size. Increase in binder solution temperature decrease the viscosity which produces smaller droplets, which results in produce small size granules. On the other hand high molecular weight binder produced larger droplets and large granules particle size.(63) In addition, the solvent system also plays a major role in determining the granule particle size, solvents due to their rapid vaporization produces smaller granules.

Instrument variables

Equipment variables like air distribution plate and pressure drop determined the fluidization behavior of the bed. Air distribution plate provides the appropriate means of supplying air to the product. They are commercially available in various sizes with 40-30% open areas and screen mesh ranging from 60-325 mesh sizes to cover the stainless steel plates. It is critical to select the appropriate distribution plate which provides the optimum list properties. For examples, powders with low bulk density may require plate with small pore size for uniform distribution. In addition, pressure drop (ΔP) generated by the blowers needs to be optimized for optimum fluidization. Also, in order to maintain appropriate ΔP, most of the granulators are equipped with blow back system to maintain clean filters. Build-up of fine material on the filers may result in higher ΔP which could disrupt the fluidization of the product. In addition, other miscellaneous equipment factor such as design of fluid bed granulator is critical to ensure consistent product quality in laboratory units and during the commercial scale-up. High drying capacity in the lab unit from some suppliers could result in longer processing time in commercial units.

Process variables

Process parameters listed in Table 1-1 are interdependent, and to fully understand a process it is essential to understand their interdependency. Optimum inlet air flow temperature is determined based on the choice of the binder solution and the thermal sensitivity of the material. Typically in aqueous based systems, higher inlet air

temperatures are preferred compared to non-aqueous solvent systems. High temperature was reported to produce finer granules and lower temperature produce larger granules.(73) In addition to the temperature, humidity of the inlet air was found to be critical for granule size; increase in humidity increased the granule size and the duration of drying.(71) To avoid filter clogging and prevent granule attrition, low air flow rate was recommended to maintain proper fluidization of the powder bed.(61,73) Several process parameters contribute to the droplet size of the binder solution; atomization air volume and pressure, and the binder spray rate must be controlled to produce consistent granule size. Higher flow rates were found to produce larger droplets and larger granules and vice-versa.(68,71,74) Droplets size was also found to be affected by the binder viscosity. Low viscous solutions produce smaller droplets and small granules.(61,73) Gerogakopoulos *et al*, reported that height and the position of the nozzle also influenced the resulting granules. Large granules with high bulk density was produce when the nozzle was placed closer to the bed height and two higher position results in finer granules due to binder spray drying.(74)

Table 1-1. List of fluid bed granulation variables. Modified from Schaefer *et. al*, Aulton *et. al*, and Lipsanen *et. al*.(61,71,72)

Product variables	Instrument variables	Process variables
Nature of starting	Air distribution plate	Inlet air flow rate
-Cohesiveness	Pressure drop	Inlet air flow temperature
-Particle size	Blow back mechanism	Air humidity
-Wettability	Nozzle height	Bed height
Binder type	Granulation bowl	Binder spray rate
Binder concentration		Atomization air pressure
Binder solvent		Spray angle
Temperature of binder		Nozzle type

Process control and end-point determination

With the availability of sophisticated controls like Programmable Logic Controllers and data acquisition systems, the granulation process is accurately controlled to achieve robust and reproducible results. Data collected from different processing conditions and locations such as inlet and exhaust temperatures, air flow rate measurement, atomization pressure, product temperature, sensors for filter blow back frequency and duration, humidity of inlet and outlet can provide feedback and help process monitoring. Moisture levels in the fluid bed granulation and drying is a critical to the quality of the intermediate granules and subsequent final dosage forms. Presence of excess residual moisture could influence the flow, compressibility of granules and the stability of a dosage form.(75) In case of tablets, capping may occur if the moisture levels are too low and picking and sticking may occur due to excess residual moisture.(76) Schaefer *et al*, reported that the optimum moisture levels to be around the equilibrium moisture during the storage of granules to avoid exchange with the surroundings.(62) However, presence of excess

moisture could result in physical, chemical and microbial instability. Several methods of end-point determination were reported in the literature. Monitoring temperature of the inlet and outlet air was one widely used criterion to determine the end-point.(77) But this method is dependent on the humidity of the inlet-air entering as material drying is dependent on the moisture content on the inlet and the outlet air.(62) In some instances humidity of the outlet air was used as an end-point determining tool.(78,79) Several authors reported the use of temperature difference (ΔT) method to determine the drying end-point.(62,80-84) The advantage of this technique is that the humidity variations on the end-point can be eliminated. Leuenberger (82) described a simple two-capillary process for drying. In first drying phase, fine capillaries draw the liquid from coarse capillaries by a capillary action. This transfer liquid to the surface of the granules where the surface remains moistened and the temperature remain constant. This state of dynamic equilibrium is described as wet bulb temperature (T_k) and the drying rate remains constant. In second stage, the surfaces of the granules begin to dry as the fine capillaries no longer able to supply liquid to the surface which subsequently increases the temperature of the surface. The dying process ends when the temperature reaches a specified temperature (T_e) the Equation 1.5 describes the theoretical principle behind the ΔT technique.(85)

$$T_e = T_k + \Delta T \qquad \text{Equation: 1.5}$$

where: T_e= End temperature; T_k= Wet bulb temperature; ΔT = Constant

The above described ΔT technique for end-point determination was found to be more consistent and reliable compared to other conventional methods as this technique is resistant to the changes in the atmospheric pressures.(80) With the advancement in the instrumentation several techniques are currently introduced in the pharmaceutical industry to monitor process parameters and determine the end-point. One such technique is the use of Near-Infrared Spectroscopy (NIRS). This technique is rapid, nondestructive and requires minimal sample preparation and can be used in-line, at-line, on-line and off-line. Several authors have reported the use of NIR in monitoring the moisture levels in the fluid bed. Franke *et al*, described the use of in-line NIRS to quantify granule moisture content and particle size allowing process monitoring and end-point determination using univariate analysis.(86) Similarly, Rantanen *et al* used three to four different wavelengths to determine the moisture content.(87) NIRS on-line monitoring was also used to quantify film coating in the fluid bed granulator using multivariate analysis.(88) Rantanen *et al*, in a series of papers described the real-time used of NIRS for process monitoring and control during fluid bed granulation and drying process. The authors have demonstrated the use of multivariate NIR chemometric models coupled with temperature and humidity data to developed models for better understanding the granulation process.(89-91) Peinado *et al*, demonstrated the development, validation and transfer of NIR model to determine the end-point for commercial production batches of an FDA approved solid oral product.(92) Alternate approaches like Focus Beam Reflectance Measurement, Self-Organizing Maps, and Artificial Neural Networks are

also used for process monitoring and end-point determination. Huang *et al* reported the use of FBRM for In-line particle size characterization using multivariate approach.(93)

1.1.18 Quality Risk Management

Pharmaceutical drug manufacturers today undergo stringent regulations in order to product safe, reliable, and cost effective products. One of the key elements to make successful product and maintaining quality throughout product's life cycle is to identify and control risk associated with it. The purpose of ICH Q(9) is to provide a systematic approach to the quality risk management to ensure high quality of pharmaceutical products by identifying and control quality issues during the process and product handling.(6) Quality risk management as defined by the ICH Q(9) guidance is "A systematic process for the assessment, control, communication, and review of risks to the quality of the drug product across the product lifecycle" (6) and two primary principle involved in the quality risk management according to the guidance document are:(6)

- *The evaluation of the risk to quality should be based on scientific knowledge and ultimately link to the protection of the patient; and*
- *The level of effort, formality, and documentation of the quality risk management process should be commensurate with the level of risk*

Traditional ways of quality risk management using empirical approaches such as compilation of observations and trends provide valuable information in handling defects and deviations. Additional risk management tools listed below can be used in conjecture

to traditional methods both provide both qualitatively and quantitative ways to estimate and identify the range of risk associated with the product.

- Basic risk management facilitation methods (flowcharts, check sheets etc.)
- Failure mode effects analysis (FMEA)
- Failure mode, effects and criticality analysis (FMECA)
- Fault tree analysis (FTA)
- Hazard analysis and critical control points (HACCP)
- Hazard operability analysis (HAZOP)
- Preliminary hazard analysis (PHA)
- Risk ranking and filtering
- Supporting statistical tools

Risk Management Tools

Risk tools such as FMEA are a bottom-up approach, where the risk is evaluated based on the severity of the failure, likelihood of the cause, and the severity of the occurrence. It uses a single point failure approach and move up to the top level. Risk Priority Number (RPN) which is the measurement of relative risk is the product of severity, occurrence, and the detectability which is used to prioritize the action

FMECA is an extension of FMEA where each failure (severity, occurrence, and detectability) from each product is evaluated for its criticality. The criticality is then translated into risk and preventive actions are taken to mitigate it. Whereas, Fault tree analysis is the top-down approach used to deduce the root cause of the top event. This can be used to evaluate the failures one at time or from two or more events. The results are represented graphically in the form a tree using logic and symbols.

According to WHO, HACCP is a systematic, proactive, and preventive tool for assuring quality, reliability and safety.(94) It involves conducting hazard analysis and identifying preventive measures for each step of the process, determining critical control points. It also involves establishing critical limits and monitoring critical control points.(6).HAZOP is a bottom-up method which uses combination of design parameters and "guideword" (e.g., No, More, Other Than, Part of, etc.) to identify deviations from the normal use. Preliminary hazard analysis based on applying prior knowledge or experience of a hazards or a failure to identify future hazardous situations or events. According to ICH Q(9) guidelines, it consists of following tools: Identification of the possibilities that the risk event happens, qualitative evaluation of the extent of possible injury or damage to health that could result and a relative ranking based on severity and likelihood of occurrence.(6) In case of complex systems, risk ranking and filtering uses both qualitative and quantitative information. A single risk score is calculated from different factors which are used for ranking risk.

1.2 Hypothesis and Specific Aims of this Research

1.2.1 Hypothesis

Following hypothesis have been put forward:

- In roller compaction, the sensitivity of Near-Infrared Spectroscopy (NIRS) to processing variations can be used to predict the quality of granules and tablets
- In-line NIRS in conjunction with humidity and temperature measurements can be used for efficient process monitoring in fluid bed granulation

1.2.2 Specific Aims

The following are the specific aims to test the above hypothesis

- To identify critical roller compaction in-process parameters influencing the properties of granules and tablets in the formulation development of immediate release dosage form
- To carry out NIRS analysis on the granules and tablets; develop and assess reliable chemometric models that predict the critical quality attributes in the formulation development of immediate release oral dosage form
- To apply in-line NIRS and multivariate batch modeling for process understanding in fluid bed granulation

1.3 Scope and Organization of this Dissertation

Chapter 2 of this dissertation focuses on the identification of critical roller compaction and product quality attributes in the formulation development of ciprofloxacin hydrochloride oral tablets. In the early stages of product development, quantitative risk assessment was performed using Failure-Mode-Effect-Analysis at various stages/unit operations, to identify high risk factors. Factors identified as further quantified using PB screening design.

Chapter 3 focuses on further evaluating factors identified from chapter 2, these factors were studied in detail using full factorial design. In addition, this chapter also discusses the application of Near-Infrared Spectroscopy (NIRS) at various stages of formulation development to develop reliable qualitative and quantitative chemometric models to predict CQA's such as granules size, crushing force, and disintegration time.

Chapter 4 deals with the in-line real time application of the NIRS in quantifying moisture levels in the fluid bed granulation process. Also discussed are utilizing novel Pyrobutton® data logger to monitor humidity and temperature. Multivariate statistical process control charts were constructed using real-time moisture, temperature and humidity data obtained from batches performed under normal conditions. To demonstrate their application, control charts (Scores, DModX, and Hotelling T^2) were further used to monitor evolution of batch process for real time fault analysis on three batches which deviate from normal processing conditions. Chapter 5 provides concluding remarks and future direction.

Chapter 2 Quality-by-Design I: Application of Failure Mode Effect Analysis (FMEA) and Plackett-Burman design of experiments in the identification of "main factors" in the formulation and process design space for roller compacted ciprofloxacin hydrochloride immediate release tablets.[1]

2.1 Abstract

As outlined in the ICH Q8(R2) guidance, identifying the critical quality attributes (CQA) is a crucial part of dosage form development; however, the number of possible formulation and processing factors that could influence the manufacturing of a pharmaceutical dosage form is enormous obviating formal study of all possible parameters and their interactions. Thus, the objective of this study is to examine how quality risk management can be used to prioritize the number of experiments needed to identify the CQA, while still maintaining an acceptable product risk profile. To conduct the study, immediate release ciprofloxacin tablets manufactured via roller compaction

[1] This section of the dissertation was coauthored along with Raafat Fahmy, Ramesh Dandu, Walter Xie, Gregg Claycamp, and Stephen Hoag and was previously published in AAPS PharmSciTech, 2012, 9, 1-12.

were used as a prototype system. Granules were manufactured using an Alexanderwerk WP120 roller compactor and tablets were compressed on a Stokes B2 tablet press. In the early stages of development, prior knowledge was systematically incorporated into the risk assessment using failure mode and effect analysis (FMEA). The factors identified using FMEA were then followed by a quantitative assessed using a PB screening design. Results show that by using prior experience, literature data and preformulation data the number of experiments could be reduced to an acceptable level, and the use of FMEA and screening designs such as the PB can rationally guide the process of reducing the number experiments to a manageable level.

2.2 Introduction

The regulatory framework outlined in the ICH guidance Q8(R2) Pharmaceutical Development, ICH Q9 Quality Risk Management and ICH Q10 Pharmaceutical Quality Systems was introduced to improve pharmaceutical product quality and provide regulatory flexibility for the industry to improve their manufacturing processes.(1-3) Figure 2-1 shows the principal steps needed for the development of a new drug using the Quality by Design (QbD) paradigm as outlined in the ICH Q8(R2), Q9 and Q10 guidance.

The first step in this process is to define the Quality Target Product Profile (QTPP). The ICH Q8(R2) guidance defines the QTPP as "A prospective summary of the quality characteristics of a drug product that ideally will be achieved to ensure the desired

quality, taking into account safety and efficacy of the drug product."(1) In other words, one has to determine the performance attributes that need to be designed into the dosage form so that it achieves the desired performance aims. Performance attributes can include factors such as therapeutic dose, route of administration, and type of dosage form, release profile that complements the pharmacokinetic characteristics of the active pharmaceutical ingredient (API) and optimizes drug delivery. This definition includes all of factors that influence product performance, from API and excipient stability/compatibility all the way through to packaging. For a successful dosage form, the characteristics that make up the QTPP should be designed into the drug product and serve as road map for the development process.

After defining the QTPP and developing a lead formulation and manufacturing process, the next step is to develop a process understanding by which the material inputs and manufacturing process parameters that affect the dosage performance or QTPPs can be identified; i.e., determine the CQAs see Figure 2-1. According to ICH Q8(R2) "A CQA is a physical, chemical, biological, or microbiological property or characteristic that should be within an appropriate limit, range, or distribution to ensure the desired product quality. CQAs are generally associated with the drug substance, excipients, intermediates (in-process materials) and drug product."(1) Examples of CQAs include those aspects affecting product purity, strength, drug release and stability; for solid oral dosage forms, raw materials properties such as particle size distribution, bulk density, and moisture content can all be examples of CQAs that can affect product performance. Thus, a key goal of QbD is to identify the most important CQAs, i.e. formulation as well as process

parameters, that have the greatest influence on the QTPP, and to understand their relationships to product performance.

The QbD paradigm requires process understanding and the determination of the design space, which requires identifying the principal CQAs. The main challenge faced with process understanding is identifying the CQAs from the numerous possible formulation and process variables that could affect drug product quality, i.e., the QTPP. The problem is worsened by the fact that most pharmaceutical operations have no fundamental first principle models that can be used; thus, most of our knowledge of unit operation behavior is based upon empirical correlation; which is typically assessed by use of statistical methods. Traditional pharmaceutical product development uses factorial (full and/or fractional) statistical designs and response surface methodologies to systematically evaluate formulation/process variables and relate them to critical product quality attributes.(4) These designs provide comprehensive process understanding and are invaluable in assessing the manufacturing process and the factors that affect end product quality. However, statistical methodologies suffer from the practical limitation that for each variable added to the study many more experiments must be done and one can easily create a situation in which the number of experiments needed to complete an experimental design is not practically feasible. This is an issue, especially in the early stages of development where formulation and/or the process are not fixed and there are many sources of variability, from the API, excipients as well as those arising from each unit operation of the manufacturing process. The fundamental problem is that studying too many variables directly increases development costs, and requires more time to bring

new products into market, which can potentially delay new therapies for patients who have life threatening illnesses. In addition, there are many unmet therapeutic needs that have small market sizes and if it is too expensive to develop a drug then no new therapies will be forth coming. Alternatively, studying too few variables has the risks of insufficient process understanding, which can increase the likelihood of product failures or recalls and safety issues due to poor product performance, which also poses some risk to patients.

One way to optimize the use or resources in development is to use risk methods to prioritize the variables to be studied, i.e., identify the variables that present the most risk to product quality and study those variables more carefully. The goal of this chapter is to illustrate how quality risk management tools can be used to rationally balance walking the fine line between too many and too few experiments during product development, and to focus resources on the factors that can have the greatest impact on patient health/product quality. Specifically, the goal is to apply quality risk management in the early stages of tablet formulation development of an IR tablet for the poorly soluble drug ciprofloxacin. The identification of key factors (sources of variability) in early stages of development was done using the failure mode and effect analysis (FMEA) followed by the Plackett-Burman (PB) design of experiments (DOE) method.(5, 6)

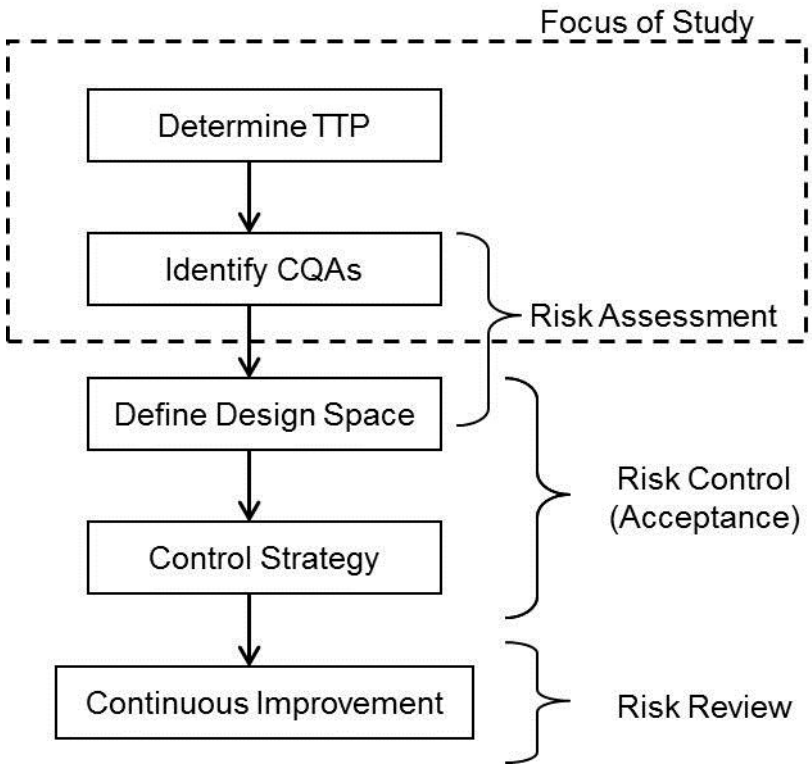

Figure 2-1. QbD drug product development flow chart showing principal steps.

2.3 Materials and Methods

2.3.1 Materials

Ciprofloxacin HCl USP (Lot # 6026) was purchased from R.J. Chemicals, Coral Springs, FL (Manufactured by Quimica Sintetica, Madrid, Spain). Microcrystalline cellulose, Avicel® PH 102 (Lot # P208819026) and Avicel® PH 101 (Lot # P108819435) grades were obtained from FMC Biopolymer (Philadelphia, PA). Pregelatinized starch, Starch 1500® grade (Lot # IN502268) was obtained from Colorcon (West Point, PA) and Spress®B825 grade (Lot # S0430676) was obtained from grain processing corporation (Muscatine, IA). Hydroxypropyl cellulose, Klucel® EXF (Lot # 89510) and Klucel® JF (Lot # 89014) grades were obtained from Aqualon/Hercules (Wilmington, DE). Magnesium stearate, vegetable source (Lot # MO5676) was obtained from Covidien (Hazelwood, MO), and animal source (Lot # WQ0272) was obtained from Spectrum pharmacy products (Hazelwood, MO). Fumed silica, Aerosil® 200 (Lot # A07319D) was obtained from Evonik (Piscataway, NJ).

2.3.2 Roller compaction and Tablet Production

To prepare a batch size of 500 gm, the intragranular components (472.5 gm) were blended in a twin shell blender (Patterson-Kelley Company, East Stroudsburg, PA) without an intensifier bar for 5 min. The powder blend was compacted on a roller compactor (Model: WP 120 V Pharma, Alexanderwerk Inc., Horsham, PA) equipped

with rollers (25 mm diameter) having a knurled surface. Granulation was performed using a fixed roll-gap of 1.5 mm. Studies carried out previously (7-9) have shown that there is no significant differences in the physical-mechanical properties of roller compacted products processed at different feed screw speed (FSS) and roller speed (RS) settings if the ratios were kept constant; therefore, for the current study we choose to investigate the influence of different FSS:RS ratios. Granules were produced at roll pressures (RP) of 80 and 140 bars, FSS: RS ratio(s) of 5:1 (FSS - 35 rpm, RS - 7 rpm) and 7:1 (FSS - 49 rpm, RS - 7 rpm) and granulator speed of 25 and 50 rpm. Ribbons were fed through the attached granulator and milled in two stages (coarse and fine) using screen size 10 and 16, respectively. The lubricant was combined with a portion of the previously prepared mix and passed by hand through a 20-mesh wire screen. This mix was then added to the same twin-shell blender with the remaining powder blend (27.5 gm) and mixed for additional 2 min. Tablets were made on a Stokes® B2 rotary tablet press (Warminster, PA) rotating at 30 rpm and equipped with force transducers to monitor compression force.

2.3.3 Granule Characterization

Granule size was measured by laser diffraction using the Malvern Mastersizer X/S (Malvern Inc., Worcestershire, UK) and the Fraunhofer model analysis routine. The dry powder feeder was operated at an air pressure of 20 psi, a feed rate setting of 2.5 (arbitrary instrument setting) and a sample size of 5 gm. The average D[4,3] particle size of 3 replicates was reported. The bulk density (Db) of a powder blend and the roller

compacted granules were determined using USP method <616>, Method II. Tapped density (Dt) was determined using JEL Stampf® Volumeter Model STAV 2003 (Ludwigshafen, Germany) in accordance with USP method <616>. Due to material limitations tapped density were not replicated. Carr's compressibility Index (CI) was determined using the formula equation 2.1.(10) A lower CI% value (< 20) is generally an indication of good flow:(10)

$$CI\% = \left(\frac{Dt - Db}{Dt}\right) * 100 \qquad \text{Equation: 2.1}$$

2.3.4 Tablet Characterization

Dissolution studies were done using USP Apparatus II, model SR8Plus (Hanson Research; Chatsworth, CA). In accordance with the USP monograph for ciprofloxacin HCl, the dissolution was carried out in 900 mL of 0.01 N HCl at 37 ± 0.5 ^{o}C and the paddles were operated at 50 rpm. Samples were collected at regular time intervals of 10, 20, 30, 45 and 60 min using an autosampler, Autoplus Maximizer and further diluted with 0.01 N HCl using Autoplus™ Multifill™ (Hanson Research; Chatsworth, CA). The amount of Ciprofloxacin HCl released was measured using UV-Visible spectroscopy (Pharmaspec UV-1700, Shimadzu) at 276 nm wavelengths. Disintegration testing was performed using a basket-rack assembly, in accordance with USP method <701>. Water was used as media and the temperature was maintained 37 ± 0.5^{o}C. Six tablets were tested and the time to for each tablet to pass through the wire mesh was recorded. Tablet crushing force was determined using hardness tester (Model HT-300) manufactured by

Key International, Inc. (Englishtown, NJ) and average value of 6 tablets were reported. In accordance with USP method <476>, friability test was performed using Vankel Inc. (Cary, NC) friability apparatus (Model 45-1000) on whole tablets corresponding to a total of 6.5 gm.

2.3.5 Statistical Methods

For the Half-normal plots, if the responses fall in line with the expected values from a normal distribution, then the effect was considered insignificant. Conversely, if a responses fall out of line with the expected values the effect was considered significant. To confirm the normal plots, *t*-tests and Pareto charts were generated using Design Expert® (version 8.0.4; Stat-Ease, Inc., Minneapolis, MN); a significant threshold of $p < 0.05$ was used. The Pareto charts help to visualize the relative size of each effect.

2.4 Results and Discussion

The following sections describe the application of risk tools for the identification of the critical quality attributes. The analysis includes defining the target product profile, followed by qualitative risk assessment using FMEA, and finally a PB DOE will be used to quantitatively identify the main effects, i.e., principal CQAs.

2.4.1 Quality Target Product Profile of Ciprofloxacin

As discussed above, the Quality Target Product Profile (QTPP) describes the design criteria for the product, and should therefore form the basis for determining the CQAs, critical process parameters (CPPs), and Control Strategy. The first step is to define the QTPP, i.e., decide what you want the product to do, the type of dosage form and manufacturing method. The desired QTPP depends upon scientific and nonscientific considerations. For example, a scientific consideration might be determining if the drug is moisture labile and can withstand being wet granulated and dried at elevated temperatures. A nonscientific consideration might be the specification of a specific branded appearance of a dosage form or route of administration by the marketing department. Ciprofloxacin HCl was chosen for this study in part because most of the issues with the QTPP have been previously determined. Thus, other than describing our QTPP, the steps to define the QTPP are not discuss; however, when working with a new drug the importance of these steps cannot be over emphasized, as they guide all the critical decisions in the drug development process.

Ciprofloxacin HCl belongs to Biological Classification System (BCS) Class II (poorly soluble and highly permeable), the API is a monohydrochloride monohydrate salt of 1-cyclopropyl-6-fluoro-1, 4-dihydro-4-oxo-7-(1-piperazinyl)-3-quinolinecarboxylic acid, which is a broad spectrum antibiotic. It is amphoteric with pKa values of 6.2 and 8.59 at 37^0C,(11) and its solubility is pH dependent with high solubility at pHs below 5 (10-30 mg/ml in water) and at pHs above 10. Ciprofloxacin has low solubility at neutral

pH of 7.5 (0.07 mg/ml in phosphate buffer).(12) For this study, 200 mg ciprofloxacin HCl, immediate release tablet formulation for oral dosing was chosen as a model product. A list of the key QTPP, which generally follows the USP monograph for the ciprofloxacin tablets are given in Table 2-1, and it is these parameters that will be the focus of this study. Obviously, other factors such as stability are important, but we will limit our discussion to these key factors.

2.4.2 CQAs Identification using a Quality Risk Management Approach

The desired quality attributes defines the objectives for formulation and process design; however, the CQAs are also very dependent upon the type of dosage form, formulation and manufacturing method chosen among many possible and clinically equivalent alternatives. For example, it is possible that if the drug has a good stability profile, then wet granulation and dry granulation via roller compaction could produce equivalent granules for an immediate release tablet, but the CQA could be very different for the two processes.

Table 2-1.Tablet quality target product profile (QTPP) of Ciprofloxacin tablets.

Critical Quality Attribute	Values
Potency & Assay	200 mg range 90 to 110%
Friability	< 1.0%
Tablet weight and content uniformity	400 $\pm$ 10 (mg)
Tablet crushing force	10-20 (kp)
Disintegration time	< 10 min
Dissolution Rate	Not less than 80% released in 30 min

Thus, before beginning to identify the CQAs, some feasibility studies need to be performed to determine the dosage form type, lead formulation and unit operations that make up the manufacturing process. Unfortunately, for solid oral dosage forms there are no first principle models that can be used to design a dosage form *a priory*. Consequently, formulation and process development typically rely on empirical prior knowledge and small scale feasibility studies and empirical statistical studies.

To develop a formulation, preformulation studies that included API solubility as a function of pH, particle size analysis, thermal and flow characterization of the API and excipients were carried out. In addition, early development work examined API suitability for tablet compaction and roller compaction. The preformulation studies demonstrated that the drug was very stable, that flow and consequently content uniformity were poor and achieving the desired drug release rate would be the biggest

formulation challenges. To address the problem of powder flow dry granulation using slugging and roller compaction were tested and found to significantly improve powder flow. The Carr index of the formulation was significantly lowered from 33.98% before roller compaction to 24.85% and 20.34% after roller compaction for roll pressures of 40 and 80 bars, respectively, indicating the suitability of roller compaction. To achieve the desired release rate, formulations consisting of varying levels of Klucel® JF (7-9%) and Starch 1500® (2-5%) were granulated and compressed at varying compression forces (8, 12, and 16 kN). These studies showed that the Klucel® levels, disintegrant levels, roll pressure, and compression force are important factors influencing the disintegration time and dissolution rate. These studied led us to identify the base formulation and processing conditions, see Table 2-2. As mentioned above, the compatibility and stability studies showed the drug to be very stable in our formulation, so the issues of stability won't be addressed further, but obviously this is a critical issue.

Based upon the preformulation and feasibility studies, we defined the following formulation and manufacturing method for 400 mg immediate release tablets containing200 mg ciprofloxacin. Each tablet contains the following excipients: Avicel® PH 102 (filler), Klucel® EXF (binder), Starch 1500® (disintegrant) and Magnesium Stearate (lubricant). 50% of the disintegrant and lubricant amount was added extragranularly prior to tableting. The manufacturing process involves blending, roller compaction of the blend with microcrystalline cellulose, magnesium stearate and pregelatinized starch, followed by the addition of extragranular portion (magnesium state

and pregelatinized starch) second blending with magnesium stearate, which was followed by compression on a rotary tablet press.

Table 2-2. Base formulation and processing conditions used for PB-DOE studies. The feed screw speed (FFS) to roller speed (RP) ratio was used as the independent variable; the table shows the individual values that make up the ratio.

Excipient	**Amount (wt%)**
Ciprofloxacin (intra granular)	50
MCC (intra granular)	37
Starch 1500 (intra granular)	5
HPC (intra granular)	2
Mg Stearate (intra granular)	0.5
Starch 1500 (extra granular)	5
Mg Stearate (extra granular)	0.5
Processing Conditions	**Parameter Value**
Blending time 1: Intragranular blend i.e. API + excipients other than magnesium stearate	5 min
Blending time 1: Intragranular blend i.e. lubricant blend (magnesium stearate)	2 min
Roll pressure	80 bar
Feed screw speed (FSS/RP ratio = 5)	20 rpm
Roll speed (FSS/RP ratio = 5)	4 rpm
Blending time 3 – Extragranular blend: granules + extragranular excipient fraction	2 min
Compression force	12 kN

2.4.3 Qualitative Risk Analysis of CQAs

The Failure Mode and Effect Analysis (FMEA) method was used to perform the qualitative risk assessment, which could identify the CQAs that have the greatest chance of causing product failure, i.e. not meeting the QTPP.(13) The first step in the risk assessment was to systematically gather up all the possible factors that could influence product quality.(14) To identify these factors we reviewed the literature, our past experiences,(15, 16) and data collected during the initial formulation development studies described above. These factors were organized hierarchically using an Ishikawa or "fishbone" diagram, see Figure 2-2.(17) The parameters outlined in the Ishikawa chart aided in the identification of the failure modes (i.e., the ways or modes by which a system, process step or piece of equipment might fail). FMEA are also used to describe the effects or consequences of specific failure modes. Using FMEA, the modes of failure can be prioritized for risk management purposes according to the seriousness of their consequences (effects), how frequently they occur and how easily they can be detected. From this information, the variables (CQAs) that need to be further studied and controlled can be identified. Another important aspect of FMEA, especially for larger organizations, is that the process of doing the analysis facilitates systematically gathering the current knowledge within the organization, and with a knowledge management system, it allows the information on risk to be stored for future use. This is important for companies in which turnover results in the loss of institutional memory.(6)

The outcome of an FMEA is a risk priority numbers (RPN) for each combination of failure mode severity, occurrence probability and likelihood of detection, which can be used to rank the risk. FMEA defines the RPN as:

$$RPN = \begin{bmatrix} 5 \\ 4 \\ 3 \\ 2 \\ 1 \end{bmatrix} O \times \begin{bmatrix} 5 \\ 4 \\ 3 \\ 2 \\ 1 \end{bmatrix} S \times \begin{bmatrix} 1 \\ 2 \\ 3 \\ 4 \\ 5 \end{bmatrix} D \qquad \text{Equation: 2.2}$$

Where *O* is the occurrence probability or the likelihood of an event occurring; we ranked these 5 likely to occur, 3, 50:50 chance of occurring and 1 as unlikely to occur. The next parameter *S,* the severity, which is a measure of how severe of an effect a given failure mode would cause; we ranked these 5 severe effect, 3 moderate effect and 1 no effect. The final parameter D is the detectability or the ease that a failure mode can be detected, because the more detectible a failure mode is the less risk it presents to product quality. For D we ranked 1 as easily detectable, 3, as moderately detectable and 5 as hard to detect. Using this procedure, we created the ranking shown in Table 2-3.

In the present study, the greatest RPNs were used to identify the parameters that pose the most risk to product quality, and thus needed to be studied in more detail. Table 2-3, is a partial listing of the factors considered when doing the FMEA. To begin the FMEA we broke the failure modes down into those coming from the formulation or raw material inputs and those coming from the process. The process failure modes were

further broken down by unit operations; which were blending intragranular ingredients, roller compaction, blending extragranular ingredients and compression.(15,16)

Changes to humidity leading to variability in product moisture content were considered to be lower risk because all the development work was conducted under GMP conditions and previous compatibility studies to assess the kinetic and equilibrium moisture content of the drug substance, excipients and formulation blends) demonstrated that there was no significant impact on the product quality attributes under relative humidity of 40 to 75% RH. In addition, variables that could affect *in vivo* performance have generally been scored high, while variables that are naturally controlled such as humidity, tooling shape) were scored lower. This difference in scoring is linked to both the detectability and severity associated with each failure effect. For those failure effects that could have an impact on processing and product physical quality, detectability was high, occurring either during the unit operation, or finished product testing.

The initial quality risk assessment has allowed the highest risks to be identified. The highest risks have been identified as those associated with changes to the input raw materials (changes in API particle size, change to magnesium stearate source and change to the level of disintegrant:binder level) and process parameters for the roller compaction (roller pressure, ratio between roller speed:feed screw speed, and compression force) .

2.4.4 Quantitative CQA Identification using Plackett-Burman Study Design

Based on the FMEA rankings see Table 2-3, the following potential CQAs were identified for further study: the API and filler-binder particle size, degree of starch gelatinization, viscosity and particle size of the hydroxypropyl cellulose and source of the lubricant. Similarly, the key processing variables to be studied were roll pressure, roll speed to feed screw speed ratio (FSS:RS), granulator speed (also called a Chilsonator® style mill that grinds the ribbon flakes into granules), lubricant blending time and tablet compression force were selected for further investigation. Using statistical methods like a full factorial design would require 2^{11} (or 2048) experiments. Clearly, at the early stages of development when there is only a preliminary lead formulation, a full factorial designs may not be an optimal use of resources due to the large number of experiments and the scarcity of API. At this stage, the goal is to identify the CQAs for which future development efforts can be focused based upon the risk associated with each parameter. Thus, we chose the PB experimental design, which is a widely used screening designs for the identification of "main factors" that cause variability in product quality.(5,18) The advantage of the PB design is that many factors can be screened with a relatively few number of trials. The disadvantage of these designs is that interactions between variables are generally confounded and cannot be easily determined, as there aren't enough degrees of freedom. Also, unless treatments are replicated variability cannot be evaluated. While these are significant limitations, when a large number of studies would be needed to implement higher resolution factorial designs, the PB can be a pragmatic solution.(19)

Table 2-3. Summary of FMEA analysis, where, Severity (S) of excursion S=1 (low) 5 (high), probability of occurrence (O) of the excursion =1 (low), 5 (high), Detection (D) of excursion D= 1(easy), 5 (hard) and Risk priority number (RPN)=SxOxD.

Unit OP	Failure Mode	Impact of Change	S	Potential Cause or Route of Failure	O	Detection or Control Method	D	RPN
Blending	Blending Time	CU	5	Poor monitoring	1	NIR	1	5
	Fill Level	CU	5	Operator's error	2	NIR	1	10
	Blender Speed	CU	5	operator's error, equipment failure	3	NIR	1	15
	Humidity	CU	3	poor air handling	1	NIR/Hygrometer	1	3
RC	Roll Speed	Poor granule quality	5	Machine failure, poor development	3	Carr Index, particle size	4	60
	Feed Screw Speed	Granule uniformity	5	Machine failure, poor development	3	HPLC/NIR	4	60
	Roll Pressure	Particle Size, hardness	5	Machine failure, poor development	5	Malvern/ Hardness tester	5	125
	Mill Speed	Particle Size, hardness	5	Machine failure, poor development	3	Malvern	4	60
	Roller Texture	Ribbon density	1	Machine failure, poor development	1	Carr index	1	1
Tableting	Humidity	CU and hardness	3	poor air handling	3	Hygrometer	3	27
	Compression force	Hardness, dissolution	5	Poor granulations	5	Disintegration, Dissolution, Hardness tester	4	100
	Compression speed	CU	3	operator's error, equipment failure	3	NIR/HPLC	3	27
	Tooling Shape	CU, tablet weight	1	operator's error, equipment failure	1	NIR/HPLC	3	3
Raw Materials	Level	Dissolution, hardness	5	operator error, poor development	5	Disintegration, Dissolution, Hardness tester	5	125
	Vendor grade differences	Dissolution, hardness	4	Poor development, operator error	5	Disintegration, Dissolution, Hardness tester	4	80
	Different Sources	Physical properties	4	Physical variation	3	Visual Inspection	3	36
	Particle size	CU, dissolution, hardness	5	Material variation	3	Malvern/ Hardness tester	4	60
	1-29 Low risk	**30-59 Medium Risk**		**60-125 High Risk**				

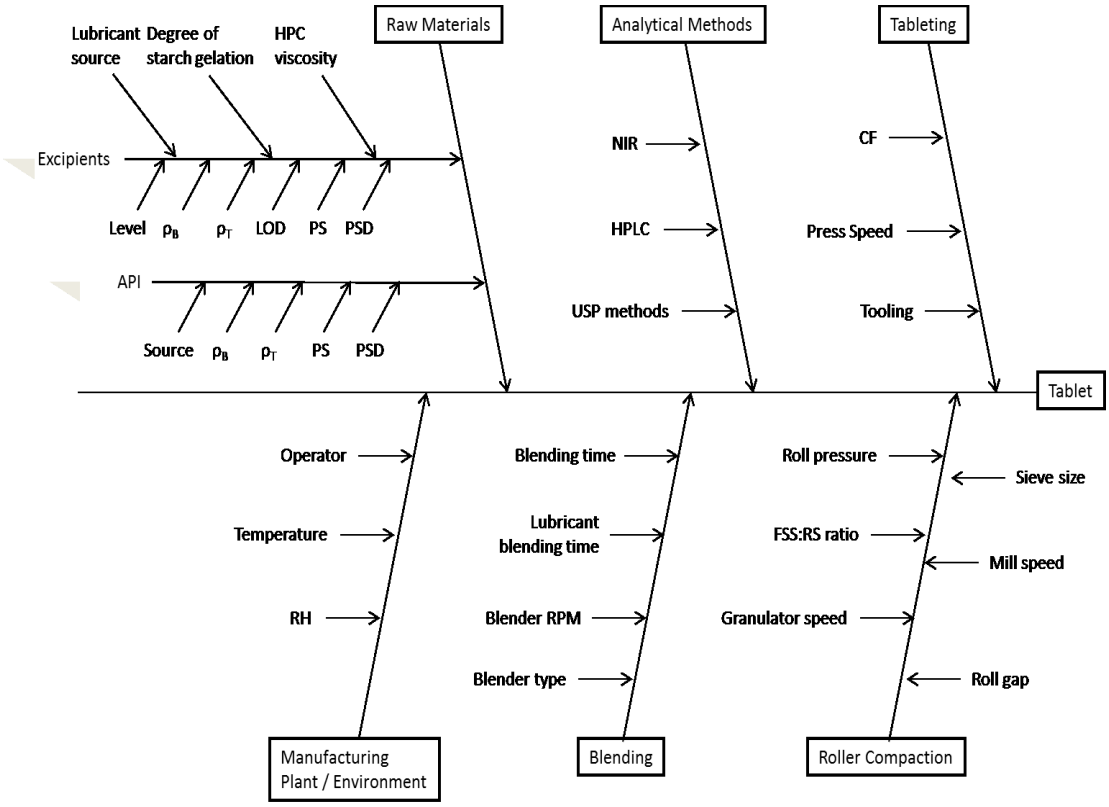

Figure 2-2. Ishikawa fish bone diagram for tablet production via roller compaction.

For the PB designs, the number of factors to be evaluated is up to one less than the number of runs or trials in the study. These designs do not exist for all the possible number of runs. The original paper published 8, 12, 16, 20, 24 … 96 and 100 runs. Thus, it is possible to study 7 factors in 8 runs, 11 factors in 12 runs or even 99 factors in 100 runs.(5) To analyze the results, the study data are plotted against the expected values of a set of samples taken from a distribution of the absolute value of X ($|X|$) where X is distributed normally. The effect of factor X_i is calculated using:

$$\text{Estimate of effect } X_i = \sum \bar{Y}(+1) - \sum \bar{Y}(-1) \qquad \text{Equation: 2.3}$$

where Y is the response of an experiment, the bar indicates average value. The effect of X_i was calculated for each of the variables studied and plotted using a half normal plot.(5, 18) The fit of these plots was used to determine significance of an effect; with half-normal plot the non-significant effects tend to fall on a straight line through the origin, while significant effects deviate from this line.(20)

For the PB-DOE, eleven formulation and processing parameters were chosen based upon the FMEA analysis, see above, and for each of the 11 variables two treatment levels were identified, see Table 2-4. The levels were determined by a combination of prior experience (15,16) and the preliminary formulation studies in which we did small scale experiments to determine the range of formulation and processing parameters. Once the study variables and their levels have been chosen, the variables were randomly assigned to the 12 experiments of the PB DOE grid, see Table 2-5.(5,18) The first column shows the assignments 11 variables from Table 2-4 for the 12 experiments; the following

columns show the + or - treatments. The quality attributes of the tablet that were measured included: weight variation (WV), tablet crushing force (CF), disintegration time (DT) and dissolution time (Q30). In addition, important granules properties such as granule size (X) and Carr index (%CI) were studied to better identify the CQAS important to the blending and granulation stages of manufacturing. The formulations were processed to produce granules and tablets using the conditions given in Table 4 and 5, and characterized for their properties (CQAs). The results given in Table 6 are broken into the granule properties and the final tablet properties.

2.4.5 Granule Particle Size

Variability in the formulation and roller compaction process resulted in granules in the size range of 154.9 to 274.5 μm (Table 2-6). The Half-normal probability plots, see Figure 3a, calculated from the particle size data shown in Table 2-6 show that the Mg stearate type and roller pressure have a significant influence on granule particle size. The calculation of the t-values, see Figure 2-3b, confirmed that both parameters are significant. Thus, for the systems studied the substitution of the vegetable grade Mg stearate with the animal grade resulted in increase in the particle size of the granules. Increase in roll pressure from 80 to 140 bars increase the granule size.

Table 2-4. Eleven factors studied in the Plackett-Burman DOE, and the associated treatment levels.

Factor	Level(+1)	Level (-1)
X1 (A) - Level of disintegrant gelatinization (categorical)	Partially gelatinized - Starch 1500	Fully gelatinized – Spress® B825
X2 (B) - Tablet compression force (Pmax) (numerical)	12 kN	16 kN
X3 (C)- Speed of granulator after roller compaction (numerical)	50 rpm	25 rpm
X4 (D)- Roll pressure (dry granulation) (numerical)	80bar	140 bar
X5 (E)- API particle size (categorical)	Cipro Unsieved (d(0.5)=15.47μ)	Cipro Sieved (d(0.5)=8.87μ)
X6 (F)- Source/supplier of lubricant (categorical)	Vegetable source – Covidien	Animal source - Spectrum
X7 (G) - Filler particle size (numerical)	Avicel PH 102 (90μ)	Avicel PH 101 (50μ)
X8 (H)- Binder grade (Hydroxypropyl cellulose) (categorical)	Low viscosity and small particle size - Klucel® EXF	Medium viscosity and larger particle size Klucel® JF
X9(J) - Ratio of roll speed to feed screw speed (numerical)	Ratio = 5 (35/7)	Ratio = 7 (49/7)
X10(K) - Blending time (API/excipient blend + lubricant blend + extragranular blend) (numerical)	5 + 2 + 2 minutes	20 + 2 + 2 minutes
X11(L) - Glidant level (numerical)	No Aerosil (0%)	Aerosil (0.25%)

Although no difference in the physical properties such as particle size, bulk density, tapped density and compressibility index was observed between the animal and plant sources of Mg stearate they differ in fatty acid composition and surface area. It was reported that lubrication efficiency was different for tablets. Ejection forces were reported to be lower for tablets consisting of vegetable grade compared to animal grade during slugging experiments.(21) It was also reported that Mg stearate has been known to affect ribbon density and mechanical strength,(22) and it is the ribbon strength that affects the particle size of the granules when the ribbon is milled into granules.

Increase in roll pressure from 80 to 140 bars increase the granule size. Generally, increasing the compression force on the material in the nip zone results in a higher degree of consolidation. The higher consolidation, which results from more bounding between particles and higher density, produces a ribbon with a higher tensile strength, and when these ribbons are milled they retain a relatively larger size compared to the ribbons produced at lower roll pressure. This type of behavior is commonly observed, see Dave *et al*. for example.(15,16)

2.4.6 Granule Carr's Index

The Carr index of the granules produced in the DOE, Table 2-5, ranged from 17.1 to 23.8, see Table 2-6. According to Carr's classification,(10) these values range from excellent to poor flow properties. The Half-normal probability plots showed that the addition of the glidant Aerosil®.

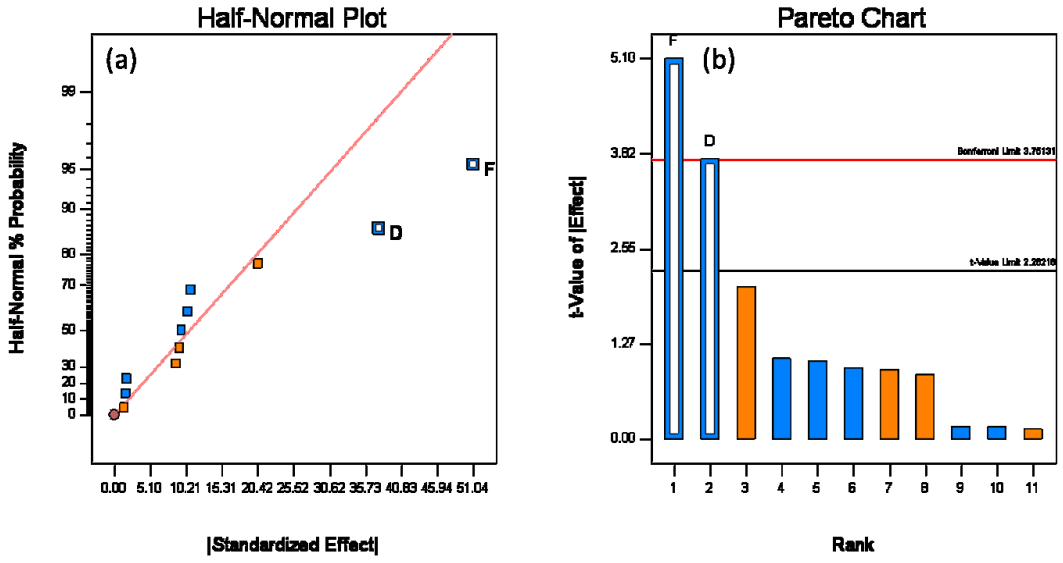

Figure 2-3. Half-normal probability (a) and Pareto plots (b) for granule particle size. Roll pressure (D) and lubricant source (F) were found to be significant.

The statistical tests see Figure 2-4b, show that the Aerosil® was significant and that roller pressure was not quite significant. The Carr index values were positively correlated, i.e. without Aerosil incorporation; the Carr index values were significantly higher, which is an indication of poor flow. The incorporation of Aerosil® (0.25% w/w) decreased the Carr index, which can be attributed to the glidant properties of silica.

Similarly, roll pressure had a positive effect, which means that at the lower roll pressure of 80 bars the Carr index was higher. This result coincides with the previous observation where roll pressure play a critical role in the granule size and increase in roll pressure increases the granule size and thereby improving the flow characteristics. While statistical analysis shows that the roll pressure effect was not significant, it is still an important factor that needs to be controlled as it affects important properties such as flow and content uniformity.

2.4.7 Tablet Weight Variation

As shown in Table 2-6, the tablet weight (Wt.) varied around a target weight of 400 mg, and the tablet weight variation as measured by the RSD% ranged from 0.6% to 2.1%. This narrow range, which meets the QTPP, was seen for all 12 experimental runs; these results show that roller compaction significantly improves powder flow. Recalling that the ciprofloxacin has a Carr Index of ~48, see Table 2-6, which is characteristic of materials that have poor flow. These results are consistent with our preliminary studies that found direct compression formulations couldn't meet weight or content uniformity

requirements. The effect of each variable shown in Table 2-4 was calculated, rank ordered and plotted in a half-normal probability plot.(5, 18, 20) Visual inspection of the Wt. RSD% in Figure 2-5a, indicates that the ciprofloxacin particle size

Table 2-5. Twelve experiment design grid used to investigate 11 variables

	Pattern	***X*1**	***X*2**	***X*3**	***X*4**	***X*5**	***X*6**	***X*7**	***X*8**	***X*9**	***X*10**	***X*11**
1	++++++++++++	1	1	1	1	1	1	1	1	1	1	1
2	-+-+++---+-	-1	1	-1	1	1	1	-1	-1	-1	1	-1
3	--+-+++---+	-1	-1	1	-1	1	1	1	-1	-1	-1	1
4	+--+-+++---	1	-1	-1	1	-1	1	1	1	-1	-1	-1
5	-+--+-+++--	-1	1	-1	-1	1	-1	1	1	1	-1	-1
6	--+--+-+++-	-1	-1	1	-1	-1	1	-1	1	1	1	-1
7	---+--+-+++	-1	-1	-1	1	-1	-1	1	-1	1	1	1
8	+---+--+-++	1	-1	-1	-1	1	-1	-1	1	-1	1	1
9	++---+--+-+	1	1	-1	-1	-1	1	-1	-1	1	-1	1
10	+++---+--+-	1	1	1	-1	-1	-1	1	-1	-1	1	-1
11	-+++---+--+	-1	1	1	1	-1	-1	-1	1	-1	-1	1
12	+-+++---+--	1	-1	1	1	1	-1	-1	-1	1	-1	-1

may lie outside of the distribution; however, when the t value (Figure 2-5b) for the effects was calculated, this had a *t*-value < 2.22. Therefore, for these formulations and processing conditions none of the 11 variable significantly affected the Wt. RSD%.

2.4.8 Tablet Crushing Force

The tablet crushing force ranged from 9.1 to 18.6 kiloponds (kp) with the variability in the formulation and process variables, see Table 2-4 and 2-6. For these 12 experiments, only one run was outside of the QTPP. The effect of each variable tested in Table 4 was assessed by plotting the observed values on a half-normal % probability plot, see Figure 6a; this graph shows that two parameters had a significant effect on crushing force, and they were roller pressure and tablet compression force. The visual observations were confirmed by *t*-test (Figure 2-6b) which also showed these parameters had statistically significant effects on crushing force. The raw data showed that roll pressure has a positive effect on the tablet crushing force, indicating a decrease in tablet hardness with increase in roll pressure. This can be explained by the "loss of compressibility" of the microcrystalline cellulose (Avicel®) at higher roll pressures resulting in decreased tablet hardness on subsequent compaction on the tablet press. This phenomena has been is well known for microcrystalline cellulose undergoing roller compaction, see Sun *et al*.(23,24) The increase in tablet crushing force with compression force (Pmax) can be explained by the higher degree of compaction resulting in a tablet with higher tensile strength and a correspondingly higher tablet crushing force; these findings are consistent with numerous studied reported in the literature. (15,16)

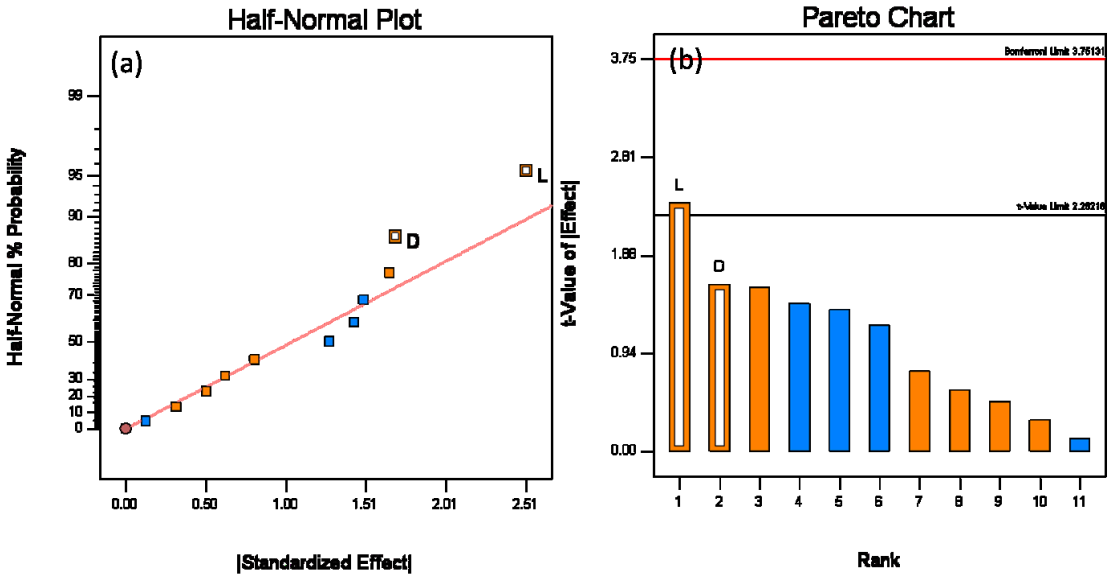

Figure 2-4. Half-normal probability (a) and Pareto plots (b) for Carr's Index (%). Glidant addition (L) was found to be significant.

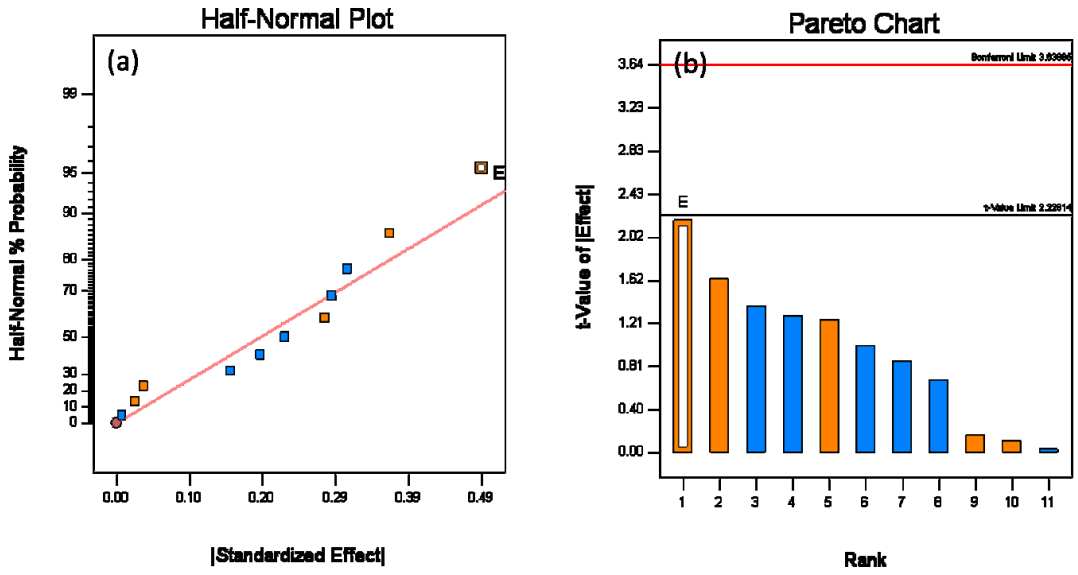

Figure 2-5. Half-normal (a) and Pareto plots (b) of rank ordered coefficient of critical quality attributes for weight variation RSD%.

Table 2-6. Granule and tablet properties – Note, due to material limitations the tapped density was not replicated, hence there is no standard deviation for Dt and the CI. For all of the formulations tested, the friability values were less than 1%, so this data was omitted from the table.

	Granule Properties						Tablet Properties		
S.no	X (μm)± SD	Db (gm/cc)‡	Dt (gm/cc)	CI (%)	Wt (mg)	Wt RSD (%)	CF (kp) ± SD	DT (min) ± SD	Q30 (%) ±SD
API	15.5 ± 3.8	0.23	0.45	48.4	NA	NA	NA	NA	NA
F1	183.5 ± 5.6	0.59	0.76	22.4	406.5	1.1	13.4 ± 0.6	**15.0 ± 2.2**	**63 ± 14.7**
F2	154.9 ± 6.2	0.60	0.76	22.0	401.8	0.7	14.2 ± 0.9	1.0 ± 0.0	99 ± 2.2
F3	202.6 ± 10.5	0.62	0.77	19.7	402.7	2.1	11.3 ± 1.0	4.0 ± 0.0	93 ± 7.9
F4	190.1 ± 6.0	0.59	0.75	21.9	398.7	0.8	18.6 ± 0.5	**52.8 ± 2.0**	**46 ± 10.3**
F5	265.4 ± 11.1	0.64	0.78	17.4	407.8	1.6	10.7 ± 0.9	**37.5 ± 4.3**	**57 ± 14.3**
F6	252.1 ± 14.2	0.69	0.83	17.1	401.2	0.6	11.3 ± 0.3	**51.3 ± 4.8**	**37 ± 5.2**
F7	225.3 ± 7.0	0.60	0.75	20.0	395.3	1.0	15.0 ± 0.2	2.0 ± 0.0	98 ± 7.8
F8	274.5 ± 9.4	0.62	0.81	23.8	403.0	1.0	14.8 ± 0.7	**40.0 ± 3.0**	**70 ± 11.1**
F9	213.6 ± 5.5	0.61	0.79	22.7	401.2	0.8	**9.1 ± 0.5**	2.0 ± 0.0	98 ± 6.0
F10	254.5 ± 10.3	0.64	0.77	17.6	394.2	1.3	10.0 ± 0.5	2.2 ± 0.4	95 ± 5.8
F11	245.6 ± 10.9	0.59	0.76	22.2	403.0	0.8	12.9 ± 0.7	**14.8 ± 6.9**	96 ± 14.5
F12	237.8 ± 16.9	0.62	0.77	19.9	394.7	1.7	18.2 ± 1.0	2.3 ± 0.5	98 ± 3.4

‡ All standard deviations were SD<0.012

X - particle size, Db - bulk density, Dt - tapped density, CI –Carr's index, Wt±weight variation RSD (i.e., 100x standard deviation / average), CF - crushing force, DT - disintegration time, Q30 - amount released in dissolution media at 30 mins RSD, NA – not applicable

2.4.9 Tablet Disintegration and Dissolution

For the 12 experiments, the disintegration time varied from 1 minute to 53 minutes, and the amount that dissolved in 30 minutes (Q30) ranged from 37% to ~ 100%, see Table 6. The dissolution graphs are shown in Figure 2-7. These results show the formulation and processing conditions can significantly affect product quality, as six runs failed disintegration and five runs failed dissolution. Based upon rank order, the data show that disintegration and Q30 dissolution are highly correlated; as five of six experiments that failed disintegration also failed dissolution, see Table 2-6. The half normal probability plots show that for disintegration, HPC grade and compression force significantly affected disintegration, and the *t*-test showed that HPC grade was highly significant, compression force was slightly significant, see Figure 2-8a and 2-8b. For Q30 dissolution, the normal probability plots showed that, HPC grade was highly significant, which was confirmed by the *t*-test, see Figure 2-9a and 2-9b.

Examination of the data in Figure 2-8 and Table 2-6 show that disintegration is the most important factor controlling dissolution. For the samples that passed dissolution, the average disintegration time was 4.1 ± 4.2 min and for the samples that failed dissolution the average disintegration time was 39.0 ± 12.4 min. These results match our empirical observation of dissolution; all the tablets that had rapid release quickly disintegrated in the dissolution apparatus, and all the tablets that had slow release remained intact in the dissolution media. The two grades of Klucel® used in the study

differ in three properties. Klucel® JF has higher molecular weight, viscosity and particle size than Klucel® EXF. The EXF grade produced much slower release; thus, differences in the molecular weight, viscosity, particle size, and wetting characteristics in the tablet matrix governed tablet disintegration time which drastically slowed dissolution for Klucel® EXF compared to JF. This is illustrated in Figure 2-7 where all the formulation containing EXF have closed symbols, and of these only one met the release specification.

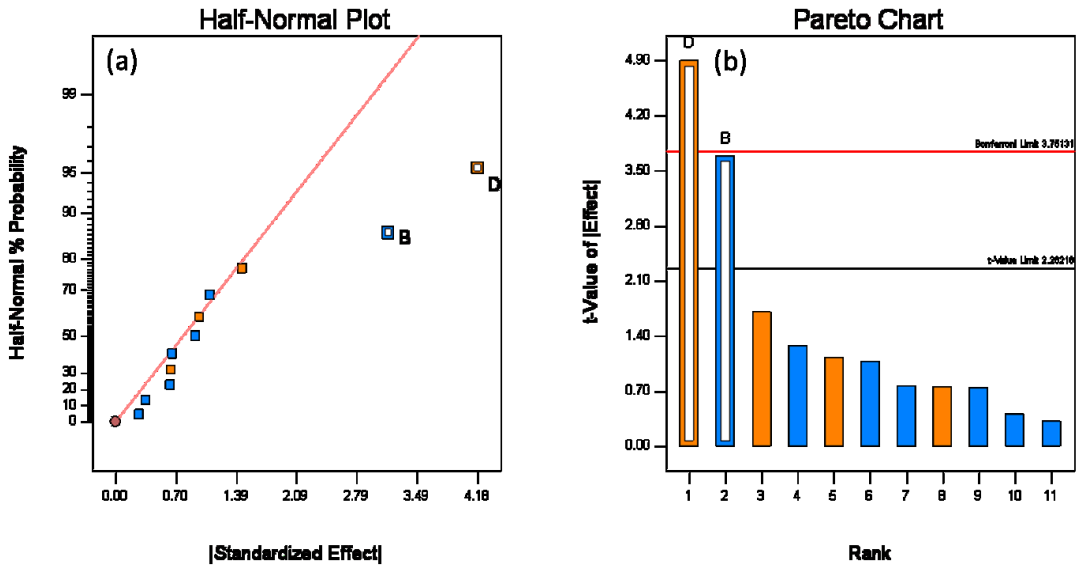

Figure 2-6. Half-normal (a) and Pareto plots (b) of rank ordered coefficient of critical quality attributes for tablet crushing force. Compression force (B) and roll pressure (D) were found to be significant.

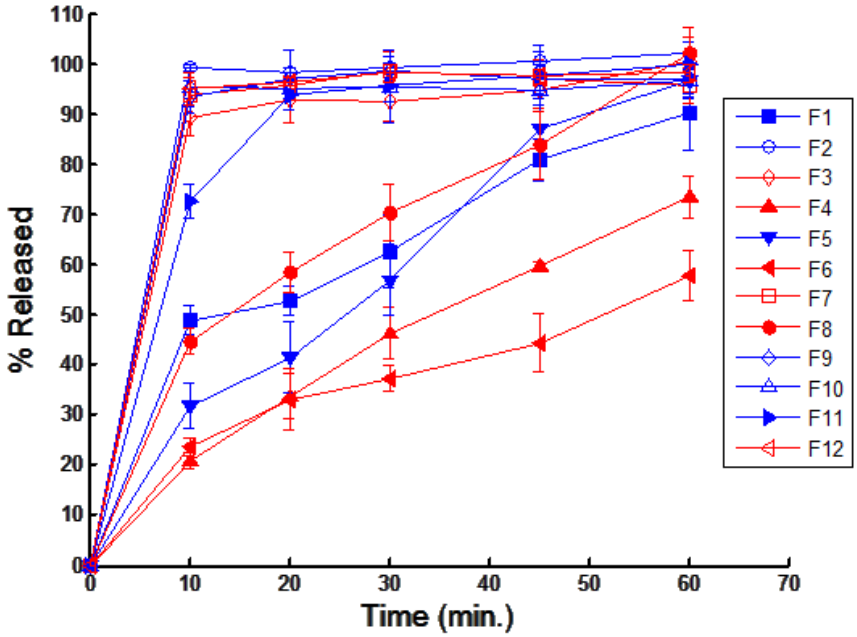

Figure 2-7. Dissolution profiles for the 12 experimental runs. The closed symbols correspond to the HPC EXF (+1 in PB), open symbols correspond to the HPC JF (-1 in PB), the red lines correspond to 16 kN Pmax (-1 in PB) and the blue lines correspond to 12 kN Pmax.

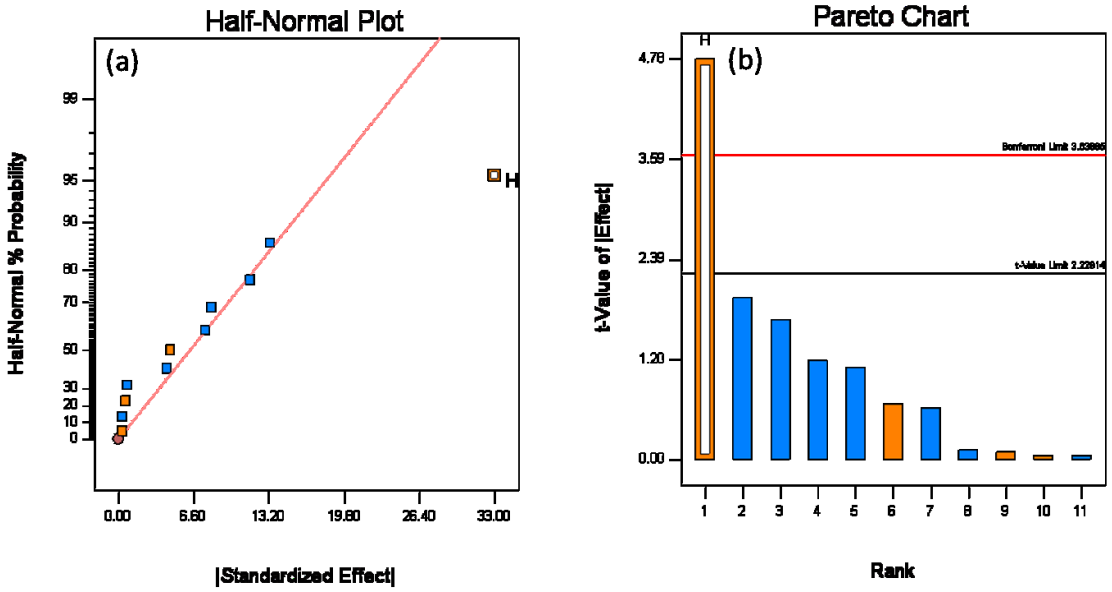

Figure 2-8. Half-normal (a) and Pareto plots (b) for disintegration time. Binder grade (H) was found to be significant.

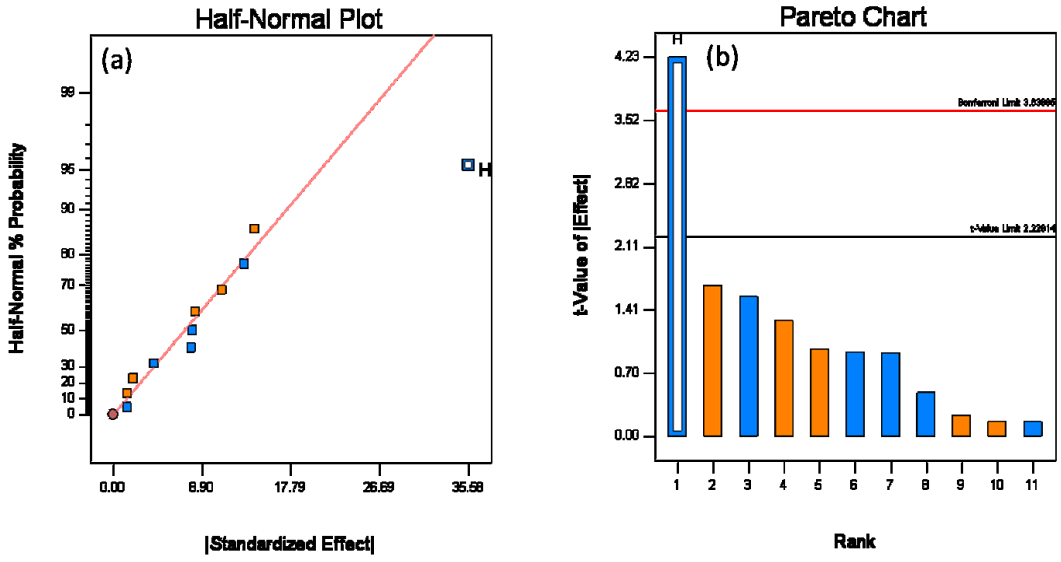

Figure 2-9. Half-normal (a) and Pareto plots (b) for Q30 dissolution. Binder grade (H) was found to be significant.

The raw data showed that increasing compression force was also found to be positively correlated to disintegration time, see Table 2-6. At higher compression forces, there is a greater volume reduction during tableting resulting in denser tablet matrixes that hold the tablet together more tightly, and reduce water uptake properties, which results in longer disintegration times. Similar results have been observed by Massimo *et al*.(25)

2.5 Conclusions

Starting with literally 100s of possible CQAs that could affect product quality, see Figure 2-2, preliminary feasibility studies and FMEA were used to reduce the number of possible attributes down to 11 factors, see Table 2-2. Then a PB screening design was

used to determine the significant main effects among these 11 factors with only 12 experiments, which compared to a full fractional designs that would have 2^{11} i.e. 2048 experiments. The granule properties (particle size, bulk density, tapped density and Carr index) and the tablets (weight variation, crushing force, disintegration time and dissolution time) were evaluated to identify which of the 11 factors affected tablet quality.

It was found that compression force and roller pressure were the most important parameters affecting tablet crushing force. Klucel® grade and Pmax were the most critical factors governing cipro release, i.e., disintegration and Q30 dissolution. In terms of granule properties (particle size, bulk density and Carr index), roller pressure is critical affecting both particle size and the Carr Index. Mg stearate type and glidant level also affected particle size and the Carr index, respectively. These results are consistent with observations made during initial feasibility studies. Thus, these parameters and their interactions warrant further study using higher resolution statistical designs. On the other hand, weight variation was not influenced by the formulation and process variables studied. In addition, several factors such as granulator speed, roll speed to feed screw speed (RS:FSS), microcrystalline cellulose particle size and mixing time (5min vs 20 min lubricant mixing) did not influence the QTPP, and can be assigned to a lower risk category requiring less scrutiny.

In summary, scientific rationale and quality risk management analysis were used to successfully and efficiently determine the CQAs coming from the formulations and the manufacturing processes.

Chapter 3 Application of Near-Infrared Spectroscopy to monitor roller compaction in-process and product quality attributes in formulation development of immediate release tablets

3.1 Abstract

The objective of this study is to use Near-Infrared Spectroscopy (NIRS) as Process Analytical Technology (PAT) tool to develop multivariate chemometric models to monitor granule and tablet quality attributes in the formulation development and manufacturing of a Ciprofloxacin hydrochloride (CIP) immediate release tablets. Critical process variables such as roll pressure (RC), compression force (CF) and formulation variables such as binder and disintegrant source identified from our earlier studies were evaluated in more detail. Multivariate principle component analysis (PCA) and partial least square (PLS) models were developed during the development stage and used as a control tool to predict the quality of granules and tablets. Validated models were used to predict the batches manufactures at different manufacturing sites to assess their robustness to change.

The results showed that RP and CF played a critical role in the quality of the granules and tablets within the range tested. Replacing binder source did not statistically influence the quality attributes of the granules and tablets. Whereas replacing lubricant type significantly impacted the granule size. Blend uniformity, crushing force,

disintegration time during the manufacturing was predicted using validated PLS regression models with acceptable standard error of prediction (SEP) values, whereas the models resulted in higher SEP for batches obtained from different manufacturing site. From this study we were able to identify critical factors which could impact the quality attributes of the CIP IR tablets. In summary, we demonstrated the ability of near-infrared spectroscopy coupled with chemometric as a powerful tool to monitor Critical Quality Attributes (CQA) identified during formulation development.

3.2 Introduction

Recently, dry granulation using roller compaction (RC) has grown in popularity, as the process is economical, energy efficient, continuous, easily automated and suitable for drugs that are sensitive to heat and moisture.(29) In roller compaction, the powder blend is compressed and compacted between two counter rotating rollers resulting in ribbon which when milled produces granules of desired size. Despite its apparent simplicity, it is quite challenging to understand the influence of RC process variables on the critical quality attributes (CQA) of a dosage form. Process parameters such as roll pressure (RP), feed screw speed (FSS) and roll speed (RP) were known to be critical and could impact process feasibility, compaction properties of the ribbons, and the tabletability of granules.(29) It is know that increasing in the FSS (at constant roll speed and roll gap) leads to the densification of the ribbon resulting in caking of material there by interrupting the flow of the powder between the rollers. Operating at low FSS could results in poor quality ribbon with low density due to insufficient powder at the nip zone region. Roll speed was found to influence the dwell time of the powder, this is critical for a plastically deforming materials such as microcrystalline cellulose where low roll speeds increase the dwell time and result in loss of compactability leading to tablets with lower hardness and friability.(34,36) In case of materials that exhibit significant elastic recovery, higher roll speed may lead to cracking, resulting in poor quality ribbon due to a shorter dwell time.(37,38) Higher roll pressure on the other hand was found to increases the density of the ribbon and in turn produces tablets with higher crushing force and low

friability.(30,35) Roller surfaces (smooth vs knurled) were shown to influence the bulk and tapped densities of the granules.(95)

In addition to process variability, material properties such as morphology and the particles size of excipients were found to influence the ribbon quality, granule size distribution, content uniformity, flowability and the compaction properties of the resulting tablets.(30) Therefore, it is critical to identify all the sources of variability arising both from process and input materials and develop a reliable and well understood process that will consistently ensure a pre-defined quality at the end of the manufacturing process. A process is considered well understood when all the sources of variability are identified, monitored and controlled through proper designing and analyzing critical in-process and material attributes that influence the quality of a dosage form.(17) To establish process control, it is critical to describe and justify how in-process controls and the controls of input materials (drug substance and excipients), intermediates (in-process materials), and drug products contribute to the final product quality. The primary goal of establishing control strategy is to shift controls upstream and minimize the need for end point quality testing (ICH Q8).(5)

Conventional method of quality testing of pharmaceutical products often involves sampling the product in a batch process and performing laboratory tests. Today, with the availability of newer technologies, significant opportunities exist in pharmaceutical industry in the area of product development, manufacturing, and quality testing of the products for real time quality testing. This shift in the process control philosophy from a

conventional end phase testing to a continuous, or nearly so, in-line systems of quality testing was primarily aimed to build quality in to the system their by avoiding the lag time associated with the off-line techniques. One such tool that is available is Near-Infrared Spectroscopy (NIRS). The advantage of NIR over other spectroscopy tools is it is rapid and nondestructive with minimal sample preparation.(17,19,96,97) In the last decade there are several articles published on the use of NIRS as PAT tool in roller compaction. Gupta *et al*, used slope of best-fit line through the near-infrared spectrum to quantify the strength of compacts using three point beam bending.(44) They also demonstrated the use of NIRS real-time to determine compact strength, tensile strength, young's modulus and particle size during roller compaction.(45) Although there are several article on application on application NIRS using roller compaction, little attention was paid on material attributes such as excipient grades and source variability on the final quality, which are critical in formulation development under Quality-by-Design (QbD) paradigm. To our knowledge, there is limited availability of literature where risk factors were systematically identified and monitored using NIRS that could potentially impact target product profiles (TPP).

Our current series of papers were aimed to address these issues. Figure 3-1 show the central steps employed in this project as outlined in the ICH guidance Q8(R2), Q9, and Q10.(5-7) In our previous studies, we examined steps 1, 2, and 3, which are defining Target Product Profiles and Identify Critical Quality Attributes (CQA)(98). These steps are associated with the guidance Q8(R2).(5) To establish TPP and determine CQAs, qualitative risk was performed using Failure Mode Effect Analysis (FMEA) followed by

Plackett-Bruman design of experiment (DOE). In these studies, RP played a critical role in granule size and Carr's index. Compressions force (Pmax) and RP was found to influence the tablet crushing force. In addition, Hydroxypropyl cellulose (HPC) grade (Klucel® EXF vs Klucel® JF) and RP were found to be critical for CIP drug release (i.e. disintegration and dissolution). However, factors that were found to be insignificant were ranked as low risk and were eliminated from further evaluation. In the subsequent paper we have examined the use of quantitative risk models to assess the risk and define the design space using approaches outlined in ICH Q10.(7) This is third in the series and the objective of this paper is to study critical factors identified from our earlier studies in details and in addition integrate NIR spectroscopy coupled with multivariate chemometric models (PCA and PLS) to monitor critical roller compaction in-process and product quality attributes that were identified from our earlier studies for process understanding and establish process control. The first part of this paper focuses on the characterization of the granules and tablets obtained at various processing parameters. Here critical formulation variables such as binder source and lubricant type that were identified from previous studies were further evaluated. HPC–Klucel® EXF and HPC-L binder grades were selected based on the previous studies performed by Desai *et al*. It was reported that, both HPC grades meet the NF criteria and exhibit no significant differences in the average molecular weight; but they were found to influence the dissolution rate of hydrochlorothiazide.(99) For lubricants, Mg stearate monohydrate (MgSt-M) and dihyrate (MgSt-D) forms were evaluated. Studied have shown that MgSt-D and MgSt-M forms of magnesium not only differ in the physical and chemical

properties but also influenced the release characteristics of the drug.(100,101) The second part of this paper focuses on developing multivariate chemometric models to quantify granules size and develop PLS calibration models to predict CQA's such as tablet crushing force and disintegration times. The third part of this paper focuses on application of validated model to external batches manufacture at different locations. In this study, Ciprofloxacin hydrochloride monohydrate was used as a model drug which belongs to Biological Classification System (BCS) Class II (poor soluble and high permeable).(102)

3.3 Materials and Methods

3.3.1 Materials

Ciprofloxacin hydrochloride monohydrate (Lot # CI06026) was obtained from R.J. Chemicals, Coral Springs, FL (Quinica Sintetica, Madrid, Spain). Microcrystalline Cellulose, Avicel® 102 (Lots # P208820014 and P209820744) was donated by FMC Biopolymer (Newark, DE), Hydroxypropyl Cellulose (HPC), Klucel® EFX (Lots # 99768 and 99769) was generously gifted by Hercules Incorporation (Hopewell, VA) and HPC-L (Lot # NHG-5111) was obtained from Nisso America Inc (New York, NY). Starch 1500® (Lots # IN502268 and IN515968) was generously donated by Colorcon (Indianapolis, IN). Magnesium stearate monohydrate (Lot # MO5676) and magnesium stearate dihydrate (Lot # JO3970) was obtained from Covidien (Hazelwood, MO).

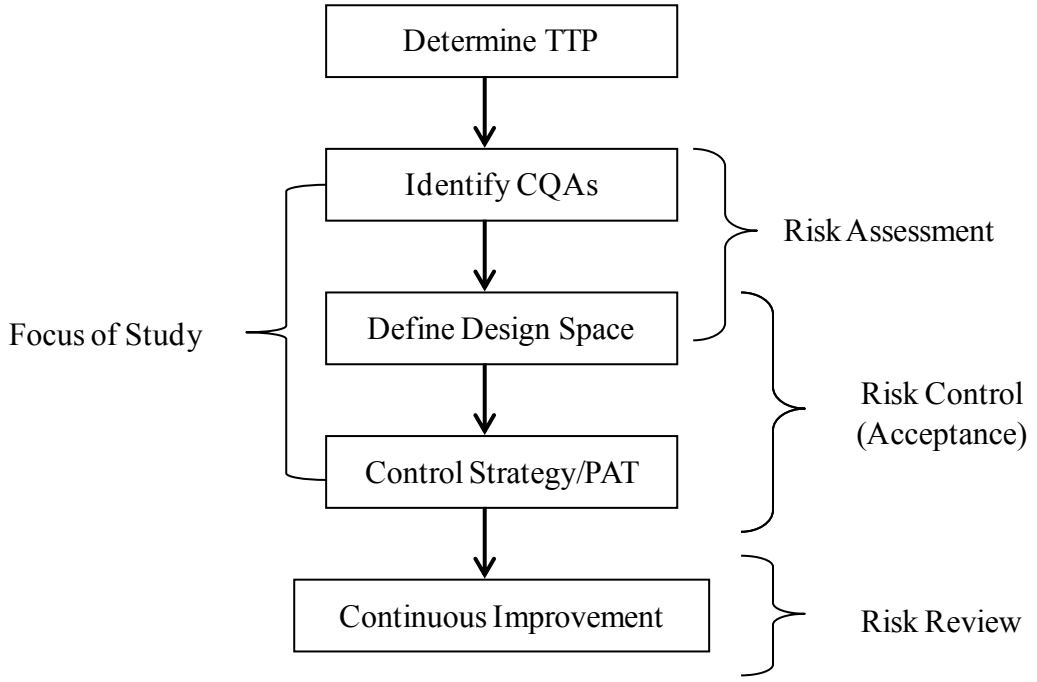

Figure 3-1. QbD drug product development flow chart showing principal steps and focus of this study.

3.3.2 Design of Experiments

Table 3-1 shows the base CIP formulation used in this study; the formulation development and the identification of the CQA is described in our previous study.(98) Table 3-2 shows the factors studied and the design employed. Two binder types, hydroxypropyl cellulose (Klucel® EFX and Nisso®-L) and two lubricant types, Magnesium stearate (MgSt-M and MgSt-D) are the formulation variables evaluated. Three roll pressures (20, 80, and 140 bar) and three compression force (8, 12, and 16 kN) were studied as processing parameters. In addition, binder and disintegrant levels were evaluated leading to total of 42 different lots. Batches 15 – 25 were manufactured at different site from batches 1 – 14, from now on batches 15-25 will be referred to as

manufacturing site 2 batches. At sight 2 roller compaction was carried out on an identical model roller compactor, granulation was carried out at the same RP, FSS/RP ratios, binder, and disintegrant levels as site 1, see Table 3-2, batches 15 - 25.

Table 3-1. Base formulation for CIP immediate release tablets.

Intra granular portion	**(%) w/w**
CIP	50
Microcrystalline cellulose (Avicel® 102)	37
Hydroxypropyl cellulose	2
Starch® 1500	5
Magnesium stearate	0.5
Extra granular portion	**(%) w/w**
Starch® 1500	5
Magnesium stearate	0.5
Total	100

Table 3-2. Formulation and process variables studied for CIP immediate release formulation development and for NIR calibration model development, and a summary of granule and tablet properties.

Batch*	RP	FSS: RP	HPC	MgSt	EFX (%) w/w	Starch (%) w/w	Avg vol* (X μ) ± Std.Dev	Span (X μ) ± Std.Dev	CF** (kp) ± Std.Dev	DT*** (min)±Std.Dev
1	20	5	+	+	2	10	98.9 ± 13.4	6.6 ± 2.9	15.5 ± 0.5	4.0 ± 0.9
2	80	5	+	+	2	10	160.7 ± 9.3	7.1 ± 2.2	9.3 ± 0.5	8.5 ± 1.4
3	140	5	+	+	2	10	183.5 ± 2.3	5.3 ± 0.5	6.8 ± 0.6	13.2 ± 2.5
4	20	5	-	+	2	10	89.1 ± 10	6.8 ± 1.9	15.3 ± 0.6	3.5 ± 0.5
5	80	5	-	+	2	10	161.5 ± 6.8	5.6 ± 0.9	9.7 ± 0.8	8.0 ± 2.2
6	140	5	-	+	2	10	193.4 ± 9.6	4.4 ± 0.7	6.6 ± 0.6	15.5 ± 1.9
7	20	5	-	-	2	10	90.2 ± 5.0	5.0 ± 0.8	16.5 ± 1.0	3.5 ± 0.8
8	80	5	-	-	2	10	173.7 ± 3.4	4.9 ± 0.1	9.0 ± 0.6	7.7 ± 1.0
9	140	5	-	-	2	10	210.9 ± 5.2	3.9 ± 0.4	6.8 ± 0.8	11.7 ± 2.5
10	20	5	+	-	2	10	95.5 ± 3.5	4.8 ± 0.1	14.6 ± 1.3	3.2 ± 0.4
11	80	5	+	-	2	10	179.8 ± 8.4	4.6 ± 0.1	10.5 ± 0.8	7.7 ± 1.6
12	140	5	+	-	2	10	231.7 ± 5.7	3.5 ± 0.2	7.2 ± 0.8	16.3 ± 0.7
13	80	5	+	+	4	10	149.0 ± 9.4	5.5 ± 0.4	9.1 ± 0.9	28.0 ± 7.5
14	80	5	+	+	4	14	151.3 ± 14.4	5.7 ± 1.9	9.1 ± 1.0	21.7 ± 0.8
15	80	5	+	+	2	10	147.9 ± 7.2	18.3 ± 5.5	4.0 ± 0.8	7.7 ± 4.5
16	80	7	+	+	2	10	254.0 ± 18.4	3.4 ± 0.3	3.3 ± 0.6	4.7 ± 1.2
17	80	3	+	-	2	10	152.8 ± 4.2	6.8 ± 1.0	6.3 ± 0.8	1.0 ± 0
18	140	7	+	-	2	10	298.4 ± 26.6	2.8 ± 0.3	2.2 ± 0.4	6.3 ± 2.9
19	140	5	+	-	2	10	333.9 ± 29.9	2.3 ± 0.3	3.6 ± 0.3	4.3 ± 1.2
20	140	5	+	+	2	10	140.0 ± 13.6	16.5 ± 6.0	3.7 ± 0.6	2.7 ± 0.6
21	140	3	+	+	2	10	263.0 ± 33.3	3.9 ± 0.3	5.3 ± 0.6	2.7 ± 0.6
22	80	5	+	+	4	10	154.6 ± 26.4	18.6 ± 10.8	5.5 ± 0.7	21.0 ± 6.2
23	80	5	+	+	4	10	154.6 ± 26.4	18.6 ± 10.8	6.5 ± 0.7	36.3 ± 6.7
24	80	5	-	+	6	8	157.3 ± 29.0	12.7 ± 7.0	5.0 ± 1.4	45.7 ± 7.2
25	80	5	-	-	3	10	251.5 ± 8.2	4.0 ± 0.4	4.6 ± 0.4	42.0 ± 4.4

HPC source, Klucel® EXF (+) and Nisso-L (-); Magnesium stearate type, MgSt-M (+) and MgSt-D (-); Average volume D(4,3), and span which is the width of the distribution as described by 10%, 50%, and 90% quantiles and are average of 3 runs; Crushing force (CF) and disintegration time (DT) are average of 6 tablets; batches 1-14 were compressed at 8, 12, and 16 kN force leading to 42 batches. Batches 15-25 are all compressed at 12 kN except for batch 23 compressed at 16 kN.

* Average of 3 runs, **Average of 6 tablets, ***Average of 5 tablets

3.3.3 NIR Measurements and Spectral Analysis

A Rapid Content Analyzer (RCA) DS 6500 spectrometer (FOSS NIRsystems, Inc., Laurel, MD) was used to scan the samples from 400-2500 nm and the final spectrum was the average of 32 scans**.** The powder blends and granules were scanned in glass scintillation vials, the tablets were scanned directly without any container; all samples were scanned in diffuse reflectance mode. The NIR models were developed using Vision® version 3.2 software. PCA score plots were obtained from Matlab 7.0.4 (The MathWorks Inc. Natick, MA) with PLS Toolbox 3.0 software (Eigenvector Research, Inc., Manson, WA). To compare the laboratory data and model predictions a paired *t*-test was performed and p values < 0.05 were considered significant. ANOVA was performed to study the influence of both formulation and processing variables on the characteristics of granules and tablets. Table 3-3 is the summary of regression coefficients (Q) and probability (p) of the responses studied. The sign for coefficients indicate the direction of the relationship where a positive sign indicate direct and a negative sign indicates inverse relationship.

3.3.4 Granule Production via Roller Compaction

Figure 3-2 illustrates the flow chart for the manufacture of CIP immediate release tablets using roller compaction. Physical mixtures of CIP, Avicel® 102, Klucel® EFX, Starch 1500® and MgSt were mixed in a 16 qt V-blender (Patterson Kelly, Co, East Stroudsburg, PA) without intensifier bar rotating at 30 rpm. The blends were compacted on a roller

compactor (Alexanderwrek® W120, Horsham, PA) equipped with rollers (25 mm diameter) having a knurled surface. The processing parameters are described in Table 3-2. For all batches the mill impeller speed was maintained at 50 rpm. The ribbons were milled in two stages (coarse and fine) using mesh size 10 and 16, respectively. The extragranular portion which consists of Starch 1500® and Magnesium stearate was added and mixed with the roller compacted granules; this blend was mixed in the same V-blender for an additional 3 min. Approximately 2 gm samples were collected before and after RC for the NIR scans, see next section for details. For site 2, same model RC fitted with identical rollers, fine, and coarse mesh was used to manufacture granules. For processing conditions, refer Table 3-2 (batches 15 – 25).

3.3.5 Blend Uniformity Study

Prior to granulation, blend uniformity was assessed for all lots using NIR and a PLS model. The blend uniformity calibration model was build using 27 off-line calibration samples comprising 9 different concentrations of ciprofloxacin ranging from 45% to 61%, see Table 3-4. The CIP concentration was adjusted with microcrystalline cellulose (MCC). The samples were prepared by weighing appropriate quantities in a vial and blending in a Turbula® mixer (Glen Mills Inc. Clifton, NJ) for 7 min. The samples were later transferred into borosilicate glass scintillation vials with screw cap (VWR®, model # 66021646) for NIR scanning. To assess blend uniformity, samples were collected from three different regions (Figure 3-3) of the V-blender using powder sampling thief (Model # 5200, Conbar, Monroeville, NJ) and the blend uniformity model was used to determine

the uniformity of subsequent formulation blends. The methods for CIP concentration determination are described below.

Table 3-3. Summary of regression coefficient for granules and tablets for batches 1-14.

Variables	Granule size (μ)		CF (kp)		DT (min)		Q(30)	
Responses	*Q*	*P*	*Q*	*P*	*Q*	*P*	*Q*	*P*
Intercept	183.7	-	7.44	-	17.08	-	84.65	-
(A) RP	27.6	< 1E-03	-2.03	< 1E-03	2.11	< 1E-03	-0.90	0.45
(B) CF	-	-	2.26	< 1E-03	7.15	< 1E-03	-3.73	0.10
(C) Binder level	-0.58	0.89	-0.87	0.02	9.22	< 1E-03	-11.08	0.01
(D) Disintegrant level	1.17	0.82	0.09	0.85	-3.62	0.02	3.82	0.42
(E) Binder source	-2.30	0.29	6.02E-04	1.00	-0.71	0.24	-0.92	0.64
(F) Lubricant type	-7.59	0.00	-0.23	0.23	-0.38	0.52	-2.34	0.23

Q: coefficients

P: probability

Table 3-4. Component and compositions used for blend uniformity study. Formulation 5 represent main batch.

	Amount (%) w/w								
Ingredients	1	2	3	4	5	6	7	8	9
Ciprofloxacin HCl	45	48	50	52	53	54	55	58	61
MCC (Avicel® 102)	47	44	42	41	39	37	36	34	31
Hydroxypropyl cellulose	2	2	2	2	2	2	2	2	2
Starch® 1500	5	5	5	5	5	5	5	5	5
Magnesium stearate	1	1	1	1	1	1	1	1	1

Table 3-5. NIR spectroscopy and HPLC results for testing the accuracy.

	Accuracy		
Blends	NIR (%) w/w	HPLC (%) w/w	Residual
1	53.20	49.93	3.27
2	54.79	52.29	2.50
3	52.56	51.46	1.10
4	53.28	52.65	0.63
5	53.54	50.72	2.82
6	52.66	51.49	1.17
7	53.02	51.64	1.38
8	52.75	51.01	1.74
9	51.49	52.49	-1.00
10	53.73	53.18	0.55
11	54.00	52.15	1.85
12	51.72	51.22	0.50
13	52.46	51.91	0.55
14	53.10	52.96	0.14
15	47.62	50.30	-2.68
16	49.84	52.80	-2.96
17	49.20	51.30	-2.10
18	48.21	51.30	-3.09
19	51.06	51.60	-0.54
20	49.52	53.50	-3.98
21	49.58	51.10	-1.52
22	49.64	50.90	-1.26
23	49.43	48.50	0.93
Avg	51.58	51.58	0.00
Std.Dev	2.04	1.14	2.01
t-test	0.49		

3.3.6 Ciprofloxacin HCl Assay

The amount of CIP was analyzed using High Performance Liquid Chromatography (HPLC). Mobile phase consists of 0.025 M phosphoric acid (adjusted to pH 3.0 ± 0.1 with triethylamine): acetonitrile (87: 13 v/v). For tablet analysis the tablets were crushed and diluted in mobile phase to a concentration of 0.2 mg/mL. The solution was sonicated

for 20 min and filtered through Millex® 0.45 µm (Millipore, MA, US) membrane filter. Then 10 µl of this solution (0.2 mg/mL mobile phase) was injected into HPLC (Waters® Corporation, Milford, MA) at a flow rate 1.5 mL/min and the amount of CIP was determined at 278 nm. For dissolution studies, the samples collected were filtered using 0.45 syringe filters and injected in to chromatographic system and the amount of CIP was analyzed as described above.

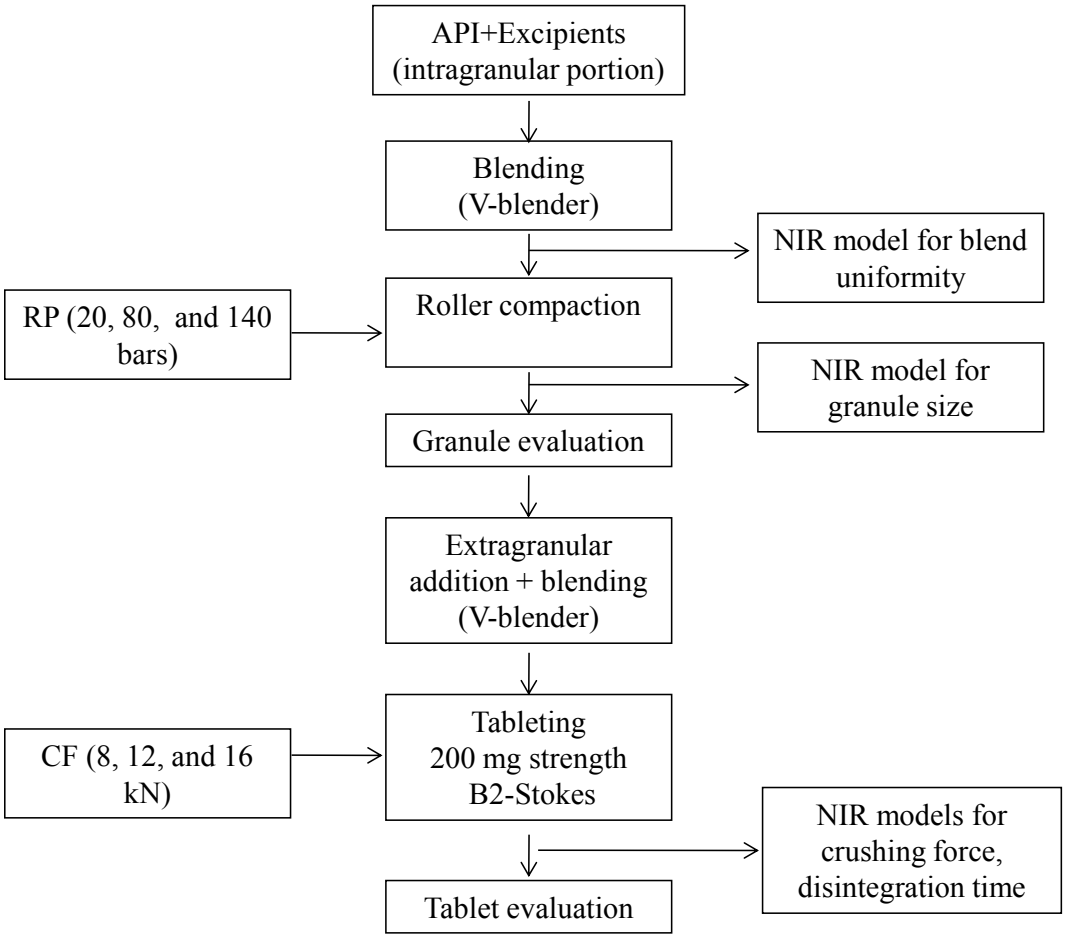

Figure 3-2. Process flow chart for Ciprofloxacin hydrochloride immediate release tablets.

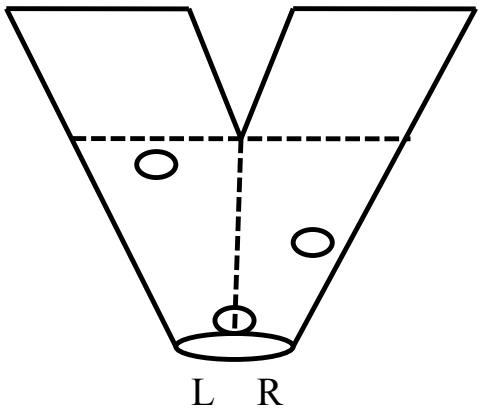

Figure 3-3. V-blender showing sampling locations.

3.3.7 Tablet Manufacturing

The blends were compressed into 200 mg strength CIP tablets fitted with 11.11 mm (7/16 in.) biconcave tooling on an instrumented Stoke B2 rotary press (Key Industries, NJ) rotating at 30 rpm. The compression force was monitored using an instrumented eye bolt connected to a 4 channel isolation amplifier (NI-SCXI-1121) and signal conditioning chassis (NI-SCXI-1000) manufactured by National Instruments Corporation (Austin, TX). Signals were monitored using a Labview software (version 8.20) data acquisition system. An identical rotary press using the same processing conditions was employed to manufacture tablets from the granules obtained from second manufacturing site.

3.3.8 Characterization of Granules and Tablets

The granules were characterized for granule size (X), bulk density (Db), tapped density (Dt) and Carr's index (CI %). Tablets were characterized for breaking force (BF), disintegration time (DT), weight variation (Wt) and dissolution (Q30). Particle size was measured by laser diffraction method using Malvern® Mastersizer (Malvern Inc., Worcestershire, UK). The dry powder feeder was operated at air pressure of 20 psi at a constant feed rate of 2.5 and samples size of 5 gm. The reported mean granule size D[4,3] and span $(D_{90}-D_{10})/D_{50}$ are the average of three runs. Bulk densities (Db) were determined on a Sargent-Welch (VWR® Scientific Products) and tapped densities (Dt) was determined using JEL Stampf® Volumeter Model STAV 2003 (Ludwigshafen, Germany) both according to USP 26 general chapter <616>. *In-Vitro* dissolution studies

were evaluated using USP method II. The dissolution media consists of 0.01N HCl and the paddles were operated at 50 rpm and the temperature was maintained at 37 ± 0.5°C. The concentration of CIP was measured using UV-Visible spectroscopy model Spectronic® Genesis™, (Thermo Scientific, Pittsburgh, PA) at 276 nm wavelength. Tolerance limits are NTL 80% released in 30 min. Disintegration was performed used basket-rack assembly (USP 26 general chapter <701>). Water was used as media and the temperature was maintained 37 ± 0.5°C. Six tablets were used and time to completely disintegrate was recorded.

3.3.9 NIR Multivariate Calibration Model Development

For the development of calibration model the number of samples required depends on the complexity of the matrix. An appropriate preprocessing method was applied to help improve model fit. Samples selection was performed to detect spectral outliers and redundant samples based on Mahalanobis distance in the principal component space, which relates the distance of a spectrum from the center of the center of a distribution of spectrum. A variety of math pretreatments such as Baseline correction (BC), Savitzky-Golay (SG) 2nd derivative (order 2, window: 15), Normalization (NM) (1-Norm, Area = 1), Standard Normal Variate (SNV) were tried to improve model fit. For this study, appropriate pretreatments were selected based on the method that yielded lowest statistical errors (SEC and SECV).

3.4 Results and Discussion

3.4.1 Granule Properties

The summary of the granule and tablets characteristics are presented in Table 3-2. Batches 1-14 were manufactured at site 1 and batches 15-25 were manufactured site 2. Granules obtained from site 1 were compressed at three CF, 8, 12, and 16 kN resulting in 42 lots. Granules from site 2 were all compressed at 12 kN, except for batch 23, which was compressed at 16 kN resulting in 11 lots.

A first order regression model was developed using batches 1-14, for each of the granule and tablet quality attributes studied in the form shown below.

$$Y_i = b_0 + b_1 A + b_2 B + b_3 C \ldots\ldots + b_6 F \qquad \text{Equation: 3.1}$$

Y_i, response (X, CF, DT, or Q30); b_0, intercept; b_1, regression coefficient; A, linear effect of RP; B, linear effect of CF; C, linear effect of binder level; D, linear effect of disintegrant level; E, linear effect of binder source; F, linear effect of lubricant type.

Regression analysis (Table 3-3) indicates that roll pressure had a significant influence ($p = 0.0001$) on the granule size followed by the type of lubricant used ($p = 0.0011$). Increasing roll pressure from 20 to 140 bars increased the average volume granule size of the granules; this was accompanied by the decrease in relative span (spread of granule size distribution). It is well known that increasing in roll pressure produces ribbons with higher tensile strength due to higher degree of material

consolidation in the nip region,(48) when these ribbons were milled the granule size was larger compare to ribbons produced at a lower roll pressure. Granule size increased when MgSt-M was replaced with MgSt-D (Table 3-3). This behavior can be explained by differences in the particle size and surface area of monohydrate and dihydrate form.(103) Batches 1, 12, 3, and 13 from site 1 (Table. 3-2) and 15, 19, 20, and 22 from site 2 have the same formulation composition and were processed under same RP conditions. Data clearly indicates that the granules size obtained at two manufacturing sites were statistically different. The reasons for this behavior are unknown and warrant further investigation which is beyond the scope of this paper.

3.4.2 Tablet Properties

The influence of processing parameters and formulation treatments on the crushing force is presented in Figure 3-4. Increasing the roll pressure at a given compression force decreases the crushing force of the tablets. This can be explained by loss of compactability or work-hardening phenomenon commonly observed with plastic materials such as microcrystalline cellulose. Several authors have reported that this work hardening phenomenon results in a pronounced decreased in tensile strength.(34,36,104)

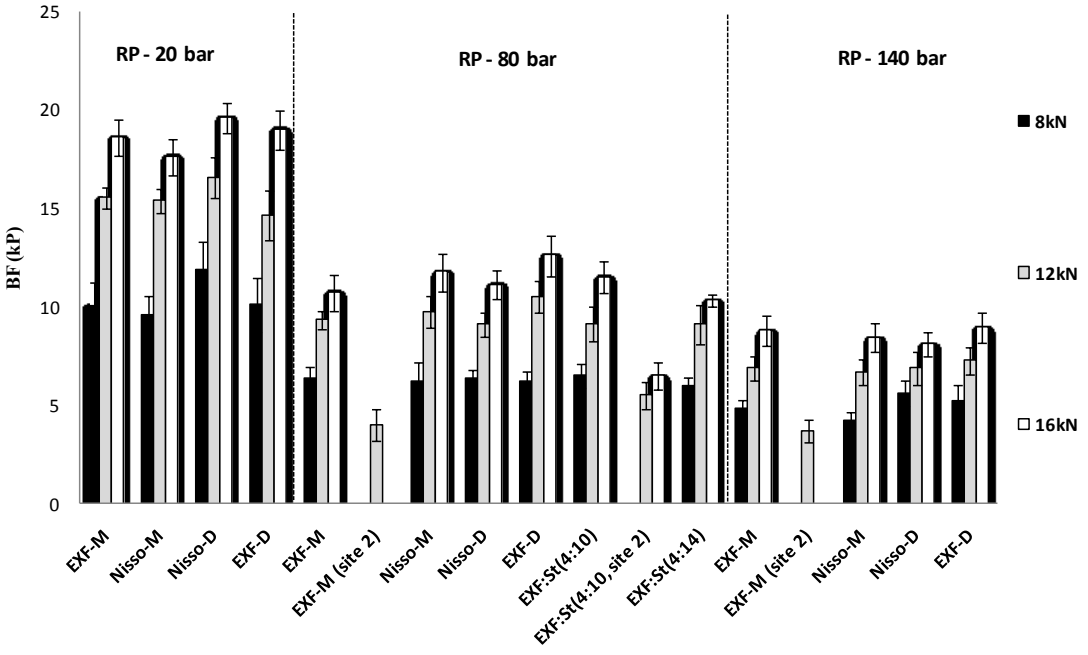

Figure 3-4. Influence of roll pressures and compression force on the crushing force. Batch composition with Klucel EXF and MgSt-M as EXF-M, Nisso-L and MgSt-M as Nisso-M, Nisso-L and MgSt-D as Nisso-D, Klucel EXF and MgSt-D as EXF-D. Batches manufactured at second site are denoted as (site 2). Batches with different binder (EXF) and starch® 1500 levels are presented as EXF-St.

In addition, for a given roll pressure, an increase in compression force increased the breaking force of the tablets. It was also observed that increase in the HPC binder level from 2 to 4 % significantly increase the breaking force of the tablets. To identify significant parameters, linear regression was performed and a $p<0.05$ is considered significant. A summary of regression coefficients and p-values is in table 3-3. For CIP release; roll pressure, compression force, binder levels and disintegrant levels were found to be statistically significant for the disintegration time (Figure 3-5), whereas, the amount of binder used was the only significant factor for CIP release after 30 min (Q30). Factors such as the binder type (Klucel® EFX vs Nisso®-L) ($p = 0.64$) and Magnesium stearate type (MgSt-D vs MgSt-M) ($p = 0.23$) were insignificant for the breaking force and the CIP release profile.

The granules manufactured at site 2 were compressed into tablets using an identical rotary press under same operating conditions. Crushing force (Figure 3-4) and disintegration data (Figure 3-5) were found to be statistically different from the tablets obtained from site 1. This could be explained due their differences in the granules size which influence the compressibility of the material.(36)

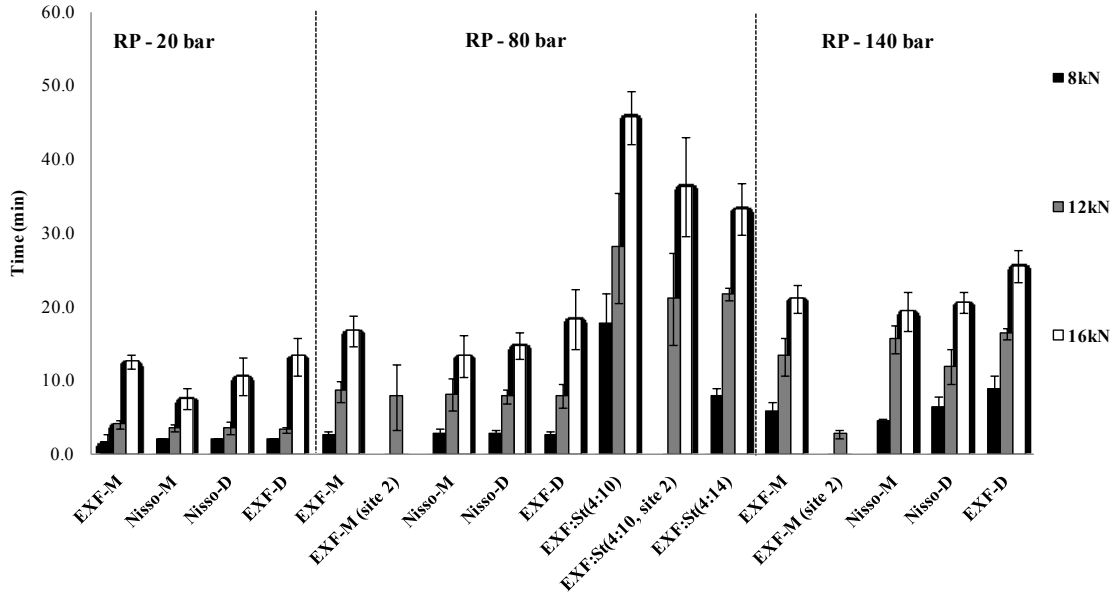

Figure 3-5. Influence of roll pressures and compression force on the disintegration time. Batch composition with Klucel EXF and MgSt-M as EXF-M, Nisso-L and MgSt-M as Nisso-M, Nisso-L and MgSt-D as Nisso-D, Klucel EXF and MgSt-D as EXF-D. Batches manufactured at second site are denoted as (site 2). Batches with different binder (EXF) and starch® 1500 levels are presented as EXF-St.

3.4.3 NIR Feasibility Study

The second derivative overlaid spectra of excipients and neat CIP powder were examined to identify the spectral characteristics of the API (Figure 3-6, panel A). Characteristic peaks were found at 1480, 1504 (CH_2, second overtones), 1604 (Aromatic-CH, first overtone), 1652 (CH, CH_2, first overtones), 1912 (R-COOH, first overtones), 2104 (N-H, combination bands), and 2204 (CH_2, combination band). In this study, spectral region 1600-1700 nm was selected to construct PLS blend uniformity model, where CIP alone

predominates and where there are no overlapping spectral peaks from the excipients. The raw NIR spectra of the granules obtained at different roll pressures (20, 80 and 140 bar) were overlaid and the spectra were analyzed for variations, a non-linear baseline shift was observed and may be due to increase in the density of the granules with higher roll pressure (Figure 3-6, panel B). Similar baseline shift was observed when the raw spectra of the tablets produced at different tablet compression forces (8, 12, and 16 kN) were examined, it was reported that increase in tablet compression force increased the tablet density which affected its absorbance via changes in the diffused reflectance path length (Figure 3-6, panel C).(17,19,96,97) Figure 3-6, panel D is the second derivative overlaid spectra of CIP. As the amount of CIP increases in the blend matrix, the intensity of the peaks increased.

Prior to the calibration model development, PCA was performed on the samples. A total of 54 tablets was selected from nine different lots processed at different RC pressures (20, 80 and 140 bars) and compressed at three different compression force (8, 12 and 16 kN). Mathematical pretreatments like normalization, SG- 2nd derivative and auto-scale were performed. The PCA 3D score plot results (Figure 3-7, panel B) indicate that 3 PC's contained 79.1% of the total variability in the data set (PC1-52.4%, PC2-17.2% and PC3-9.5%). Examination of the score plot and loadings indicated that PC1 correlated with tablet compression force and PC2 explained samples differences due to RP. The sample variation could be explained by differences in the densities arising from increased compression force during tableting and increased roll pressure during RC.

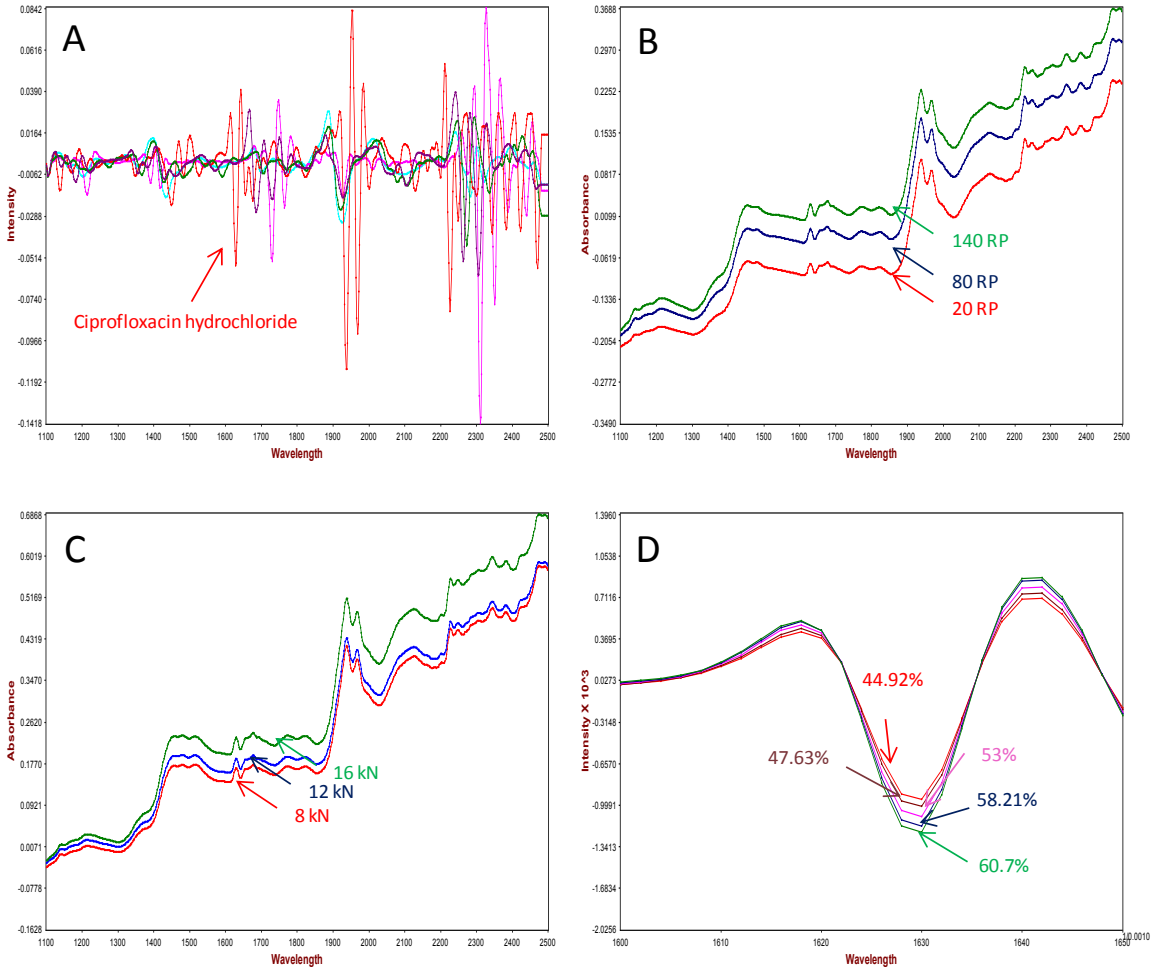

Figure 3-6. Feasibility study, 2nd derivative spectra of neat Ciprofloxacin hydrochloride and all the excipients given in Table 1 (A). Overlaid raw spectra of granules (B) obtained at different roll pressures and overlaid raw spectra of tablets obtained at different compression force (C). The 2nd derivative spectra of blends used to construct blend uniformity calibration model (D).

3.4.4 Blend Uniformity Model

Figure 3-6, panel D show the spectral regions 1600-1700 nm used for the blend uniformity which has a CIP characteristic peak. For the calibration model development, the samples were preprocessed using SG (quadratic polynomial, no of convolutions = 7) followed by 2nd D (Segment size = 10) using 1500-1700 nm spectral region. Four factors

were used to build the model and R^2, SEC and SECV obtained were 0.961, 1.0 %, and 2.1%, respectively (Figure 3-8, panel A). The model when tested with external data set resulted in SEP values of 1.8% (Figure 3-8, panel C). To test for model accuracy, paired *t*-test was performed on the NIR predicted and HPLC data. Results indicate no significant difference (P = 0.49) between the data (Table. 3-5).

3.4.5 Granule Size Model

Granules obtained at different roll pressure were subjected to PCA to identify the relationship among the variables. The raw spectrum was preprocessed using second derivative followed by autoscaling. The PCA 2D plot of 42 samples (Figure 3-7, panel A) accounts for 78.14% of the total variability in the spectra. PC1 had 48.1% of the total variability due to difference in the roll pressure. A four factor PLS calibration model was obtained when samples were pretreated with SG (cubic polynomial, 29 convolutions) and 2^{nd} derivative using 1128 – 2170 nm spectra regions. The model (Figure 3-8, panel B) resulted in R^2, SEC and SECV values of 0.949, 11.1 μm, and 15.4 μm, respectively. The model was validated using external data set using the granules not used in the model from the same roller compactor, i.e. no site change and the resulting prediction model (Figure 3-8, panel D) resulted in SEP value of 18.4 μ. Adjusting bias did not significant improve the model indicating the robustness of the model. There was no statistical significance ($p > 0.05$) between the NIR predicted data and the actual granule size measured using laser diffraction.

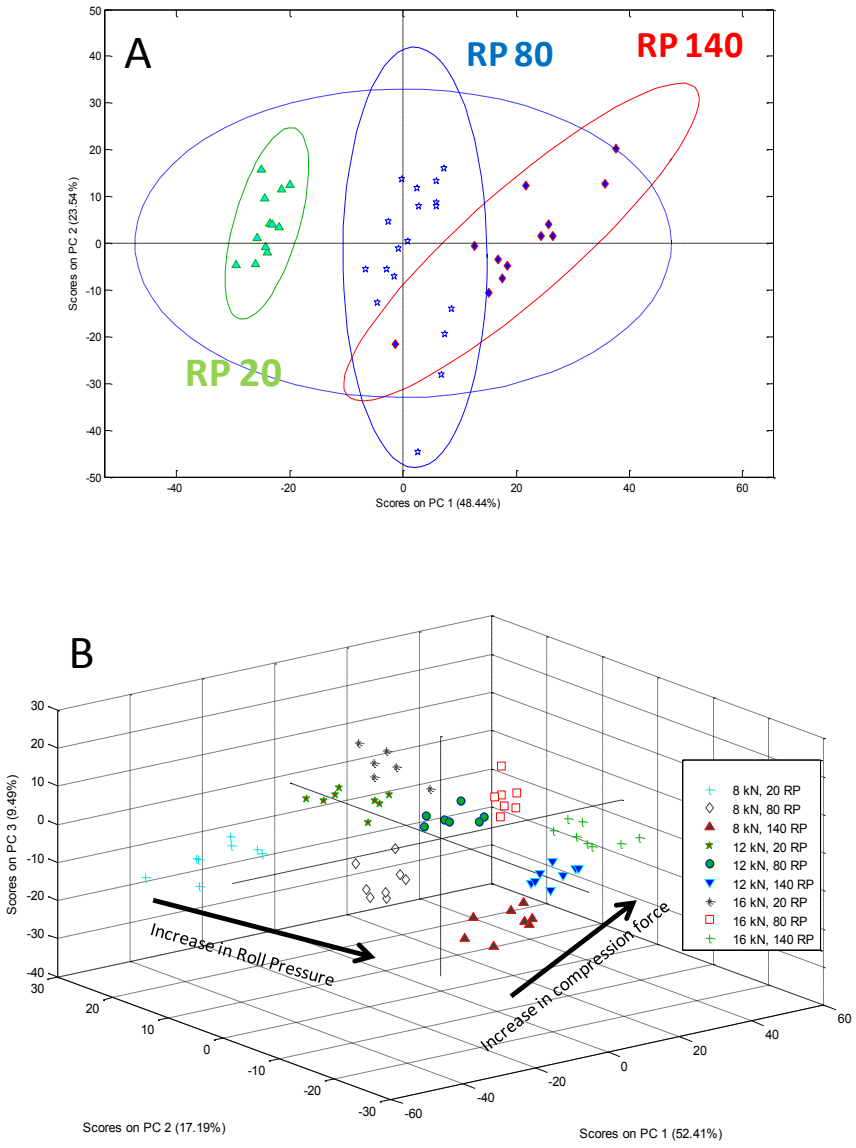

Figure 3-7. PCA and score plots of granules (A) and tablets (B).

3.4.6 Crushing Force Model

For the crushing force calibration model development, 126 tablets were selected from 6 different batches with different excipient grades, varying formulations as well as roller compacted processing parameters. For this study, PLS model provides the best fit and the final pretreated selected was SG smoothing (quadratic polynomial, 7 convolutions) and baseline correction (λ = 1800 nm). The calibration model (Figure 3-9, panel A) was build using 6 factors with R^2, SEC and SECV of 0.849, 1.7 kp and 2.0 kp, respectively, using 1122 – 2192 nm spectra regions. The models developed were tested using validation bathes obtained from the same roller compactor and tablet press not used in the calibration model consisting of 88 samples. The results (Figure 3-9, panel C) had a correlation SEP value of 2.2 kp, adjusting the bias did not change the SEP value indicating the robustness of the calibration model. Statistical analysis using student t- test indicate no significant difference ($p > 0.05$) between NIR predicted values and actual data (data not shown). However the prediction values (Figure 3-9, panel E) for the batched manufactured at site 2 resulted in higher SEP values for the batches with similar formulation and manufacturing conditions.

3.4.7 Disintegration Time Model

For this study, 126 samples were selected from 4 different batches to build calibration model. The calibration data set consisted of tablets made from different Klucel® (EFX or Nisso-L) and magnesium stearate (MgSt-M or MgSt-D) source only. Samples selection

was performed using Mahalanobis distance in the principle component space (threshold 0.95). The best-fit model was obtained when SG 1122 – 2192 nm wavelength range was used. The samples were pretreated using baseline correction (λ = 1800 nm) and SG smoothing (quadratic polynomial, 7 convolutions). The calibration model (Figure 3-9, panel B) gave R^2 value of 0.886 when 6 factors were used to build the model and SEC and SECV of 3.5 min and 4.4 min, respectively. The final model was tested using prediction set consisting of 42-sample set from four different batches resulting in a SEP value of 4.5 min (Figure 3-9, panel D). Similar to crushing force results, disintegration time prediction values (Figure 3-9, panel F) for the batches manufacture site 2 was found to be higher. The results of which are further are discussed below.

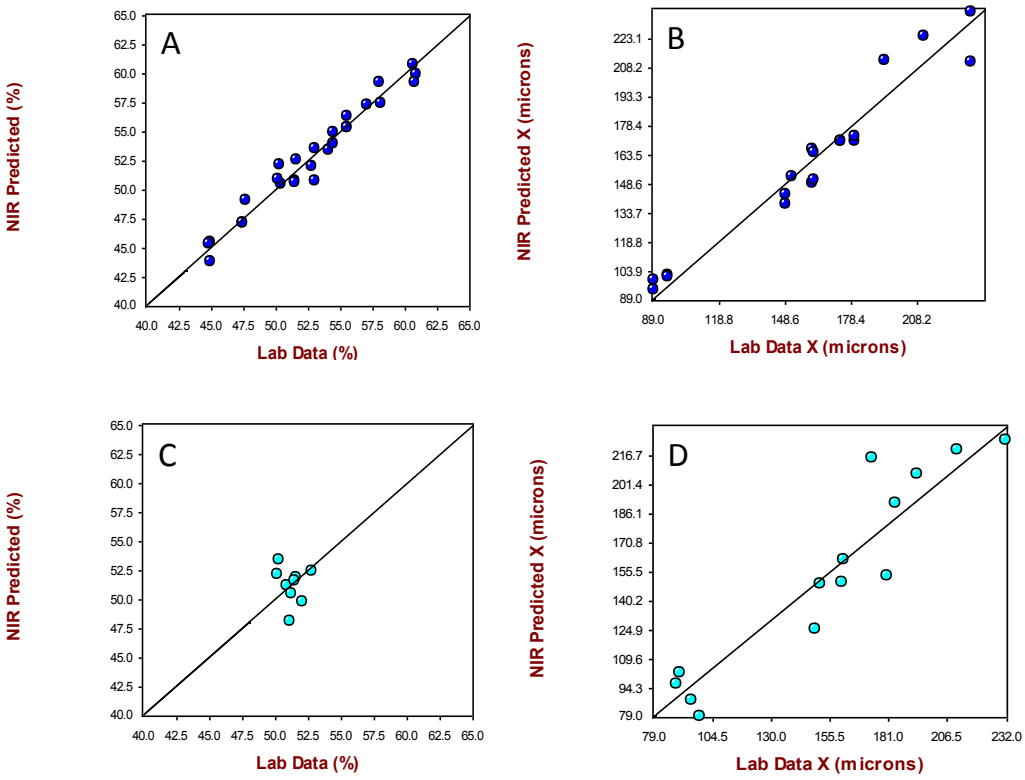

Figure 3-8. PLS calibration models for blend uniformity (A), granule size (B). PLS prediction (validation) for blend uniformity (C), granule size (D).

3.4.8 Model Prediction using External Data Set (manufacturing site 2)

To test the applicability to external data set, calibration models were applied to external batches that were manufactured at a different location using the same model roller compactor. The resulting granules were compressed on a tablet press and the compression profile was monitored using a force transducer. The prediction summary is presented in the Table 3-6. It was evident that the models (Figure 3-9, panels E and F) did not result in satisfactory SEP values for the crushing force and disintegration time.

This raises questions whether there are unknown formulations and/or processing variables that was not fully explore and not incorporated in NIR models which could have resulted in different granule and tablet characteristics. To explain this variability, PCA was performed on both the granules and on tablets obtained from both manufacturing sites (Figures. 3-10 and 11). PC-1 (43.2%) in Figure 11 and PC-2 (20.7%) in Figure 12 clearly explain the spectral variation resulting from granules and tablets used in the calibration and validation set respectively. Moreover, granules and tablets obtained at different site were evaluated for granule size, crushing force, and disintegration time and results of which further confirms that they were indeed different from calibration data set (Table 3-2).

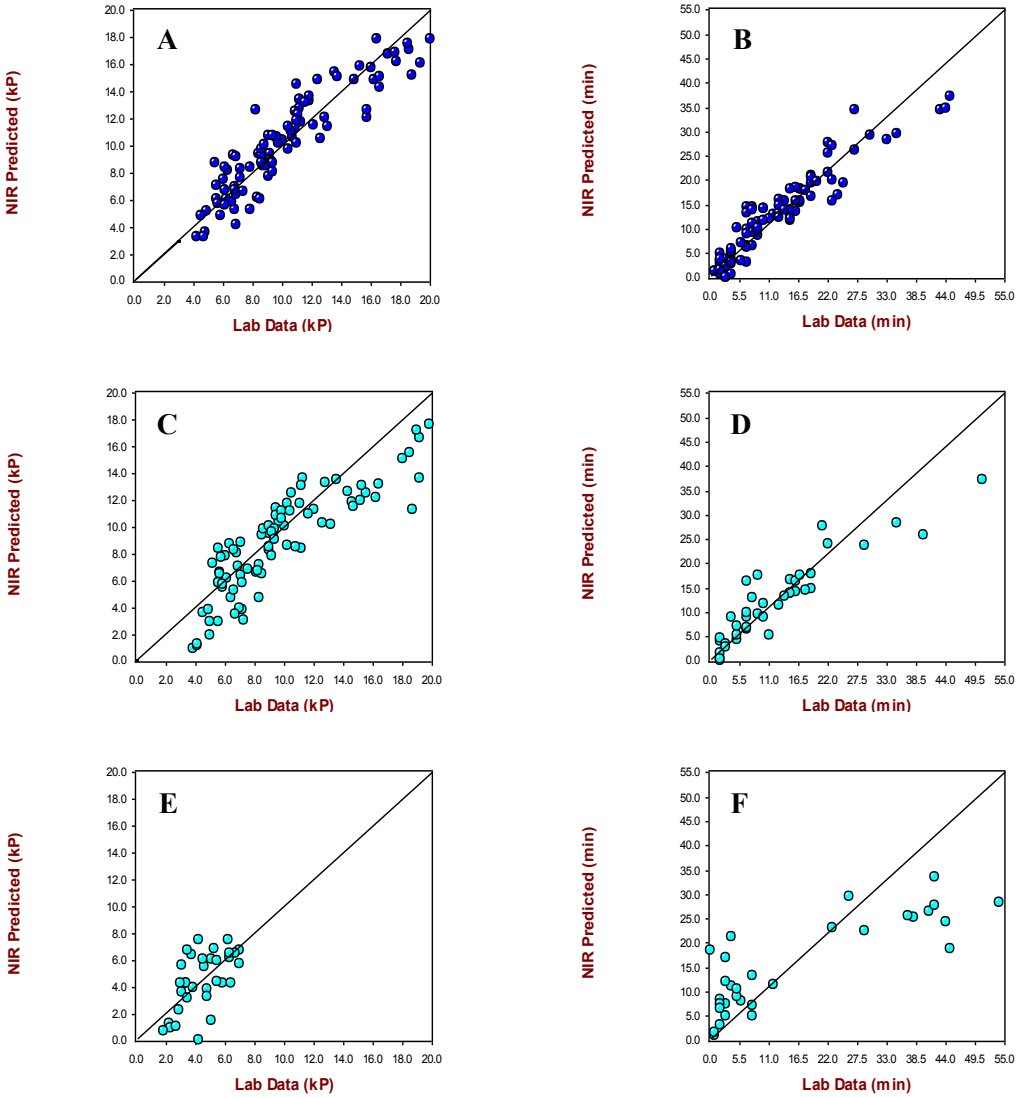

Figure 3-9. PLS calibration models for tablets. Crushing force (A) and disintegration time (B). PLS prediction using internal validation set crushing force (C) and disintegration time (D) and external validation crushing force (E) and disintegration time (F).

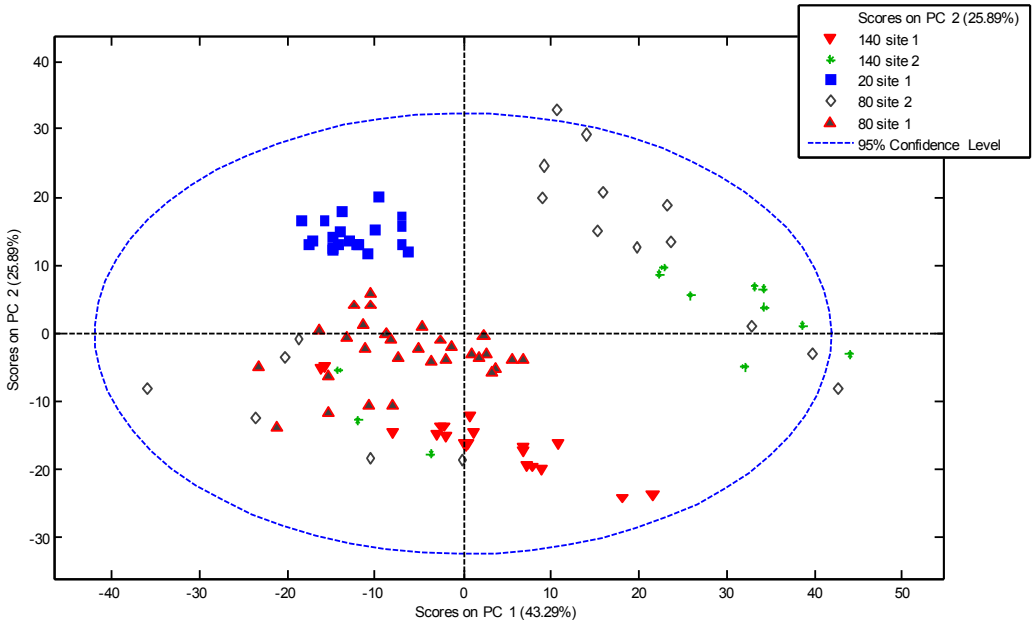

Figure 3-10. PCA analysis and score plots of granules obtained at different roll pressure and compression force.

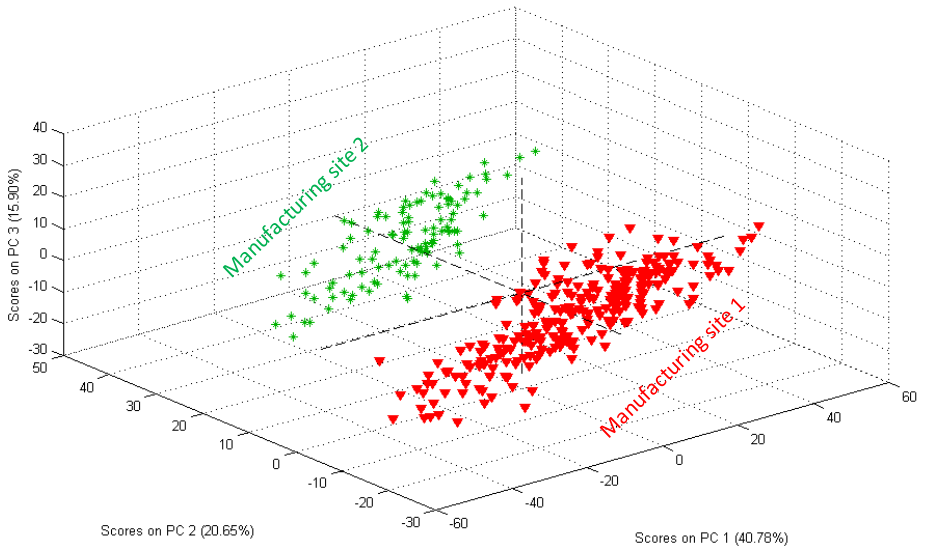

Figure 3-11. PCA analysis and score plots of tablets obtained at different sites.

Table 3-6. Summary of PLS models for the granule and tablet quality attributes.

	Calibration model						Prediction model - Site 1		Prediction model - site 2	
Models	No. of samples	Pretreatment	Factors	R^2	SEC	SECV	No. of samples	SEP	No. of samples	SEP
Blend uniformity	27	SG Quadratic 2D	4	0.961	1.0	2.1	-	-	23	1.8
Granule size	17	SG Quadratic 2D	4	0.949	11.2	15.5	14	18.4	-	-
Crushing force	126	BC, SG Quadratic 2D	6	0.849	1.7	2.0	88	2.2	27	2.2
Disintegration time	126	BC, SG Quadratic 2D	6	0.886	3.5	4.4	42	4.5	30	10.3

3.5 Conclusions

This study demonstrates the application of NIR spectroscopy as a powerful tool to monitor CQAs such as blend uniformity, granule size, tablet crushing force and disintegration time during the formulation development of immediate release tablets. As a part III of a three part study, the PLS multivariate models were developed, validated and applied during the production. The models were able to successfully predict the CQAs for the granules and tablets manufactured in the same site and on same machine. The prediction values (SEP) values however were found to be higher when applied to granules and tablets manufactured at a different location which emphasis the importance of incorporated all the variability that may arise due to process and/or instrument variability. In addition, PCA was able to clearly demonstrate their difference and was used a qualitative tool in the manufacturing.

Chapter 4 Application of in-line near infrared spectroscopy and multivariate batch modeling for process monitoring in fluid bed granulation

4.1 Abstract

Fluid bed granulation is an important unit operation in pharmaceutical industry for granulation and drying. To improve our understanding of fluid bed granulation, in-line near infrared spectroscopy (NIRS) and novel environmental temperature and RH data logger called a PyroButton® were used in conjunction with partial least square (PLS) and principle component analysis (PCA) to develop multivariate statistical process control charts (MSPC). These control charts were constructed using real-time moisture, temperature and humidity data obtained from batch experiments. To demonstrate their application, statistical control charts such as Scores, Distance to model (DModX), and Hotelling T^2 were used to monitor the evolution of batch process during the granulation and subsequent drying phase for real-time moisture levels during granulation and drying stages were determined using a validated PLS model. Two PyroButtons® were placed one near the bottom of the granulator bowl plenum where air enters the granulator and another inside the granulator in contact with the product in the fluid bed helped to monitor the humidity and temperature levels during the granulation and drying phase. The control charts were used for real time fault analysis, and were tested on normal

batches and on three batches which deviated from normal processing conditions. This study demonstrated the use of NIRS and the use of humidity and temperature data loggers in conjunction with multivariate batch modeling as an effective tool in process understanding and fault determining method to effective process control in fluid bed granulation.

4.2 Introduction

Fluid bed granulation is a wet granulation technique for producing granules by spraying a solution (typically a binder solution) on to a fluidized powder. Wet granulation is generally carried out to improve the flow characteristics, compression properties, increase the density, the drug release characteristics, blend uniformity, and reduce the dust.(56) Moisture levels during fluid bed granulation and drying are critical to the quality of the granules and subsequent final dosage form. The presence of excess residual moisture could influence granule flow, granule compressibility and drug stability in a dosage form.(75) In the case of tablets, capping may occur if the moisture levels are too low, whereas picking and sticking may occur with excessive residual moisture.(76) Schaefer *et al*, reported that the optimum moisture levels to be around the equilibrium moisture during the storage of granules to avoid exchange with the surroundings during the storage (62) and a minimum water activity of 0.35 – 0.5 may be necessary for optimum tablet hardness.(105) With fluid bed granulation, moisture levels also play a critical role in determining the outcome of the batch, and when moisture levels are not monitored or controlled, this could lead to over or under wetting of the powder bed resulting in batch

failures. Excess moisture in the powder bed can de-fluidize the bed and lead to bed collapse.

In wet granulation, the end-point is reached when the target granule size is reached. Granule growth is a complex process where the granule moisture level is a critical attribute that determines granule density and granule size. Several fluid bed factors were found to influence the quality and the end point of a fluid bed granulation process. Aulton *et al*, reported that inlet air flow rate, air temperature, air humidity, and atomization factors such as spray angle, flow rate, and atomization pressure could cause critical variations to the end-point.(61) Hence batch trajectory has a strong influence on the product quality. Therefore, it is critical to monitor the moisture levels in the granules throughout the granulation process, and not just at the end of the drying phase.

Conventional techniques for moisture determination using off-line methods such as loss on drying (LOD) and Karl-Fisher titration are slower and may delay process end-point decisions. Several methods of end-point determination were reported in the literature. Monitoring temperature of the inlet and outlet air is one widely used criterion to determine the end-point.(77) But this method is dependent on the humidity of the inlet-air entering as material drying is dependent on the moisture content on the inlet and the outlet air.(62) In some instances, humidity of the outlet air was used as an end-point determining tool.(78,79) Several authors also reported the use of the temperature difference (ΔT) method to determine the drying end-point.(62,80-84) The advantage of this technique is that the humidity variations on the end-point can be eliminated. In summary, the ideal process monitoring and endpoint determination, should involve monitoring of the fluid bed environment and the state of moisture in the granule.

With instrumentation advancements, several techniques are available to monitor process parameters and determine the end-point in real time; one such technique is Near-Infrared Spectroscopy (NIRS). This technique is rapid, nondestructive and requires minimal sample preparation and can be used in-line, at-line, on-line and off-line. Several authors have reported on the of monitoring moisture levels using NIR in a fluid bed. Franke *et al*, described the use of in-line NIRS to quantify granule moisture content and particle size allowing process monitoring and end-point determination using univariate analysis.(86) Similarly, Rantanen *et al*, used three to four different wavelengths to determine the moisture content of powder blend in the instrumented fluid bed granulator using multi-channel NIR moisture sensor.(87) NIRS on-line monitoring was also used to quantify film coating in the fluid bed granulator using multivariate analysis.(88) Rantanen *et al*, in a series of papers described the real-time used of NIRS for process monitoring and control during fluid bed granulation and drying.(87,90,91) Peinado *et al*, demonstrated the development, validation and transfer of NIR model to determine the end-point for commercial production batches of an FDA approved solid oral product.(92) Despite several successful implementation of NIR for moisture determination, this technique suffers from drawbacks such as; fouling of the optical sensor due to binder addition and limit penetration of the radiations source into the powder may limit it application and could affect its ability to determine the end point accurately. Despite several advancements over the years with the end-point determination and process control, the fluid bed granulation is still a complex phenomenon where several factors like moisture, humidity levels, temperature and other processing and formulation variable needed to be monitored and control. One objective of this research is the use of novel

data loggers and its application for temperature and humidity monitoring in fluid bed batch process. Although few authors have demonstrated the use of multivariate NIR chemometric models coupled with temperature and humidity data to developed models for better understanding the granulation process,(89-91) the use of PyroButton® for this application was never explored. These data loggers were reported for use in sterilization validation and monitoring in steam sterilization; humidity and temperature monitoring of environment and facilities such as warehouse, and processing procedures in pharmaceutical and food industry. However, there is no reported use of these in fluid bed granulation. These data loggers can be programmed for time and the duration of data collection. Due to its small size (17 mm x 6 mm size) these can be placed at various locations in and around the granulator for accurate monitoring. These loggers are self-powered by Lithium battery and internally consist of microprocessor, capacitive humidity sensor, and a quartz clock, all enclose in hermetically sealed stainless steel housing and hence these data loggers can be chemically sterilized and depyroginated and each data logger's calibration is NIST traceable.

The overall objective of this study is to couple real-time product moisture content predicted from NIR spectra with data from the environmental monitoring of humidity and temperature information to establish Statistical Process Monitoring Charts (SPMC) for fluid bed granulation and drying. This study will also use examples to show how SPMC can be used for process monitoring and fault detection. Knowledge gained from better PAT tools can be used to improve process understanding and establish better process control, which can help to reduce or eliminate end product testing.

4.3 Materials and Methods

4.3.1 Materials

Fexofenadine hydrochloride (Lot # C10 6026) was obtained from Cipla laboratories (Hyderabad, India). Microcrystalline cellulose, Avicel® 102 (Lot # P2098207) and croscarmellose sodium (Lot # TN11823647), was generously gifted by FMC Biopolymer (Philadelphia, PA). Lactose monohydrate (Lot # 10536575), Pharmatose® 110M was obtained from DFE Pharma (Princeton, NJ). Polyvinylpyrrolidone, Kollidone® K30 (Lots # G02086PT0 and G10976PT0) was obtained from BASF (Tarrytown, NY). Hydroroxypropyl cellulose (Lots # 99768 and 25604), grade Klucel® EXF was gifted by Aqualon/Hercules (Wilmington, DE).

4.3.2 Fluid-bed Granulation

Appropriate quantities of drug-excipients were weighted and sieved through # 18 mesh before mixing in a 8 qt V-blender (Patterson Kelly, Co, East Stroudsburg, PA) without intensifier bar rotating at 30 rpm for 5 min. Granulation was performed using a Magnaflow® fluid bed processor, Model 002 (Fluid Air® Inc., Aurora, IL); the parameters used for this study are described in Table 4-1. The required amount of granulation liquid consisting of 15% w/v solution of polyvinylpyrolidone (Kollidone® K30) in water was added during granulation at a constant spray rate of 5.5 gm/mL and the granules were dried until the LOD was less than 2%. Starting at 2 standard cubic feet per minute (SCFM) the inlet air flow rate was incrementally increased by 2 (SCFM) every 5 min until the required amount of binder solution was sprayed after which the air

flow rate was head constant at 6 SCFM for drying. The change inlet air flow rate was performed to maintain a more consistent state of bed fluidized during granulation. In our preliminary experiments, (data not shown) we observed that high inlet air flow rates at the beginning of the granulation led to content uniformity problems as the micronized drug gets trapped or stuck to the blow back socks; to avoid this, the inlet air was sequentially ramped as described above.

Table 4-1. Experimental batches showing formulation and process variables. Batches 1-12 were used for model building and batches 13- 15 were used as test set.

Batches	PVP binder (%w/w)	Disintegrant level (% w/w)	Inlet air temp (^{o}C)	Atomization pressure (psi)
1	6.50	1.25	70.0	10
2	6.50	1.25	70.0	10
3	6.50	1.25	70.0	10
4	6.50	1.25	60.0	10
5	6.50	1.25	60.0	10
6	6.50	1.25	60.0	10
7	6.50	1.25	60.0	4
8	6.50	1.25	60.0	10
9	5.75	0.88	55.0	7
10	5.75	0.88	65.0	7
11	5.75	1.63	55.0	7
12	7.25	0.88	55.0	7
13	7.25	1.63	65.0	13
14	7.25	0.88	55.0	13
15	6.50	1.25	70.0	10

4.3.3 NIR Data Collection

A FOSS NIRSystems XDS Process Analyzer (FOSS NIRSystems, Inc., Laurel, MD) was used to collect the spectra and the data was analyzed using Vision® software (version 3.5 SP 6). Each spectrum consists of 16 co-added scans from the NIR range of 800-2200 nm. A scoop probe (XO-2500 Purge Probe, (FOSS NIRSystems, Inc., Laurel, MD), specifically designed for this application was inserted into a granulator at 45^{o} angle to the central axis, see Figure 1. As the batch circulates in the fluid bed, it gets collected on to the "spoon" at the end of the probe. After the scan is collected, the software triggers an air purge (~ 80 psi) which returns the sample back to the granulator. The height of the nozzle, angle of probe insertion and the spray angle of the binder solution are all critical and should be optimized to obtain good correlation and also avoid powder and spray deposition around the collection window of the probe.

4.3.4 Reference Data Collection

During a granulation run, physical samples were manually collected from the sampling port at regular intervals (5 min) during the model development stage and analyzed for moisture using LOD, see Figure 4-1. The sample times were timed to match the NIR probe collection times. To measure LOD, about 1gm of sample was evenly spread on the pan of the moisture analyzer (Mettler Toledo, Model HB43) and the sample weight loss was determined at 105 ^{o}C.

4.3.5 NIR Model Development

The PLS model was build using 32 samples from 10 different developmental batches (data not shown) which was part of the design space study for the development of Fexofenadine HCl IR tablet. The samples were inspected for outliers before calibration model development. To build a PLS model, spectral range 1860-1990 nm corresponding to the –OH combination band was used. Several preprocessing techniques were tested, and it was found that the Stavitzky-Golay/first order derivative (SG: number of data points: 29, order of derivative: 1st order, convolution polynomial: cubic) gave the best fit. The calibration model was validated using external data set obtained from a different batched from the same experimental design and statistical values such as SEC, SECV and SEP were compared. Student T-test was performed on NIR predicted data and LOD (%) values to test for model robustness. To develop multi-way principal component analysis (MPCA) model, the data was preprocessed first using multiplicative scatter correction (MSC) followed by first derivative (1-D), using quadratic polynomial with segment size of 5. Data pretreatment remove unwanted systemic variations due to baseline shifts and light scattering.(10)

4.3.6 Humidity and Temperature Monitoring

To record humidity and temperature during the granulation and drying phase, a novel data recorder was used (PyroButton®**,** Opulus Ltd, Philadelphia, PA),. These NIST traceable data recorders were placed at two different locations inside and around the fluid bed (Figure 4-1. positions 1-2). The data obtained was manipulated using PyroButton-

SQL (21 CFR Part 11 compliant) software, for analysis the absolute humidity and temperature were used.

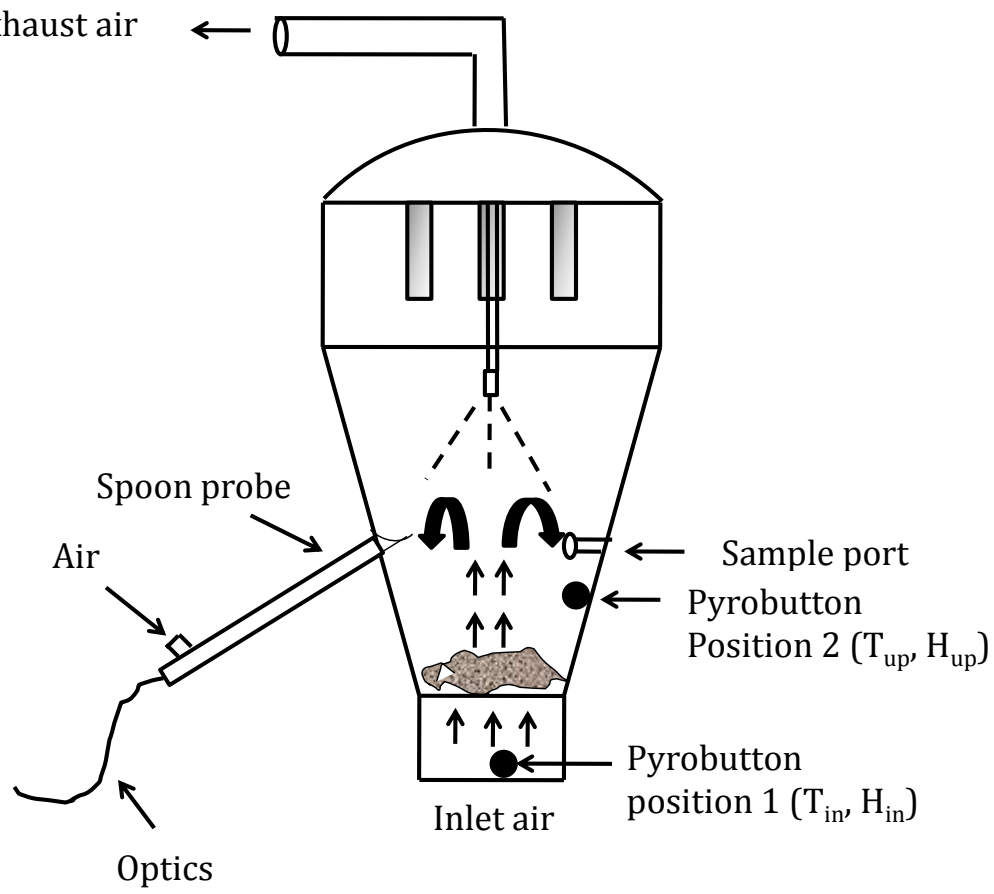

Figure 4-1. Schematics of the fluid bed set-up. NIR optic probe is inserted at 45 ^{o}angle to the central axis. Pyrobutton® data loggers are placed near inlet (in) and in the upper (up) product chamber.

4.3.7 Granule Size Measurement

Particle size was measured by laser diffraction method using Malvern® Mastersizer (Malvern Inc., Worcestershire, UK). The dry powder feeder was operated at air pressure of 20 psi at a constant feed rate of 2.5 and samples size of 5 gm. The mean granule size D[4,3] and span values of three runs was reported.

4.4 Multivariate Batch Modeling of NIR Spectra

4.4.1 Three-way Data Arrangement

In this study, a multi-way PCA technique was used to model the 3D batch process data. The data can be arranged as a three-way matrix ***X (J x K x I)***, as illustrated in the Figure 4-2, where in typical batch process in which J = 1,2,3, … , ***J*** variables, in this case NIR spectral absorbance, was measured at k = 1,2,3, … , ***K*** time intervals for i = 1,2,3, …, ***I*** batches. Different batches are arranged on the vertical direction, the variables along the horizontal, and the measurement time along the third direction. The objective of the MPCA as described by Nomikos *et al*, is to decompose the three-way data matrix X in to a series of principle components consisting of score vectors (t_r), and loading vectors (P_r), plus a residual matrix (E). The relationship can be described as follows (Nomikos *et al*):(106)

$$X = \sum_{r=1}^{R} t_r * \mathrm{P_r} + E \qquad \text{Equation: 4.1}$$

Where R is the number of principle components retained in the model. In MPCA, the data can be unfolded either batch-wise or variable-wise. Wold *et al* introduced variable-

wise batch unfolding to monitor deviations or abnormalities during the batch run.(107,108) Batches with variable length can be analyzed with this method, but cannot be applied to monitor time dependant dynamics. On the other hand, batch-wise unfolding helps to monitor time dependant dynamics and hence helpful in determining batch end point.

4.4.2 Multivariate Statistical Process Control Charts

To construct a multivariate statistical process control (MSPC) chart, DOE batches that were typical, i.e., yielded the desired granule properties such as end-point moisture content and granule size were modeled using MPCA, (Table 4-1, batches 1-10). Once constructed, these charts can be used to identify and diagnosis faults or deviations from the normal process trajectories that were established with the calibration batches.(109) In this study, scores, DModX also known as distance to model, and Hotelling T^2 were used for process monitoring. Hotelling's T^2 can be described by the following equation:

$$T^2 = \sum_{i=1}^{A} \frac{t_i^2}{s_{t_i}^2} \qquad \text{Equation: 4.2}$$

where $s_{t_i}^2$ is the estimated variance of t_i, t_i is the i_{th} PC, and A is the number of PC's selected.(110) If a totally new type of special event occurs which was not present in the reference data, then a new PC will appear. Such observation can be seen by calculating DModX, which is given by:

$$DModX = \sum_{i=1}^{k} (y_{new,i} - \bar{y}_{new,i})^2$$ Equation: 4.3

Where $\bar{y}_{new}$ is the new observation which is calculated from the reference PCA. DModX is also referred to as squared prediction error (SPE) of the residual of the new observation.(110)

4.5 Results and Discussion

4.5.1 NIR Spectral Analysis

Prior to the development of calibration model, the raw NIR spectra obtained during entire granulation and drying phase was overlaid and second derivative preprocessed data of the absorbance spectra was analyzed to identify spectral features corresponding to the moisture. Additionally, principle component analysis was performed on the raw data, here the spectra was preprocessed using Savitzky-Golay (SG: number of data points: 15, order of derivative: 1st order, convolution polynomial: quadratic) followed by auto-scaling. The preprocessing was performed to enhance the spectral features and remove any irrelevant data.

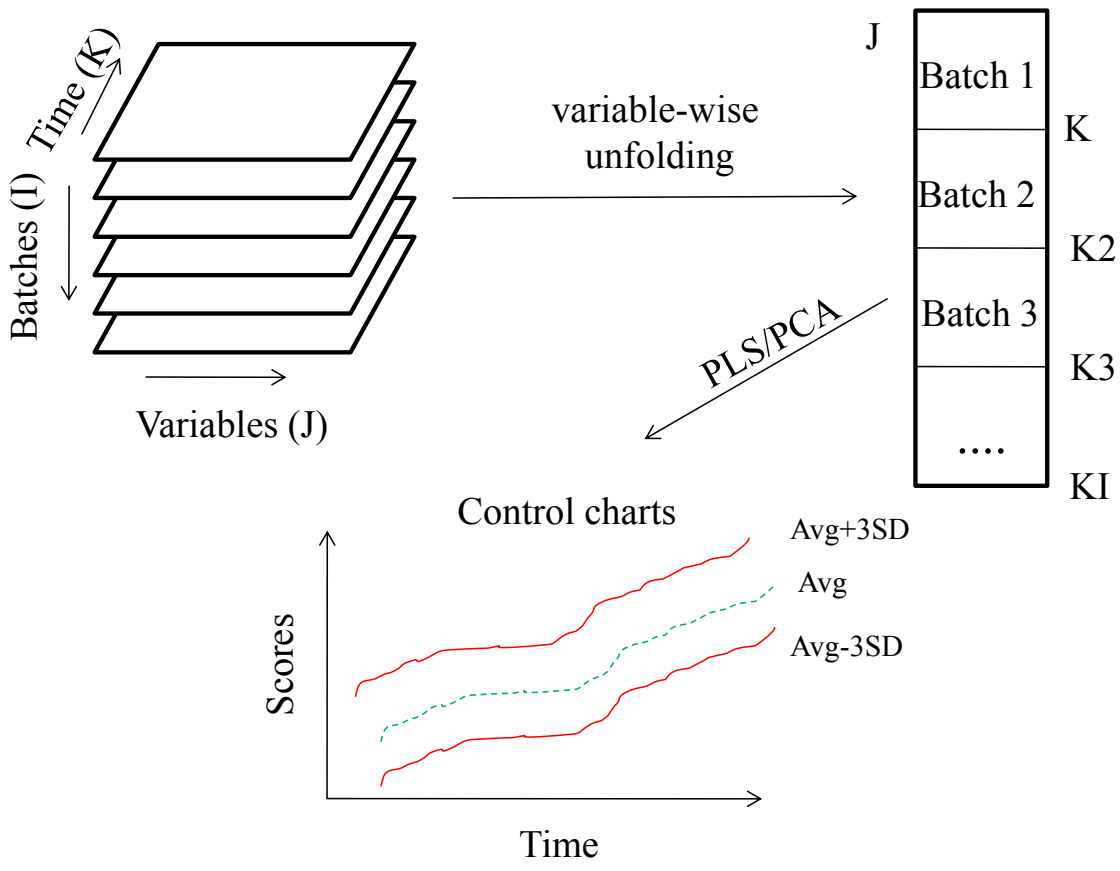

Figure 4-2. The variable wise unfolding of the 3D data matrix (x) and batch control chart limits. A PCA or PLS can be applied to generate scores and average and standard deviation of the scores are plotted against time.

Figure 4-3, panel A, illustrates the overlaid raw spectra collected during granulation and drying process which contains both physical and chemical information. Peaks corresponding to the wavelength region around 1400 nm relates to the first overtone of the –OH group. Spectra regions from 1600 – 1800 nm corresponds to the first overtone from –CH, -CH_2, and –CH_3. Figure 3, panel B is the preprocessed spectra (SG-2D) from region 1900-1950 nm, in this region the peak corresponds to water increases during granulation/binder spraying and decreases during drying.

Spectra regions from 1900-2000 nm of the normal batch was analyzed using PCA where 2 PC's explained 97.27% variability in the data with PC1 and PC2 capturing 76.95%, and 20.32% variability, respectively. Figure 4-4a shows PC1 and PC2 for batch 1 which illustrates the process trajectory of a normal batch. Loadings associated with the model are shown in the Figure 4-4b-c, where PC-2 show maxima at 1942 nm which resembles the water peak. These observations correlated with the previously reported literature.(92)

4.5.2 Moisture Model

A two factor PLS model was constructed to predict the moisture levels in the fluid bed granulator. Figure 4-5a is the relationship between NIR predicted and LOD% values and the calibration model resulting in R^2, SEC, and SECV values of 0.943, 0.99%, and 1.09% respectively. To validate the model, an external data set not used in the calibration model was predicted which resulted in SEP value of 0.88%. To test for linearity, 13 samples covering entire ranges from 2 to 15% were predicted. The plot of NIR predicted and LOD% values were linear with intercept 0 with R^2 of 0.974 (see Figure 4-5b). To further

validate the model, paired *t*-test was performed on the NIR predicted values and actual moisture content of the granules obtained from LOD% measurements and no statistical significance was observed (P<0.05 is significant).

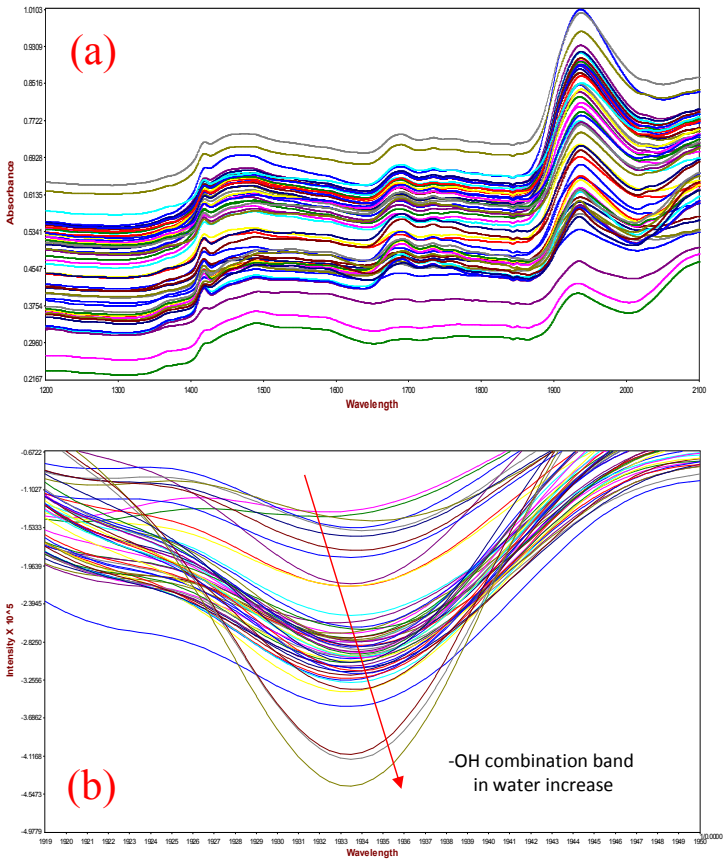

Figure 4-3. Raw spectra (a) taken in-process in the fluid bed and the preprocessed second derivative (b) overlaid spectra.

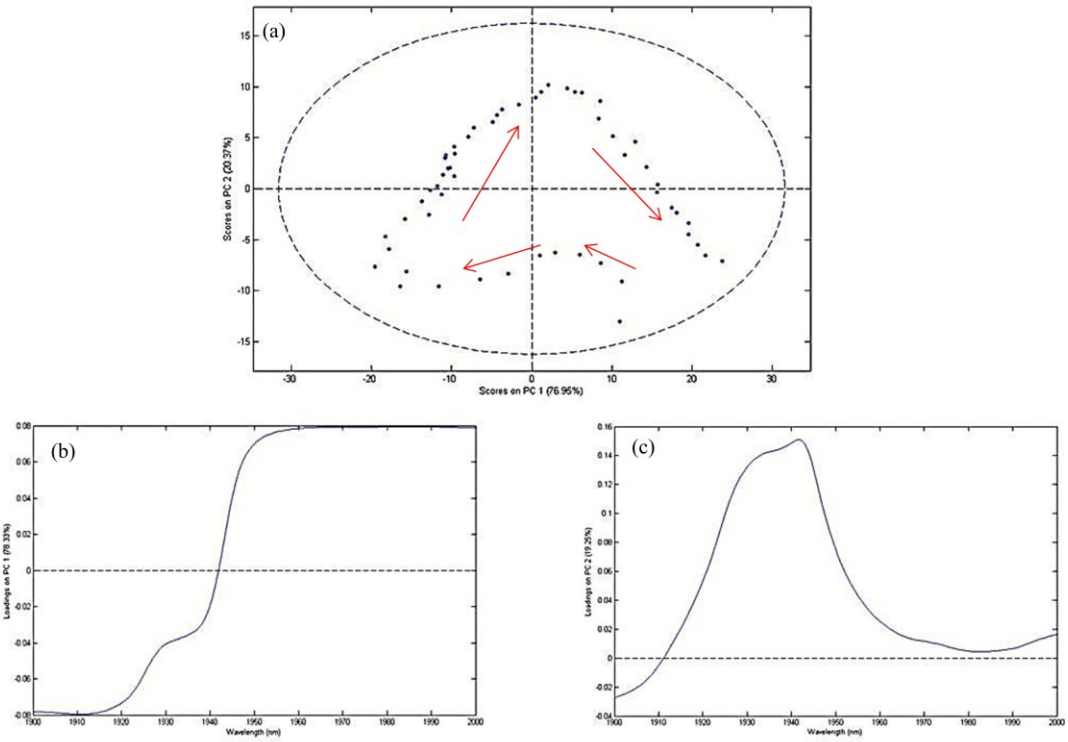

Figure 4-4. PCs score and loading plots from a normal batch. (a) PC1 vs PC2 score plot, with arrows showing process trajectory; (b) PC1 loading plot; (c) PC2 loading plot.

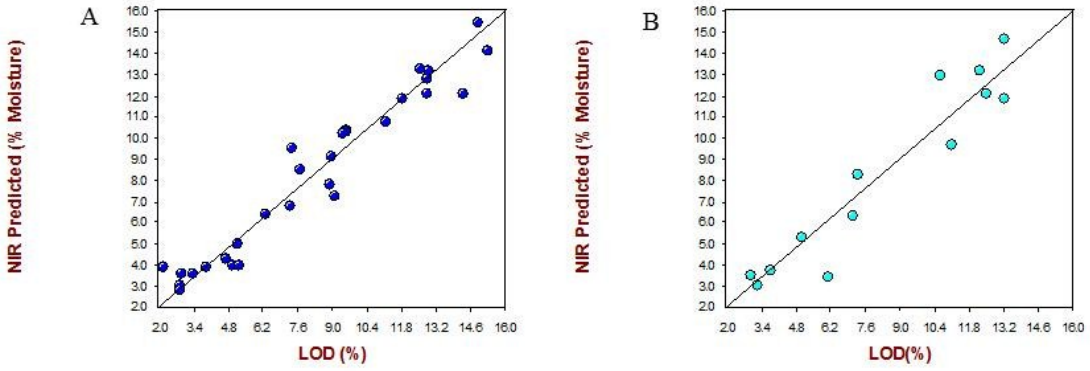

Figure 4-5. PLS calibration (a) and prediction (b) model for moisture.

4.5.3 MSPC Charts

Figure 4-6 shows the temperature and humidity, measured by the PyroButton® during fluid bed granulation process. The air inlet and the powder bed, see Figure 4-1, temperatures during the granulation and drying phase are shown in Figure 4-6a. Before t = 0, data not shown, the fluid bed without powder is equilibrated to the operating temperature for 15-20 min minutes. The operating temperatures are given in Table 4-1. At time t = 0 the powder is added to the fluid bed chamber, with the Fluid Air system this requires stopping the air flow and opening the chamber to add the powder. This causes the temperature to drop, and given the mass of the fluid air chamber the temperature slowly returns to the operation temperature. The entire granulation and drying is divided into three different stages. The first stage from A to B the powder bed is equilibrated to the desired operating temperature and additional mixing takes place. The second stage B to C where the binder solution is sprayed onto the powder bed and the third stage starting at C until the batch is completed is the drying phase.

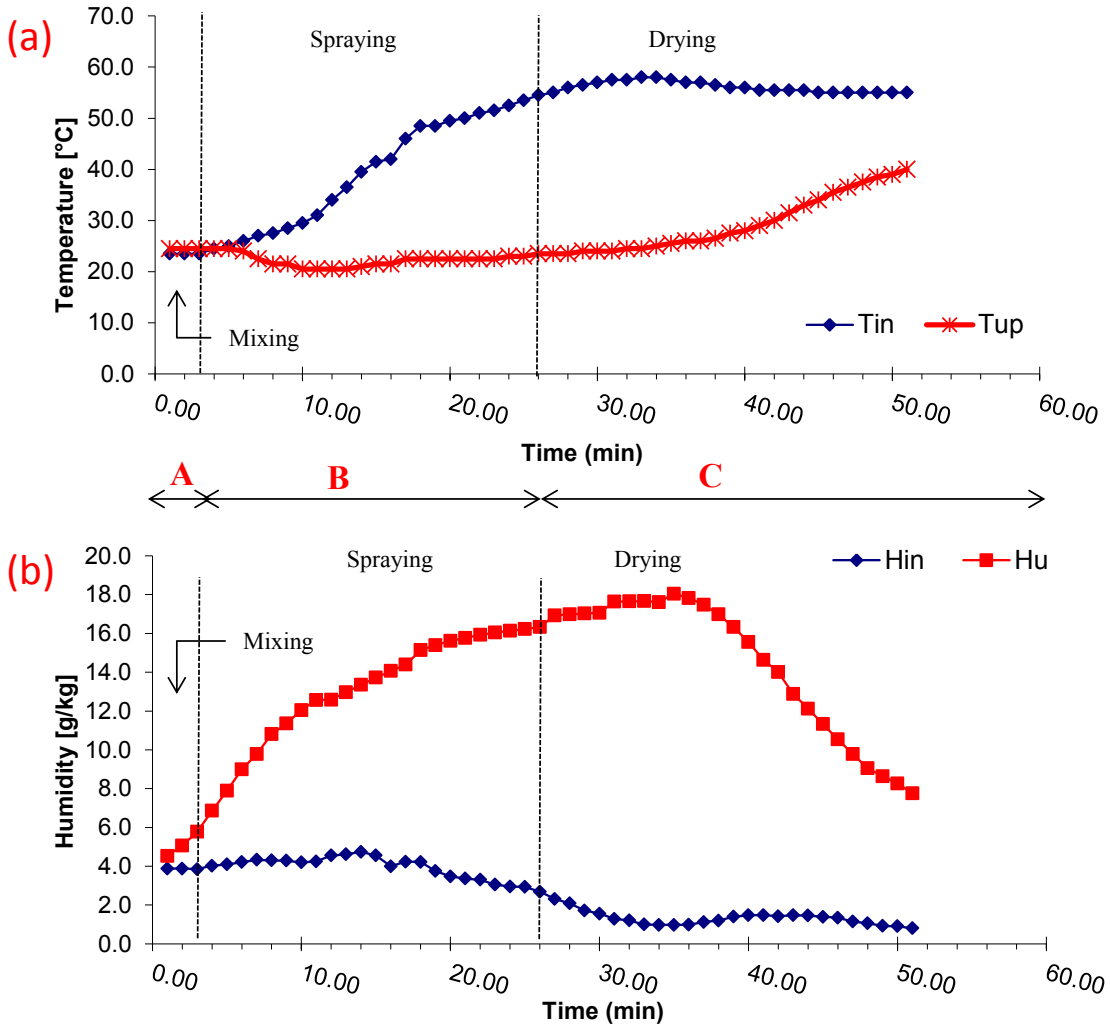

Figure 4-6. Temperature (a) and Humidity (b) data from positions 1 and 2 obtained from the Pyrobutton®.

During the granulation phase (B), once spraying begins, the temperature in the powder bed (T_{up}) is reduced due to water evaporation from the binder solution. During drying (C), the temperature slowly increases as the product becomes dry and less water leaves the system. Humidity levels of the air entering the system (H_{in}) stayed in lockstep with the T_{in} throughout the process (see Figure 4-6b). The inlet air temperature increases (T_{in}) until the system reaches steady state at the end of drying phase (B-C), see Figure 4-6a.

Figures 4-7 plots humidity vs time for the 12 batches performed at different process conditions, as described earlier see Table 4-1. The boundaries in the chart represent average (dashed line) value and ±3 standard deviation (Std.Dev) (i.e., a 99% confidence interval) for each sampling time. Figure 4-7a shows the humidity levels of the air entering the system and differences can be seen between the batches as the air entering the granulator was not pre-conditioned; unconditioned ambient air was used for these studies. On the other hand Figure 4-7b, humidity levels within the granulator or inside the product chamber (H_{up}) in the beginning of the process have broader limits and this can be attributed to process differences between the batches as the inlet air temperature of batches were different, which can change how the system reached steady state from the time it was opened to charge the powder into the system to the time it reached steady state. As the spraying continued the humidity levels increased and the variability lowered as the system reaches equilibrium. During the drying phase the boundary limits increased as the drying phase reached the granulation end point, because each batch differed in the process conditions used for the DOE (see Table 4-1 and Figure 4-7b). Similar trends were recorded for temperature with respect to variability in the data.

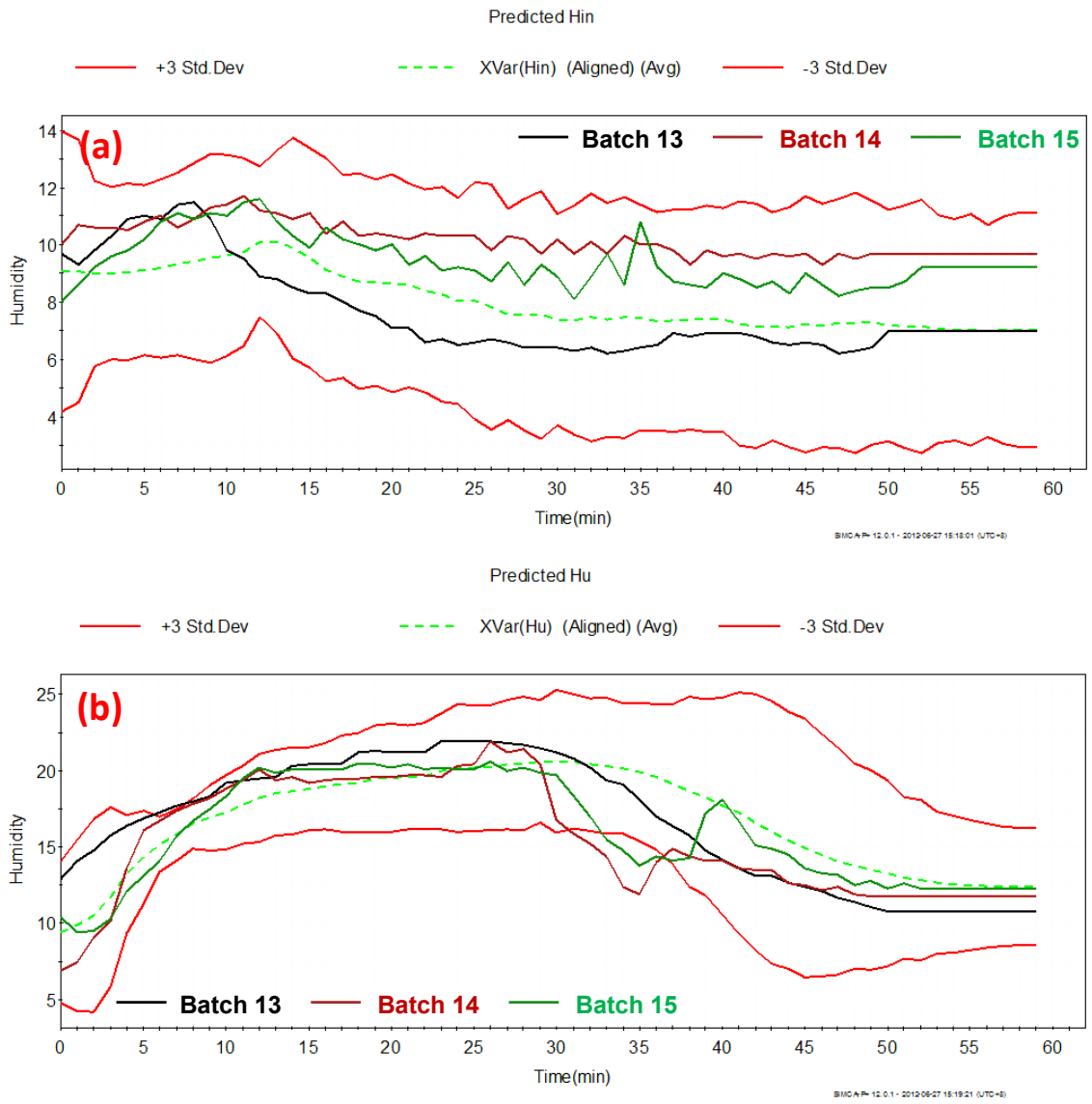

Figure 4-7. Humidity (g/kg) plots of inlet air (a) and product chamber (b).

Large variations were reported in the beginning and the end of the process and less variability once the system reached equilibrium (see Figure 4-8a-b).

Figure 4-9; shows the multivariate chart of the first principle component scores of the PLS model. The summary of multivariate models is presented in Table 4-2. Humidity and temperature data collected from the PyroButtons® from two different locations, Inlet (H_{in} and T_{in}) and product (H_{up} and T_{up}) were used, respectively, to build the model. The control limits in these charts are larger as the batches used in the modeling were performed with different processing conditions such as different inlet air temperature and binder levels, see Table 4-1. At the beginning of the granulation process, a large variability can be seen as the starting processing conditions for the batches were different. The variability lowered at the beginning of the spraying and as the spraying continued, the variability started to increase. As the process reached the end point the variability was the highest, this can be attributed to different drying times due to different amounts of binder level addition during the spraying stage and different inlet temperatures during drying phase. The NIR spectra PLS score plot of first principle component is illustrated in the Figure 4-10, the process trend charts show narrow control limits during spraying as shown by the red boundaries, but the limits were higher during drying this is for the same reasons described above where different binder levels and different inlet temperature resulted in batch to batch variability during drying phase. In addition to score plots, Hotelling's T^2 and DModX charts were built from normal batches and 95% confidence intervals were established (see Figures 4-11, 12). These charts with the set boundary limits were then used to monitor new batches.

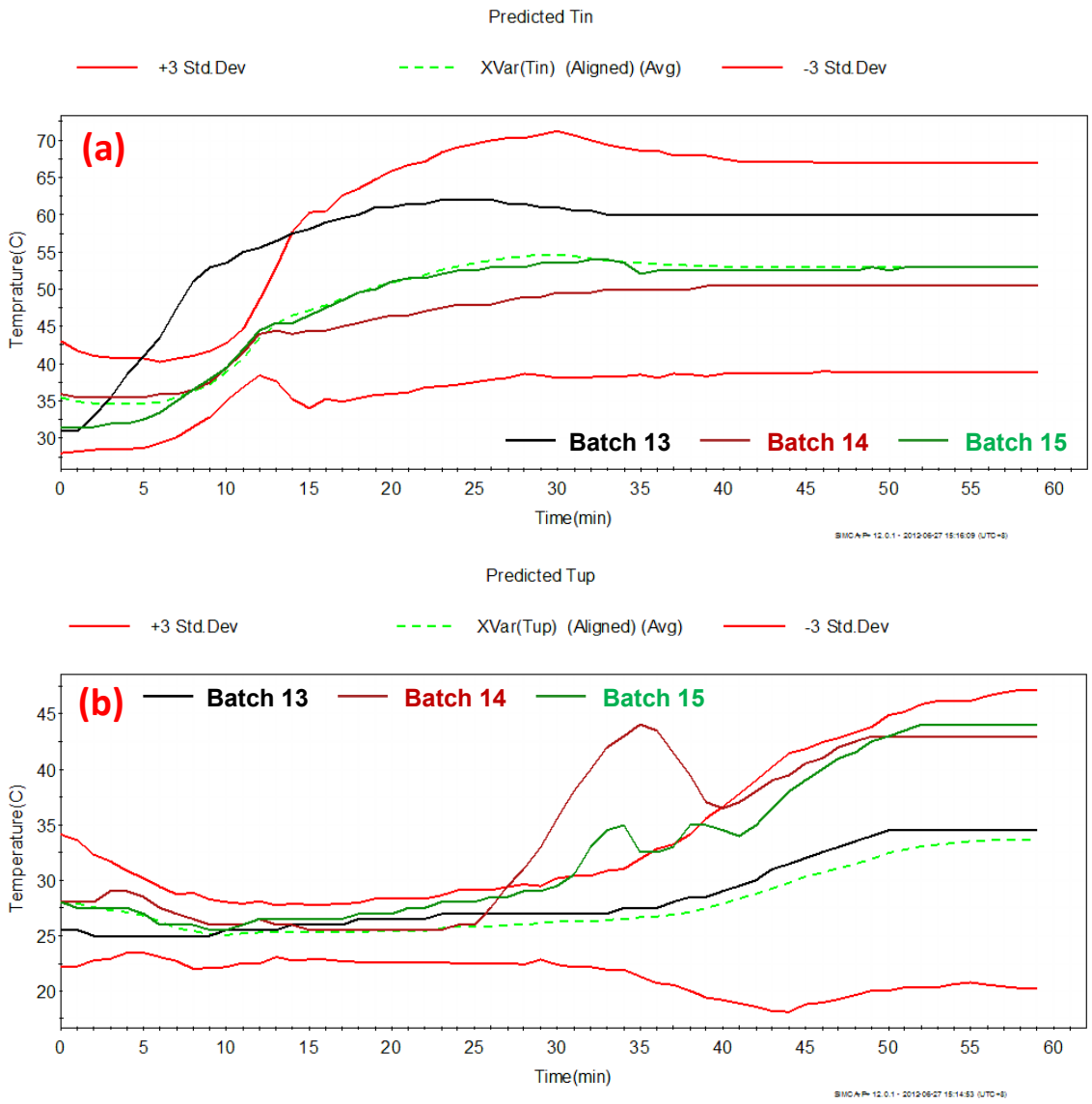

Figure 4-8. Temperature plots of inlet air (a) and product chamber (b).

Table 4-2. Summary of multivariate models where PC is number of principle components, R2 X (cum) and R2 Y (cum) is the cumulative sum of squares of the entire X and Y explained by the models, respectively. Q2 is the fraction of total variation of Y that can be explained by the model.

Model	PC	R^2 X(cum)	R^2 Y(cum)	Q^2
NIR Spectra	3	0.684	0.839	0.836
Temperature and Humidity	2	0.631	0.717	0.716

4.5.4 Fault Detection Using MSPC Charts

In this section, the use of MSPC charts to identify faults during fluid bed granulation process using multivariate models derived from batches that were within the specification ranges will be demonstrated. Scores, Hotelling's T^2 and DModX charts developed using normal batches were used to monitor batch process.

For batch 13, scores and T^2 plots indicated process slightly deviated at time points 19, 20 and 29 min see Figures 4-10 and 4-12. Moisture values predicted by the in-line NIR probe (Figure 4-13) show that the moisture levels lowered at those time points, these data points can be considered as outliers as the moisture levels was back to normal range and hence no process changes was performed for this batch process and moisture, temperature and humidity charts followed normal trends thereafter. This batch was successful and yielded desired end point moisture of LOD of less than 1% and desired granule size similar to that of normal batches (Table 4-3).

Table 4-3. Summary of granules size distribution (n=3).

Batches	D(10)±Std.Dev	D(50)±Std.Dev	D(90)±Std.Dev	Span*±Std.Dev
1	15.27±2.5	110.69±2.5	224.62±1.6	1.89±0.1
2	12.47±8.1	104.24±7.2	212.24±13.6	1.90±0.1
3	24.38±1.4	112.67±0.1	225.31±0.8	1.78±0.0
4	15.11±1.2	96.18±6.4	215.03±5.2	2.19±0.1
5	30.12±1.8	114.77±2.8	227.45±0.6	1.72±0.0
6	29.75±5.9	117.83±4.7	234.19±6.7	1.74±0.1
7	29.72±6.0	114.04±3.3	228.73±4.2	1.75±0.1
8	21.99±0.8	114.71±3.6	231.56±6.6	1.62±0.4
9	24.62±1.5	115.46±1.3	233.75±2.0	1.81±0.0
10	37.90±0.5	119.94±1.6	232.17±2.1	1.62±0.0
11	30.08±0.2	116.33±0.4	230.57±2.1	1.72±0.0
12	35.58±0.3	116.23±0.7	230.82±1.6	1.68±0.0
14	21.69±1.1	115.28±2.2	233.54±2.5	1.84±0.0
15	31.61±0.1	118.02±2.3	230.53±3.6	1.69±0.0

* span = [(D90-D10)]/D50]

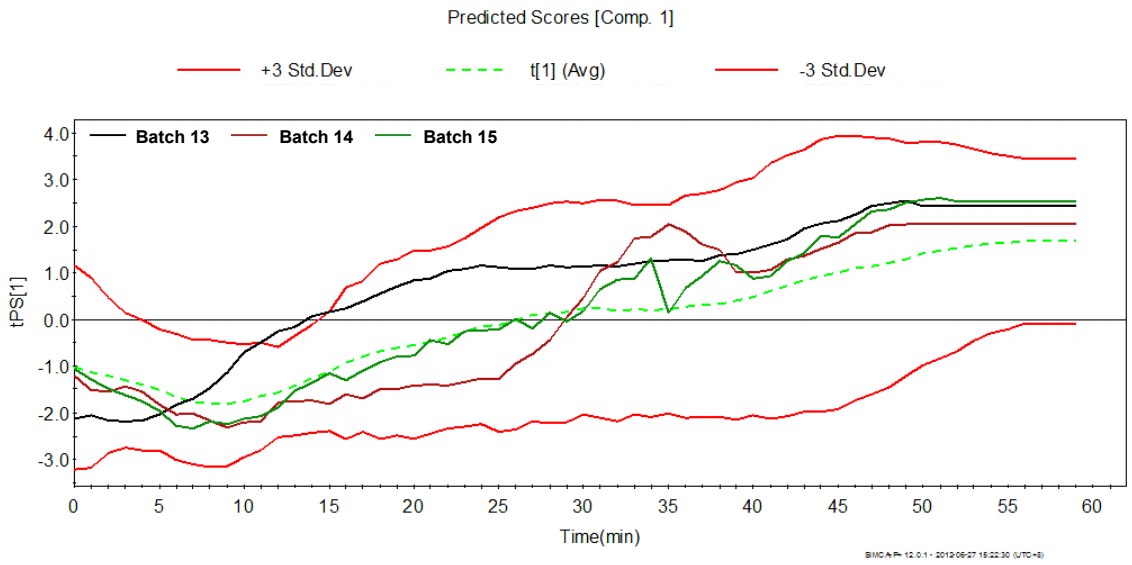

Figure 4-9. The PLS 1 score plot of the humidity and temperature of batches. Average and control limits (±3 Std.Dev) were built using batches 1- 13. Batches 13-15 deviated from the normal process.

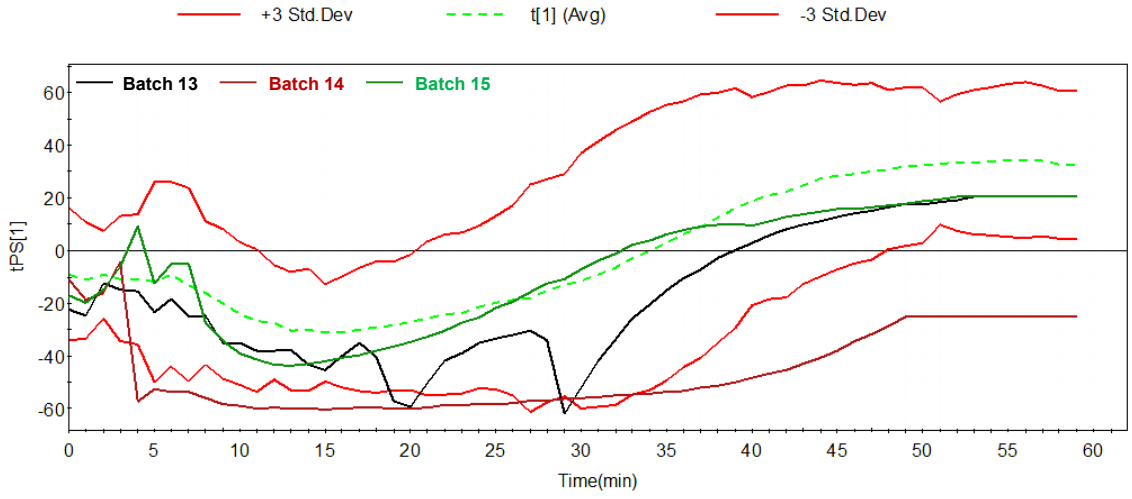

Figure 4-10. The PLS 1 score plot of the NIR spectra. Average and control limits (±3 Std.Dev) were built using batches 1- 13. Batches 13-15 deviated from the normal process.

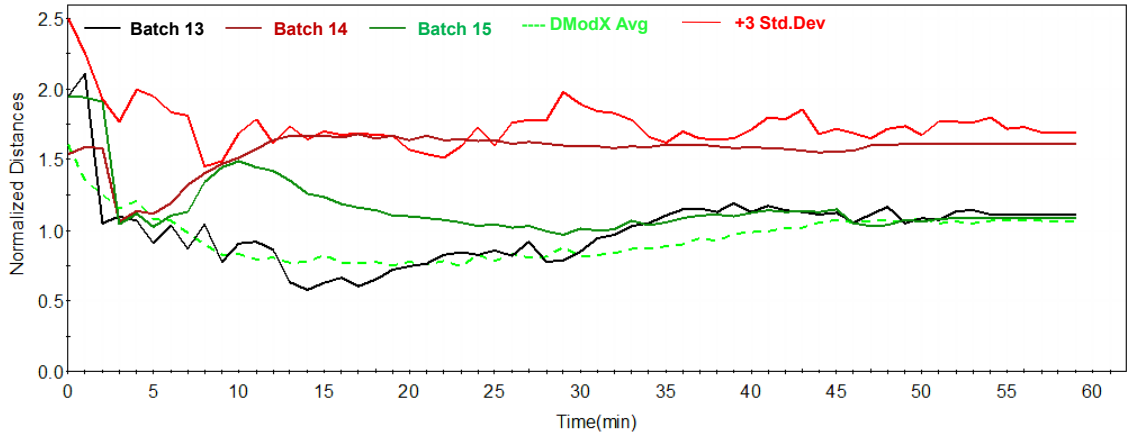

Figure 4-11. The DModX plot of the NIR spectra of batches 13-15.

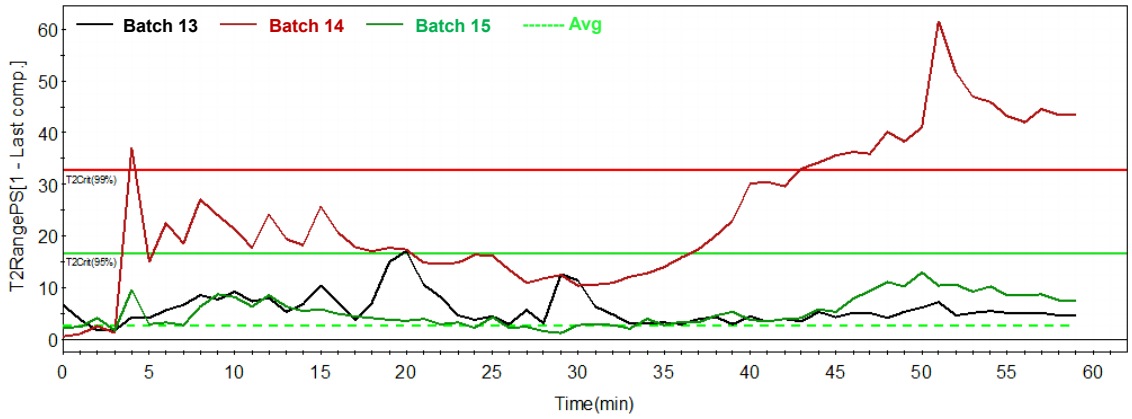

Figure 4-12. The Hotelling T^2 plot of the NIR spectra of batches 13-15.

For batch 14, the scores started deviating from the very beginning i.e. time point 4 min and stayed deviated throughout the process run. DModX and Hotelling T^2 also show similar deviations at that time point. To identify the root cause, moisture trends and humidity and temperature score charts were evaluated. No deviation in inlet temperature and humidity (Figures 4-7,8) from normal operating conditions was observed; however, late in the process at around the 35 min time period the product humidity and temperature did deviate, see Figures 4-7b and 4-8b, whereas the moisture trends for batch 14 clearly show higher moisture levels from the beginning of run, this data clearly explained that the process deviation was induced by excessive binder solution around NIR probe due to improper binder spray angle. Continuous addition of binder solution resulted in powder accumulating around the probe resulting in non-homogeneous or uneven powder wetting. The bed started to collapse around 28 min time point during which time the inlet air flow was increased in order to maintain the fluidize bed state. Score and variable plots show a process deviation during the same time point. Increase in inlet air flow rate subsequently increased the product temperature and decreased the humidity levels resulting in efficient drying. The final product in the end did not meet the end point criteria and it was considered a failed batch.

For batch 15, processing conditions such as amount of binder sprayed and inlet temperature was similar to that of batch 12. The score, T^2, and DModX plots were normal and didn't show any process deviations from normal batches, but the real-time moisture levels predicted by the NIR were found to be considerable higher than the normal batches, i.e. 25% at 14 min (Figure 4-13), and the reason for such high moisture level is unknown and needs further investigation, to prevent batch failure and bed collapse, the

inlet air level was increased from 6 SCFM at 20 min to 12 SCFM to maintain proper bed fluidization. In the end this batch was successful and produced desired end point moisture and granule size (Table 4-3).

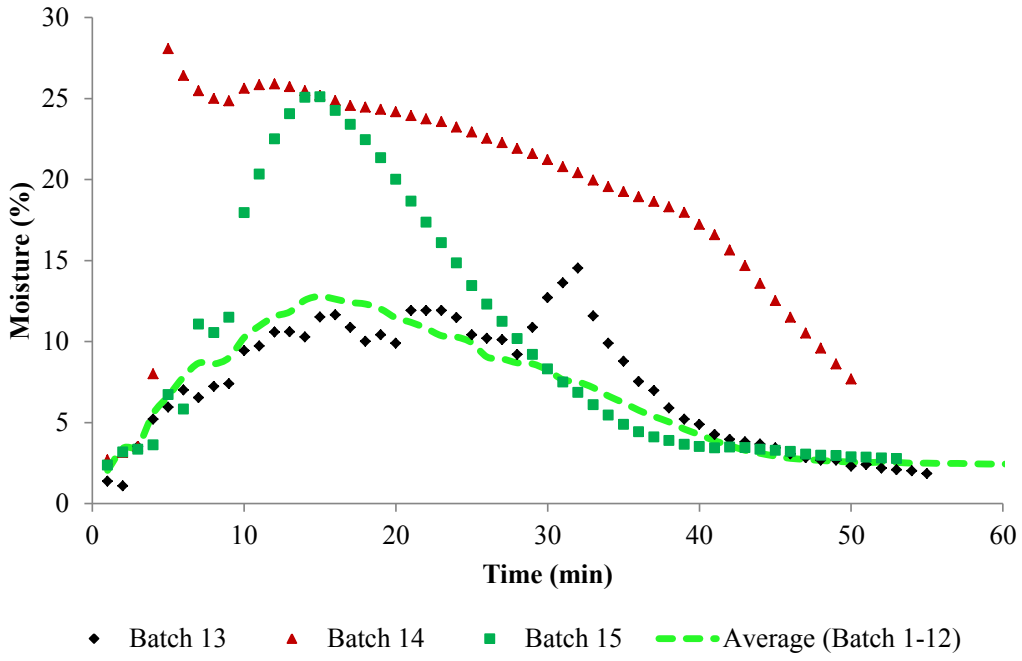

Figure 4-13. Real-time moisture trends chart from routine analysis for granulation/drying.

4.5.5 Conclusions

For fluid bed granulation to say the process can be controlled our studies show that one must monitor the humidity and temperature in the granulation environment and the state of moisture within the granules. The system setup using pyroButton® and a NIR probe work very well at this. In this study we have demonstrated the use of in-line NIR spectroscopy coupled with multivariate statistical process control methodology as an

effective way for process monitoring in fluid bed granulation. The novel commercially available data loggers known as PyroButton® were used in this study for temperature and humidity at different regions of the fluid bed granulator. A quantitative PLS model was established using NIR spectra and granule moisture from loss on drying measurement. The established model demonstrated high linearity between absorbance and the moisture during all phase of granulation. The calibrated model was validated using external data set; linearity and robustness of the model was determined. This data together with real time moisture from NIRS was used to construct process trajectories and establish process boundaries.

This study also demonstrated that using SPC charts such as scores, Hotelling T2, and DModX collectively was effective in identifying process abnormalities and determine the root cause for such failures. Information collected during fluid bed granulation using NIRS and PyroButton® data logger during product development stage can be used for effective process control and to established process design space.

Chapter 5 Summary, Conclusions, and Future Directions

Process understanding and process monitoring are an integral and critical component in the pharmaceutical manufacturing which will consistently ensure predefined quality at the end of the manufacturing process.(1) Such procedures are basic tenet of quality by design intended to mitigate risk associated with product failures and simultaneously reduce regulatory burden. Process understanding typically involves identifying, managing, and predicting all critical source of variability accurately and reliably over the design space established for raw materials, processes parameters, manufacturing, environment, and other factors.(1) Of several Process Analytical Technology (PAT) tools currently available for this application, near-infrared spectroscopy (NIRS) has gained wide spread acceptance due to its rapid, non-destructive, easy sample preparation without pretreatment, and the use of fiber optics for separating sample location from the spectrophotometer.(4,10)

The current studies focuses on two unit operations commonly employed in pharmaceutical industry for the preparation of granules. One is a dry granulation technique using roller compaction and another is wet granulation using fluidized bed. The first part of this dissertation examined the application of Plackett-Burman design and Failure-Mode-Effect-Analysis risk assessment in the identification of critical roller compaction in-process and product quality variables in the release of Ciprofloxacin hydrochloride immediate release tablets. Quality risk management tools such as Failure-Mode-Effect-Analysis (FMEA) was used to prioritize the number of experiments needed to identify the CQA, while still maintaining an acceptable product risk profile.

Preliminary feasibility studies and FMEA helped to reduce the number of possible attributes down to 11 manageable factors. Then Plackett-Burman (PB) screening design helped to identify the main effects among these factors. Results indicated that the roll pressure from 80 to 140 bars significantly affected the particle size and Carr's index; increase in roll pressure increased the ribbon density which further increased the granule size. As the granule size increased, it improved the flow properties, which is critical for the content uniformity. The binder grade (Klucel®) and the tablet compression force were found to be critical for the release characteristics (i.e. dissolution and disintegration) of Ciprofloxacin hydrochloride model drug. In addition, results show that the Mg stearate type and glidant addition affected particle size and the Carr index, respectively. Substitution of the vegetable grade Mg stearate with the animal grade resulted in increase in the particle size of the granules. Factors which did not influence the quality target product profiles were assigned low risk and avoided from further consideration. The results from this study showed that scientific rationale, quality risk management, and screening designs such as PB-DOE can be used to identify critical factors coming from formulation and process parameters.

The second part of this research deals with studying the parameters identified from earlier studies for potential interaction using high resolution statistical design. Four high risk factors identified from earlier studied; roll pressures, compression force, binder source, and the lubricant type were evaluated further. First order regression results showed that granule size increased when Mg stearate dihydate (MgSt-D) form is replaced with monohydrate (MgSt-M) form which was in accordance to the reported literature where the particle size of dihydate form resulted in higher strength ribbons which when

milled resulted in larger granules. In addition, compression force played a critical role in the crushing strength of the tablets. As the compression force increased from 8 to 16 kN, crushing force of all the formulation increased. However, increase in roller pressure from 20 to 140 bars reduced the hardness of the tablets due to loss of compressibility commonly observed during roller compaction. No interaction terms were identified from regression analysis for the parameters tested.

To establish a control strategy during formulation development, NIRS was used to develop robust chemometric models for blend uniformity, granule size, crushing strength, and disintegration time. The models were further validated using independent data set (i.e. not used in the model development) which resulted in acceptable prediction statistics. Before roller compaction, the blend uniformity of the 23 batches were predicted using partial least square (PLS) calibration model build using 1500–1700 nm spectral regions which is the characteristics peak for ciprofloxacin and not interfered with other excipient peaks. The spectra was then preprocessed using SG-2nd derivative and the resulting model yielded standard error of prediction (SEP) values of 1.79 %. Similarly, NIRS PLS model was developed to predict the granule size after the roller compaction. The best fit and most predictive model for the granules used math pretreatment of SG-2D, whereas for the crushing force and the disintegration time, the best fit was obtained when baseline correction followed by SG-2D was employed. All the models yielded satisfactory SEP values and successfully predicted both granule and tablet properties for the batches manufactures at the same location. To test for accuracy, the actual tests (i.e HPLC for blend uniformity, disintegration test, etc) were performed on the same material and *t*-test was carried out to test the robustness of the models. However, the batches

manufactured at different location (i.e. manufacturing site 2) yielded higher SEP values. The reason for difference in the granules and tablets due to site change is still unknown and warrants further investigation. The results of this section further expand the application of NIRS and reiterated the importance of establishing a process monitoring and process control in-line with the Process Analytical Technology (PAT) guidance to mitigate the propagation of risk downstream during the manufacturing.

The last section of this dissertation deals with the application of PAT tools of in-line NIRS spectroscopy and Pyrobutton® data loggers in conjunction with multivariate batch modeling for process understanding the fluid bed granulation. The goal is to develop statistical process control charts using the real-time moisture data from the NIRS and humidity and temperature variations obtained from the data loggers as the batch progress. The spectra was math pretreated using SG first derivative and the best file and most predictive PLS model was obtained using two factors when spectral regions corresponding to –OH combination bands were used (1860 – 1990 nm).

Data loggers placed at two different locations in the fluid bed monitored the humidity and temperature as the batch progress. The data generated from normal batches were used to develop multivariate statistical charts such as Score, Distance to Model, and Hotelling T^2. These charts were successful in identifying the process abnormalities which deviated from the normal processing conditions. This study have demonstrated the use of NIRS and other PAT tools such as Pyrobutton® data loggers as an effective process control technique. These charts can be further applied for fault detection during the manufacturing and could aid in process modification during batch failures.

In summary in this dissertation, the application of NIRS and chemometrics on two unit operations commonly used in pharmaceutical manufacturing were studied. Risk tools and screening designs were employed to identify high risk factors influencing critical quality attributes in roller compaction during the manufacturing of immediate release tablets were studied. With the help of NIRS critical quality attribute such as blend uniformity, granules size, crushing force, and the disintegration time were quantified using PLS models and used as control strategy tool. In addition, this study demonstrated the use of statistical process control charts as an effective process monitoring and fault detection tools. Several observations made from these studies provide a platform for future directions for this research which entails a comprehensive understanding on: (i) investigating the effect of Mg stearate forms on the ribbon properties and granules during roller compaction, (ii) Factors contributing to the changes in the granule size and tablet properties as a result of location/manufacturing site change, (iii) Developing robust models which predict product quality attributes due to the site change, (iv) Real-time application of the process control charts and development of feed forward and feedback ward systems using these charts for effective process control.

Appendix A: Supplemental Data for Chapter 3

In this section, the dissolution of Ciprofloxacin hydrochloride in different pH's and ionic strengths are presented. Also discussed are the formulation and processing variables studies in the manufacturing of Cipro clinical batches.

A.1. Influence of pH and ionic strength on the release of Ciprofloxacin hydrochloride IR tablets:

Tablets for Table 3-2 (Chapter 3), Batch 2 (Fast), compression force (CF) at 12 kN; Batch 13 (Medium), CF 8 kN; and Batch 13 (Slow), CF 12 kN were used. Dissolution was carried at out according to USP II method at 37 ± 0.5 ^{0}C with paddle rotated at 50 rpm. Studies were carried out at pH's of 2.2, 4.5, and 5.5 and at ionic strengths (μ) of 0.01, 0.05, and 0.2.

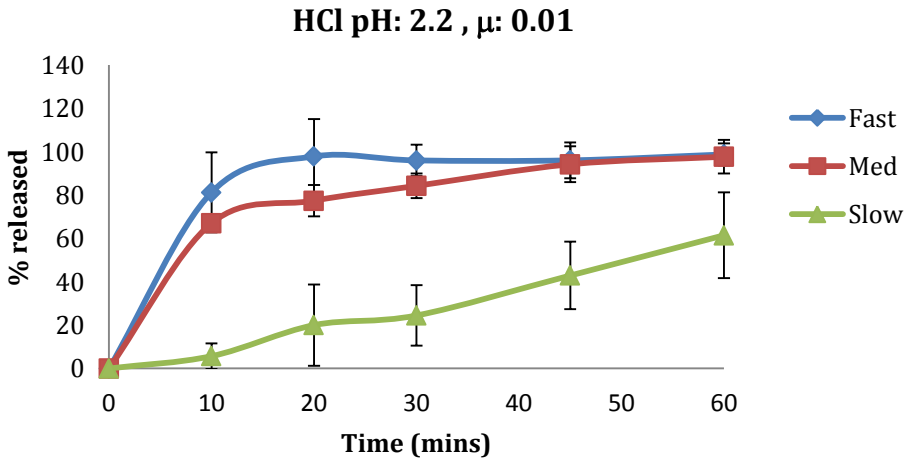

Figure A-1. Dissolution of CIP at pH 2.2 and ionic strength of 0.01, (n = 5).

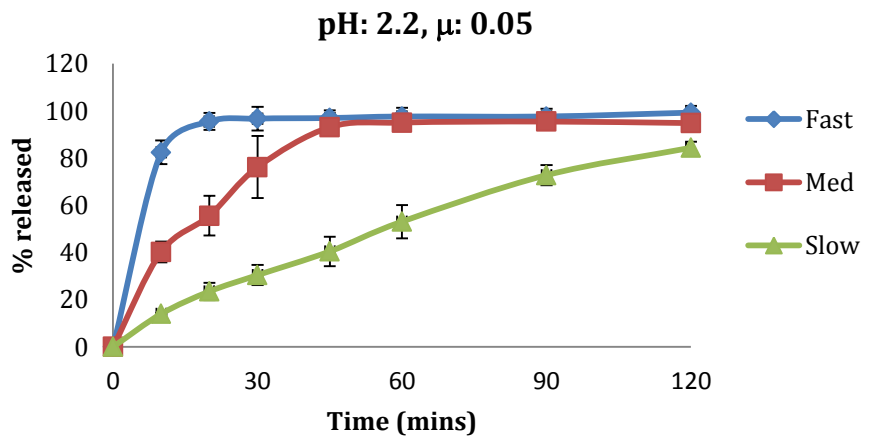

Figure A-2. Dissolution of CIP at pH 2.2 and ionic strength of 0.05, (n = 5).

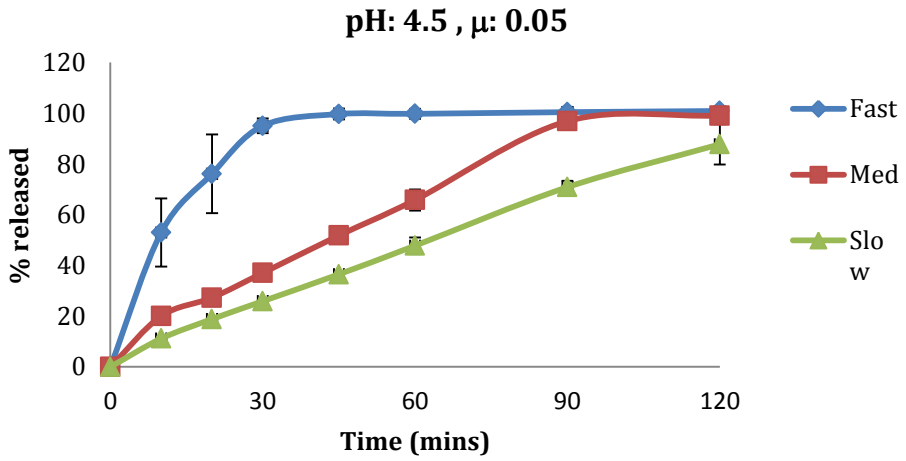

Figure A-3. Dissolution of CIP at pH 4.5 (acetate buffer) and ionic strength of 0.05, (n = 5).

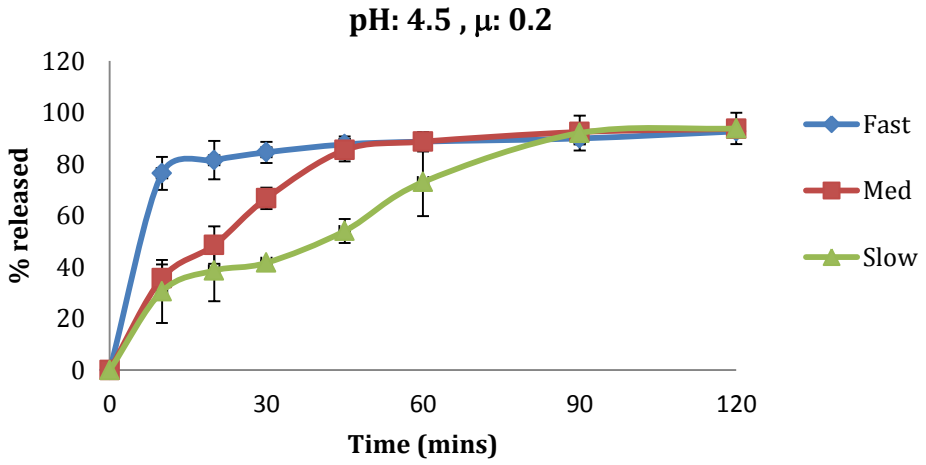

Figure A-4. Dissolution of CIP at pH 4.5 (acetate buffer) and ionic strength of 0.2, (n = 3).

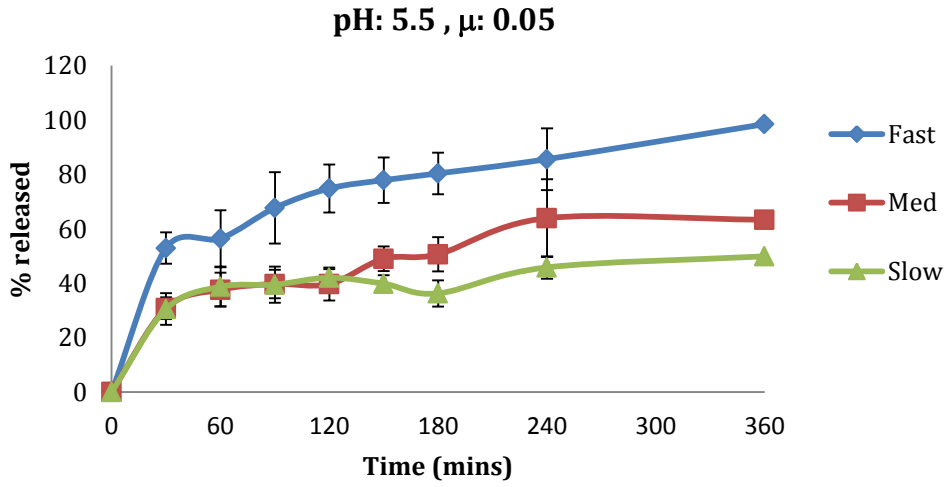

Figure A-5. Dissolution of CIP at pH 4.5 (acetate buffer) and ionic strength of 0.05, (n = 3).

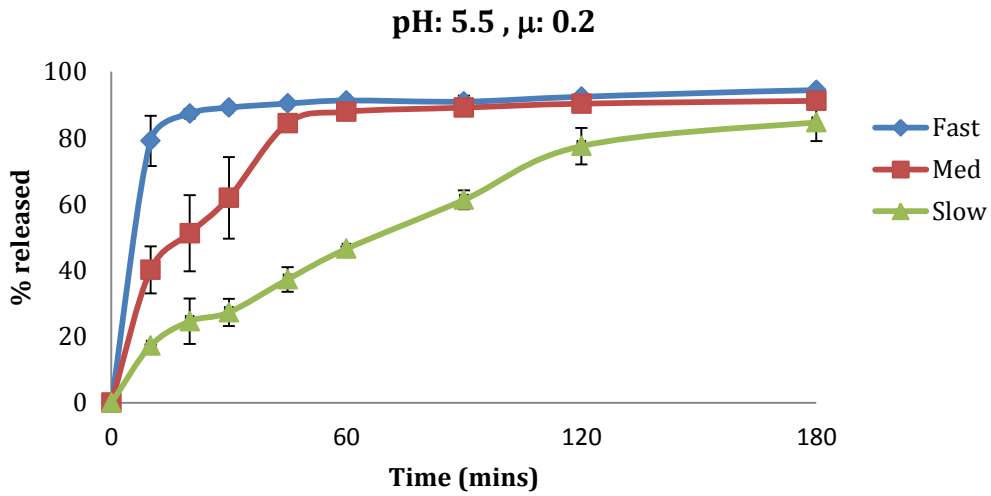

Figure A-6. Dissolution of CIP at pH 4.5 (acetate buffer) and ionic strength of 0.2, (n = 3).

A.2. Manufacturing of Ciprofloxacin hydrochloride oral tablets (clinical batches)

A total of 10 batches were manufactured and the parameters evaluated are presented below (Table A-1).

Table A-1. Parameters studied for the manufacturing of Ciprofloxacin hydrochloride clinical batches. (Highlighted in grey are the batches selected for clinical)

Clinical lot number	Mass (kg)	Formula	Roll Press (bars)	FSS/ RS	HPC (source) EFX-0; Nisso-1	MgSt (type) Mono-0, Di-1	EFX level%	1500 level%	Pmax
UMB-201006-01	2	CipA1	80	5	0	0	2	10	12
UMB-201006-02	1	CipA2	80	7	0	0	2	10	12
UMB-201006-03	1	CipA3	80	3	0	1	2	10	12
UMB-201006-04	1	CipA4	140	7	0	1	2	10	12
UMB-201006-05	1	CipA5	140	5	0	1	2	10	12
UMB-201006-06	2	CipA6	140	5	0	0	2	10	12
UMB-201006-07	1	CipA7	140	3	0	0	2	10	12
UMB-201006-08	2	CipB1	80	5	0	0	4	10	12,16
UMB-201006-09	1	CipC1	80	5	0	0	6	8	12
UMB-201006-10	1	CipD1	80	5	1	1	3	10	12

Dissolution: *In-Vitro* dissolution studies were evaluated using USP method II. The dissolution media consists of 0.01N HCl and the paddles were operated at 50 rpm and the temperature was maintained at 37 ± 0.5°C. The amount of CIP was analyzed using High Performance Liquid Chromatography (HPLC). Mobile phase consists of 0.025 M phosphoric acid (adjusted to pH 3.0 ± 0.1 with triethylamine): acetonitrile (87: 13 v/v). The solution was sonicated for 20 min and filtered through 0.45 µm membrane filter. 10 µl of this solution (0.2 mg/mL mobile phase) was injected into HPLC (Waters® Corporation, Milford, MA) at a flow rate 1.5 mL/min and the amount of CIP was determined at 278 nm. The samples collected were directly injected in to chromatographic system and the amount of CIP was analyzed.

Table A-2. Formulation of clinical batches

Ingredients	Fast tabs UMB-201006-03	Slow tabs UMB-201006-09
Intra granular portion	*(%) w/w*	*(%) w/w*
Ciprofloxacin hydrochloride	50	50
MCC (Avicel® 102)	37	35
Hydroxypropyl cellulose EXF	2	6
Starch® 1500	5	4
Magnesium stearate	0.5	0.5
Extra granular portion	*(%) w/w*	*(%) w/w*
Starch® 1500	5	4
Magnesium stearate	0.5	0.5
Total	100	100

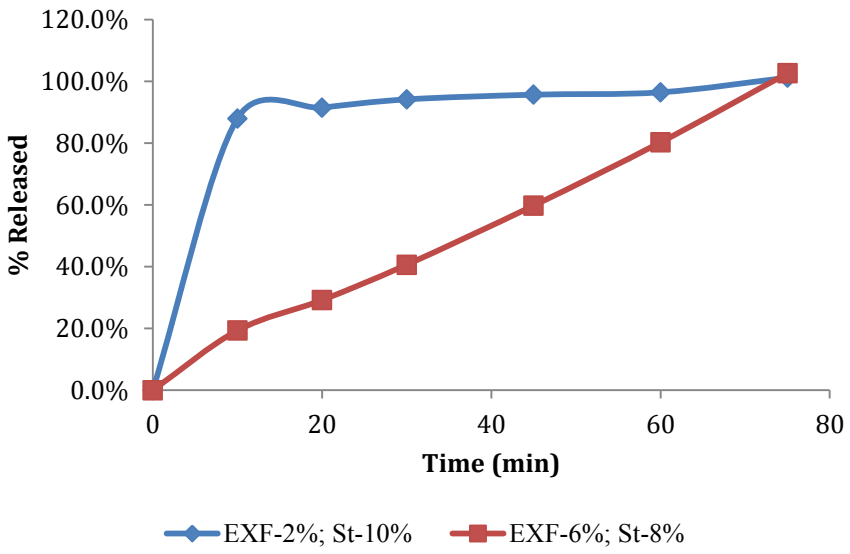

Figure A-7. Dissolution of Cipro, carried according to USP test method (n = 3).

Appendix B: Supplemental Data for Chapter 4

Section B.1, deals with the manufacturing of Fexofenadine hydrochloride clinical batches under GMP. Also discussed in the section are the design employed (Figure B.1) and variables studied (Table B.5-1), followed by dissolution of the batches identified (Figure B.2). Section B.2, discusses the central composite design employed to identify critical formulation and process variable that influence the CQA's. Design, variables, and results are presented in the tables B. 5-5-7.

B.1. Manufacturing of Fexofenadine hydrochloride oral tablets

In this study, three critical parameters were evaluated using a 2 level full factorial DOE + 3 Star points (Figure B-1) were employed leading to a total of 15 batches. Factors studied were listed in the table B-1.

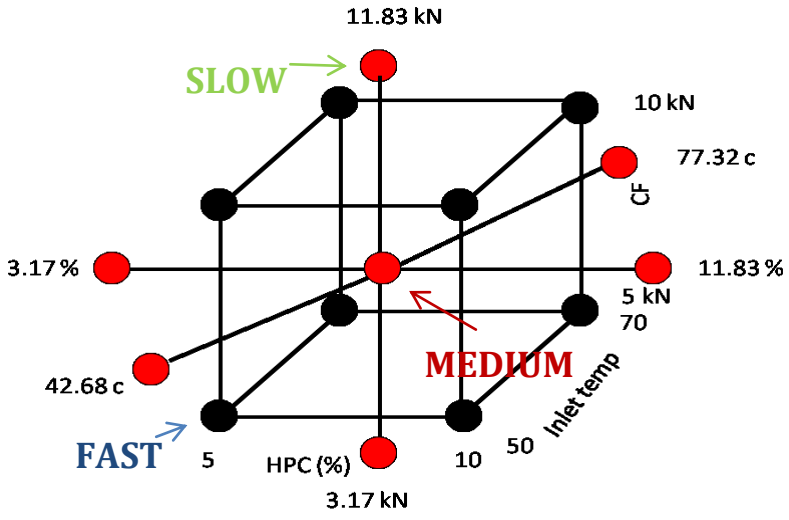

Figure B-1. Design employed for clinical manufacturing. Binder (Klucel® EXF), Inlet air temperature, and compression force (CF) are the three parameters evaluated.

Table B-1. Process parameters studied for the manufacturing of clinical batches.

		Process Parameters		
Batches	UMB Lot No	HPC (%)	Inlet.temp (^{o}C)	CF(kN)
Fexo A (Fast)	UMB-201203-23	5	50.00	5.00
Fexo B	UMB-201203-24	10	50.00	5.00
Fexo C	UMB-201203-25	5	70.00	5.00
Fexo D	UMB-201203-26	10	70.00	5.00
Fexo E	UMB-201203-27	5	50.00	10.00
Fexo F	UMB-201203-28	10	50.00	10.00
Fexo G	UMB-201203-29	5	70.00	10.00
Fexo H	UMB-201203-30	10	70.00	10.00
Fexo I	UMB-201203-31	3.17	60.00	7.50
Fexo J	UMB-201203-32	11.85	60.00	7.50
Fexo K	UMB-201203-33	7.5	42.68	7.50
Fexo L	UMB-201203-34	7.5	77.32	7.50
Fexo M	UMB-201203-35	7.5	60.00	3.17
Fexo N (Slow)	UMB-201203-36	7.5	60.00	11.83
Fexo O (Medium)	UMB-201203-37	7.5	60.00	7.50

Table B-2. Formulation of Fexofendaine hydrochloride clinical batches.

Ingredients	%w/w		
Intragranular portion	*Fast*	*Medium*	*Slow*
Fexofenadine HCl	15	15	15
Avicel® PH 102	38.63	38.63	38.63
Lactose monohydrate 110M	38.63	38.63	38.63
Ac-Di-Sol®	1.25	1.25	1.25
Kollidone® K30	6.5	6.5	6.5
Extragranular portion			
Granules	85	85	85
Avicel® PH 102	10.5	6.5	6.5
Klucel® EXF	3.5	7.5	7.5
Mg-stearate	0.5	0.5	0.5
Aerosil® 200	0.5	0.5	0.5
Total	100	100	100

Dissolution

Dissolution was performed according to USP apparatus II monograph in 900 ml of 0.001N HCl solution with paddles rotating at 50 rpm at 37 ^{o}C using Hanson® SR8 Plus dissolution apparatus connected to flow through cell. The samples were analyzed using UV-Vis spectrophotometer (Shimadzu, UV160U) at 220 nm wavelength.

Fexo A (UMB-201203-01) met the USP release criteria for immediate release, i.e. not less than (NLT) 60% release in 10 min and NLT 80% in 30 min. Fexo O (UMB-201203-15) was identified as medium release tablets. It consists of as more extragranular binder (7.5%) as formulation variable and processed at higher compression force (7.5 kN) as compared to Fast formulation. Batch Fexo N is identified as slow release tablets consists of same formulation as the medium release tablets, however they are compressed at higher compression force (11.83 kN) than the medium release tablets. In conclusion, HPC binder level and compression force was critical for the release of the Fexofenadine hydrochloride.

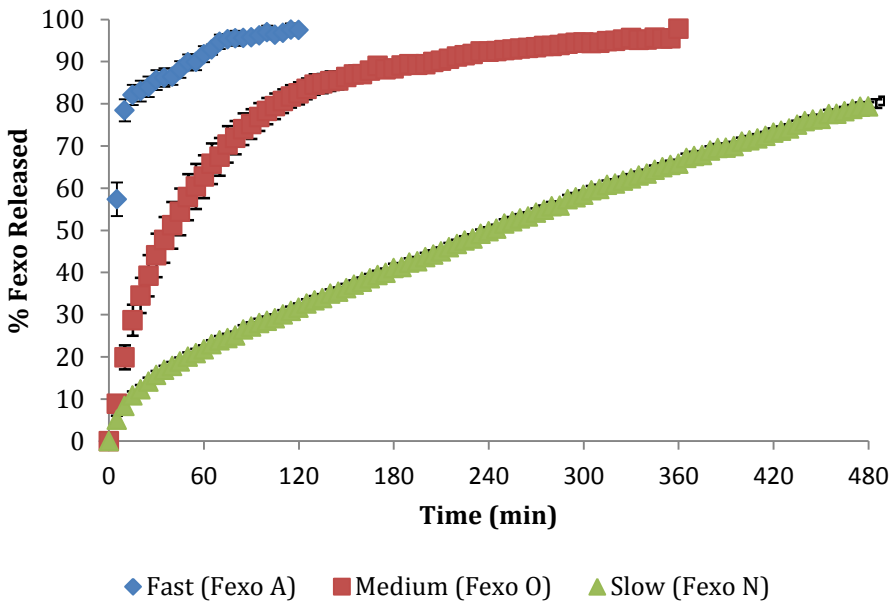

Figure B-2. Dissolution of Fexo, carried according to USP test method (n = 6).

Table B-3. Summary of granule and tablet properties of Fexofenadine hydrochloride tablets for clinical.

	Granule properties					Tablet Properties	
Batch	CI%*	d(10) ± Std.Dev (μ)**	d(50) ± Std.Dev (μ)**	d(90) ± Std.Dev (μ)**	d(4,3) ± Std.Dev (μ)	Wt ± Std.Dev (mg)***	CF ± Std.Dev (kp)***
Fexo A	17.6	13.5 ± 3.5	109.5 ± 3.9	230.0 ± 6.0	118.6 ± 3.5	474.7 ± 5.5	11.6 ± 0.5
Fexo B	17.8	17.0 ± 2.9	114.2 ± 6.7	228.4 ± 3.9	119.4 ± 2.5	474.8 ± 6.4	12.2 ± 0.9
Fexo C	19.8	15.3 ± 2.5	110.7 ± 2.5	224.6 ± 1.6	117.5 ±1.8	468.8 ± 5.7	8.9 ± 0.8
Fexo D	19.8	12.5 ± 8.1	104.2 ± 7.2	212.2 ± 13.6	110.0 ± 9.8	471.5 ± 5.9	12.2 ± 0.9
Fexo E	15.1	36.1 ± 2.2	118.9 ± 2.1	232.0 ± 1.9	127.5 ± 1.6	473.6 ± 5.4	14.7 ± 1.2
Fexo F	18.4	36.9 ± 0.7	119.7 ± 0.8	229.8 ± 2.0	127.4 ± 0.1	471.5 ± 5.0	15.4 ± 1.2
Fexo G	20.2	24.4 ± 1.4	112.7 ± 0.1	225.3 ± 0.8	120.5 ± 0.3	471.5 ± 7.3	15.3 ± 0.8
Fexo H	18.8	5.1 ± 1.2	96.2 ± 6.4	215.0 ± 5.2	104.1 ± 6.2	471.6 ± 4.6	16.5 ± 0.9
Fexo I	19.6	29.7 ± 6.0	114 ± 3.3	228.7 ± 4.2	122.8 ± 3.8	468.3 ± 5.5	13.9 ± 0.7
Fexo J	17.3	30.1 ± 1.8	114.8 ± 2.8	227.4 ± 0.6	123.1 ± 16	469.0 ± 5.6	15.1 ± 1.6
Fexo K	16.6	36.5 ± 2.8	116.8 ± 2.2	229.2 ± 2.8	125.7 ± 2.0	471.5 ± 4.8	12.1 ± 0.7
Fexo L	16.4	16.5 ± 2.9	112.4 ± 3.3	229.0 ± 7.4	120.1 ± 3.8	474.0 ± 6.1	11.2 ± 0.5
Fexo M	21.2	29.8 ± 5.9	117.8 ± 4.7	234.2 ± 6.7	126.5 ± 4.87	473.0 ± 6.4	5.7 ± 0.4
Fexo N	16.9	29.3 ± 4.2	117 ± 2.9	230.6 ± 5.2	125.0 ± 2.7	471.8 ± 6.8	16.2 ± 1.4
Fexo O	12.3	30.2 ± 1.0	115.2 ± 3.2	227.3 ± 5.0	123.4 ± 3.1	477.0 ± 3.2	11.1 ± 0.7

* No. of runs (n) = 1
* *No. of runs (n) = 3
*** No. of runs (n) = 6

B.2. Studies to identify critical product and process variables

Table B-4. Base formulation for Fexofenadine hydrochloride tablets

Ingredients	%w/w
Intragranular portion	
Fexofenadine HCl	15
Avicel® PH 102	38.63
Lactose monohydrate 110M	38.63
Ac-Di-Sol®	1.25
Kollidone® K30	6.5
Extragranular portion	
Granules	85
Avicel® PH 102	10.5
Klucel® EXF	3.5
Mg-stearate	0.5
Aerosil® 200	0.5
Total	100

Table B-5. Variables and their levels studied. Base formulation (level = 0) highlighted

Factors	Levels				
	-1	*-0.5*	***0***	*0.5*	*1*
X1: Binder level (%)*	5	5.75	**6.5**	7.25	8
X2: Disintegrant level (%)	0.5	0.88	**1.25**	1.63	2
X3: Extragranular binder level (%)**	2	2.75	**3.5**	4.25	5
X4: Inlet air temperature (^{o}C)	50	55	**60**	65	70
X5: Atomization pressure (psi)	4	6	**10**	13	16

* Sprayed during granulation

**Added extragranular

Table B-6. Central composite design employed for Fexofenadine hydrochloride tablets

	DOE Parameters				
Batch	HPC (%w/w)	PVP (%w/w)	Ac-Di-Sol (% w/w)	Inlet air (^{o}C)	Atm pressure (psi)
C1.5	2.75	5.75	1.63	55	13
C1.6	4.25	5.75	1.63	55	7
C1.17	3.50	6.50	1.25	60	10
C1.1	2.75	5.75	0.88	55	7
C1.23	3.50	6.50	1.25	60	10
C1.8	4.25	7.25	1.63	55	13
C1.20	3.50	6.50	1.25	60	10
C1.16	4.25	7.25	1.63	65	7
C1.10	4.25	5.75	0.88	65	7
C1.19	3.50	6.50	1.25	60	10
C1.14	4.25	5.75	1.63	65	13
C1.21	3.50	6.50	1.25	60	10
C1.3	2.75	7.25	0.88	55	13
C1.4	4.25	7.25	0.88	55	7
C1.18	3.50	6.50	1.25	60	10
C1.15	2.75	7.25	1.63	65	13
C1.13	2.75	5.75	1.63	65	7
C1.2	4.25	5.75	0.88	55	13
C1.11	2.75	7.25	0.88	65	7
C1.9	2.75	5.75	0.88	65	13
C1.22	3.50	6.50	1.25	60	10
C1.24	3.50	6.50	1.25	60	10
C1.12	4.25	7.25	0.88	65	13
C1.7	2.75	7.25	1.63	55	7
S2.2	5.00	6.50	1.25	60	10
S2.1	2.00	6.50	1.25	60	10
S2.10	3.50	6.50	1.25	60	16
S2.4	3.50	8.00	1.25	60	10
S2.7	3.50	6.50	1.25	50	10
S2.8	3.50	6.50	1.25	70	10
S2.12	3.50	6.50	1.25	60	10
S2.3	3.50	5.00	1.25	60	10
S2.6	3.50	6.50	2.00	60	10
S2.5	3.50	6.50	0.50	60	10
S2.9	3.50	6.50	1.25	60	4
S2.11	3.50	6.50	1.25	60	10

Table B-7. Granule properties for the central composite design

Batch	Db (gm/cc)	Dt (gm/cc)	CI%	d10 X (μ)	d50 X (μ)	d90 X (μ)
C1.5	0.31	0.40	22.31	32.5 ± 0.38	116.13 ± 2.05	232.12 ± 5.23
C1.6	0.34	0.45	23.27	31.62 ± 0.05	118.02 ± 2.26	230.53 ± 3.58
C1.17	0.35	0.45	20.52	36.36 ± 0.06	118.65 ± 0.18	231.89 ± 0.17
C1.1	0.38	0.47	19.26	37.90 ± 0.52	119.94 ± 1.58	232.17 ± 2.11
C1.23	0.36	0.44	19.32	40.22 ± 1.14	121.62 ± 2.58	234.41 ± 3.40
C1.8	0.35	0.44	20.42	38.26 ± 0.70	123.09 ± 0.22	240.63 ± 1.59
C1.20	0.35	0.46	24.63	34.11 ± 1.57	117.49 ± 1.83	232.38 ± 1.77
C1.16	0.32	0.41	21.34	36.25 ± 0.81	123.67 ± 1.09	239.76 ± 2.98
C1.10	0.35	0.45	21.25	30.08 ± 0.18	116.33 ± 0.37	230.57 ± 2.12
C1.19	0.35	0.45	21.74	34.43 ± 0.97	121.15 ± 1.32	239.30 ± 4.51
C1.14	0.37	0.44	16.25	32.03 ± 0.48	113.06 ± 1.92	226.53 ± 2.83
C1.21	0.36	0.43	17.63	31.97 ± 0.77	115.49 ± 1.15	230.80 ± 1.85
C1.3	0.34	0.41	18.06	16.75 ± 1.34	107.66 ± 1.22	213.38 ± 4.91
C1.4	0.32	0.37	14.88	30.79 ± 0.47	114.02 ± 1.15	221.87 ± 1.55
C1.18	0.28	0.38	26.86	33.57 ± 1.78	114.66 ± 2.09	219.54 ± 7.14
C1.15	0.33	0.42	21.38	37.92 ± 4.24	118.87 ± 5.45	231.41 ± 3.53
C1.13	0.36	0.45	20.24	29.57 ± 1.43	115.51 ± 2.02	230.35 ± 3.87
C1.2	0.34	0.43	22.23	22.77 ± 0.37	110.45 ± 1.39	224.52 ± 1.86
C1.11	0.36	0.45	19.30	32.37 ± 1.80	118.46 ± 1.98	228.95 ± 2.34
C1.9	0.35	0.45	22.15	30.47 ± 0.29	113.47 ± 1.38	225.76 ± 2.66
C1.22	0.32	0.40	21.92	36.58 ± 0.43	117.91 ± 0.62	227.75 ± 1.53
C1.24	0.34	0.44	23.89	33.83 ± 0.09	121.22 ± 0.53	234.22 ± 1.14
C1.12	0.32	0.41	22.45	36.10 ± 0.38	121.82 ± 0.98	237.11 ± 1.97
C1.7	0.34	0.42	17.97	35.60 ± 1.17	121.54 ± 1.65	234.64 ± 3.40
S2.2	0.35	0.44	20.84	33.37 ± 0.94	120.43 ± 2.74	234.09 ± 3.43
S2.1	0.30	0.39	22.46	35.24 ± 0.21	122.66 ± 1.84	237.95 ± 2.73
S2.10	0.31	0.39	21.20	31.80 ± 0.70	120.79 ± 1.60	237.53 ± 2.30
S2.4	0.33	0.42	20.77	29.43 ± 1.49	113.48 ± 2.30	220.90 ± 2.07
S2.7	0.38	0.46	18.94	36.13 ± 0.71	123.27 ± 1.09	240.38 ± 3.04
S2.8	0.33	0.43	23.18	19.27 ± 2.19	112.74 ± 1.68	229.71 ± 3.41
S2.12	0.31	0.40	20.99	24.62 ± 1.47	115.46 ± 1.28	233.75 ± 1.98
S2.3	0.33	0.46	26.53	25.10 ± 0.78	110.97 ± 0.83	224.33 ± 1.38
S2.6	0.34	0.42	20.16	30.06 ± 1.33	116.11 ± 1.24	231.28 ± 1.74
S2.5	0.29	0.39	26.83	27.11 ± 2.05	123.94 ± 0.99	241.25 ± 1.85
S2.9	0.33	0.44	23.70	21.99 ± 0.83	114.71 ± 3.56	231.56 ± 6.56
S2.11	0.32	0.40	21.74	29.75 ± 1.66	123.33 ± 1.73	240.48 ± 2.10

Table B-8. Tablet properties for the central composite design

	Wt (mg)	CF (kp)	DT (sec)	Q10 (%)	Q(10) Std.Dev	Q30 (%)	Q(30) Std.Dev
C1.5	459	11.98 ± 0.71	13	80	3.7	87	4.6
C1.6	471	11.52 ± 0.32	17	75	3.9	82	5.0
C1.17	481	11.42 ± 0.66	24	85	4.7	90	3.3
C1.1	466	10.60 ± 0.57	32	73	6.1	83	7.1
C1.23	468	9.67 ± 0.39	18	77	3.4	83	2.4
C1.8	464	11.10 ± 0.46	54	86	1.9	94	3.0
C1.20	469	9.88 ± 0.52	10	80	2.7	85	3.5
C1.16	472	9.63 ± 0.52	17	77	5.3	85	6.8
C1.10	468	9.47 ± 0.77	10	79	2.4	85	2.5
C1.19	472	10.73 ± 0.69	19	77	7.5	83	7.4
C1.14	465	9.62 ± 0.55	12	69	5.4	74	4.2
C1.21	462	11.53 ± 0.37	7	75	1.5	82	2.1
C1.3	477	8.60 ± 1.08	7	71	5	80	3
C1.4	478	9.53 ± 0.68	17	59	23	80	14
C1.18	473	7.45 ± 0.58	19	76	6	82	7
C1.15	461	8.53 ± 0.48	4	77	4	82	5
C1.13	471	10.00 ± 0.19	1	74	3.7	82	2.4
C1.2	468	11.00 ± 0.81	33	73	6.8	81	5.1
C1.11	467	9.53 ± 0.43	13	75	10.3	86	9.2
C1.9	465	9.78 ± 0.59	17	69	4.1	76	3.7
C1.22	471	10.60 ± 0.26	21	80	6.3	88	6.5
C1.24	470	9.88 ± 0.66	21	77	2.8	85	4.3
C1.12	469	11.53 ± 0.95	51	70	6.8	87	5.9
C1.7	468	10.98 ± 0.36	21	78	2.9	84	4.1
S2.2	471	10.70 ± 0.30	4	77	4.1	82	2.3
S2.1	472	11.72 ± 0.44	10	75	3.6	82	2.6
S2.10	467	10.97 ± 0.45	10	71	5.9	78	2.7
S2.4	479	8.67 ± 0.50	13	84	4	90	4
S2.7	478	9.93 ± 0.56	11	81	5.2	86	4.5
S2.8	470	10.07 ± 0.42	9	68	5.3	74	5.1
S2.12	469	11.18 ± 0.60	10	77	1.7	81	2.5
S2.3	465	9.87 ± 0.30	5	71	4.2	77	3.8
S2.6	477	10.20 ± 0.47	13	71	6.8	77	7.1
S2.5	464	10.27 ± 0.19	24	56	19.1	80	9.4
S2.9	472	10.17 ± 0.35	6	70	2.7	76	2.0
S2.11	469	11.22 ± 0.73	27	71	4.7	80	3.2

References

(1) U.S. Department of Health and Human Services, Food and Drug Administration (2004) Guidance for industry: PAT—a framework for innovative pharmaceutical development, manufacturing and quality assurance. http://www.fda.gov/downloads/Drugs/GuidanceComplianceRegulatoryInformation/Guidances/ucm070305.pdf. Accessed December 07 2011.

(2) U.S. Department of Health and Human Services, Food and Drug Administration. http://www.fda.gov/Drugs/DevelopmentApprovalProcess/Manufacturing/QuestionsandAnswersonCurrentGoodManufacturingPracticescGMPforDrugs/UCM071836. Accessed December 07, 2011.

(3) Rathore AS, Bhambure R, Ghare V. Process analytical technology (PAT) for biopharmaceutical products. Analytical and bioanalytical chemistry 2010;398(1):137-154.

(4) Bakeev AK. Process Analytical Technology: Spectroscopic Tools and Implementation Strategies for the Chemical and Pharmaceutical Industries. 1st ed.: Wiley-Blackwell; 2005.

(5) ICH. Q8(R2) Pharmaceutical Development. Part I: Pharmaceutical development, and. Part II: annex to pharmaceutical development. http://www.ich.org/fileadmin/Public_Web_Site/ICH_Products/Guidelines/Quality/Q8_R1/Step4/Q8_R2_Guideline.pdf: 2009.

(6) ICH. Q9 Quality Risk Management. http://www.ich.org/fileadmin/Public_Web_Site/ICH_Products/Guidelines/Quality/Q9/Step4/Q9_Guideline.pdf: 2005.

(7) ICH. Q10 Pharmaceutical Quality System. http://www.ich.org/fileadmin/Public_Web_Site/ICH_Products/Guidelines/Quality/Q10/Step4/Q10_Guideline.pdf: 2008.

(8) Yu L. Pharmaceutical quality by design: product and process development, understanding, and control. Pharm Res 2008;25(4):781-791.

(9) Rathore A. Roadmap for implementation of quality by design (QbD) for biotechnology products. Trends Biotechnol 2009;27(9):546-553.

(10) Beebe KR, Pell RJ, Seasholtz MB. Chemometrics: a practical guide. : Wiley; 1998.

(11) G R. Near-infrared spectroscopy and imaging: Basic principles and pharmaceutical applications. Adv Drug Delivery Rev 2005;57:1109-1143.

(12) Vision 3. FOSS NIRSystems; 2004.

(13) Williams P, Norris K, Zarowski W. Influence of temperature on estimation of protein and moisture in wheat by near-infrared reflectance. Cereeal Chem 1982;59:473-477.

(14) Cogdill R, Drennen J. Near-infrared spectroscopy. In: Brittain H, editor. Spectroscopy of Pharmaceutical Solids. 1st ed. New York, NY: Taylor & Francis; 2006. p. 313.

(15) Reich G. Near-infrared spectroscopy and imaging: Basic principles and pharmaceutical applications. Adv Drug Delivery Rev 2005;57:1109-1143.

(16) Training Course from FOSS NIRSystems, Inc. Vision for XDS.

(17) Tabasi S, Fahmy R, Bensley D, O'Brien C, Hoag S. Quality by design, part I: application of NIR spectroscopy to monitor tablet manufacturing process. J Pharm Sci 2008;97(9):4040-4051.

(18) Martens H, Naes T. Multivariate calibration. : Chichester: John Wiley & Sons; 1989.

(19) Tabasi S, Fahmy R, Bensley D, O'Brien C, Hoag S. Quality by design, part II: application of NIR spectroscopy to monitor the coating process for a pharmaceutical sustained release product. J Pharm Sci 2008;97(9):4052-4066.

(20) Miller RW. Roller compaction technology. In: Parikh DM, editor. Handbook of Pharmaceutical Granulation Technology. New York, NY: Marcel Dekker; 1997. pp. 99–150.

(21) Parrott EL. Densification of powders by concavo-convex roller compactor. J Pharm Sci 1981;70(3):288-291.

(22) Miller RW. Advances in pharmaceutical roller compactor feed system designs. Pharm.Technol.Eur 1994:58-68.

(23) Ende MTA, others. (2007) Improving the content uniformity of a low-dose tablet formulation through roller compaction optimization. Pharm Dev Technol :391-404.

(24) Ghorab M, Chatlapalli R, Hasan S, Nagi A. Application of thermal effusivity as a process analytical technology tool for monitoring and control of the roller compaction process. AAPS PharmSciTech 2007;8(1):23-23.

(25) Kleinebudde P. Roll compaction/dry granulation: pharmaceutical applications. Eur J Pharm Biopharm 2004.

(26) Johanson JR. A Rolling Theory of Granular Solids. Transactions of the {ASME}: J.Appl.Mech 1965:842-848.

(27) Bindhumadhavan G, others. (2005) Roll compaction of a pharmaceutical excipient: Experimental validation of rolling theory for granular solids. Chem Eng Sci :3891-3897.

(28) Kleinebudde P. Roll compaction/dry granulation: pharmaceutical applications. European Journal of Pharmaceutics and Biopharmaceutics 2004 9;58(2):317-326.

(29) Teng Y, Qiu Z, Wen H. Systematical approach of formulation and process development using roller compaction. European journal of pharmaceutics and biopharmaceutics 2009;73(2):219-229.

(30) Bacher C, Olsen PM, Bertelsen P, Kristensen J, Sonnergaard JM. Improving the compaction properties of roller compacted calcium carbonate. Int J Pharm 2007;342(1-2):115-123.

(31) Freitag F, others. (2003) How do roll compaction/dry granulation affect the tableting behaviour of inorganic materials? Comparison of four magnesium carbonates. Eur.J.Pharm :281-289.

(32) Inghelbrecht S, others. (1998) Roller compaction and tableting of microcrystalline cellulose drug mixtures. Int J Pharm :215-224.

(33) Sun C, Himmelspach M. Reduced tabletability of roller compacted granules as a result of granule size enlargement. J Pharm Sci 2006;95(1):200-206.

(34) Malkowska S, Khan KA. Effect of Re-Conpression on the Properties of Tablets Prepared by Dry Granulation. Drug Dev Ind Pharm 1983 01/01; 2011/12;9(3):331-347.

(35) Inghelbrecht S, Remon JP. Roller compaction and tableting of microcrystalline cellulose/drug mixtures. Int J Pharm 1998 2/23;161(2):215-224.

(36) Sun C, Himmelspach M. Reduced tabletability of roller compacted granules as a result of granule size enlargement. J Pharm Sci 2006;95(1):200-206.

(37) Roberts RJ, Rowe RC. The effect of punch velocity on the compaction of a variety of materials. J Pharm Pharmacol 1985;37(6):377-384.

(38) Ruegger CE, Celik M. The effect of compression and decompression speed on the mechanical strength of compacts. Pharm Dev Technol 2000;5(4):485-494.

(39) Hervieu P, Dehont F, Jerome E, Delacourte A, Guyot JC. Granulation of Pharmaceutical Powders by Compaction an Experimental Study. Drug Dev Ind Pharm 1994 01/01; 2011/12;20(1):65-74.

(40) Gupta A, Peck G, Miller R, Morris K. Effect of the variation in the ambient moisture on the compaction behavior of powder undergoing roller-compaction and on the characteristics of tablets produced from the post-milled granules. J Pharm Sci 2005;94(10):2314-2326.

(41) Inghelbrecht S, others. (1998) The roller compaction of different types of lactose. Int J Pharm :135-144.

(42) RW. M. Roller compaction optimization—NIR in-process mapping. : J Pharm Tech Yearbook Supplement: 30–39; 1999.

(43) Gupta A, Peck G, Miller R, Morris K. Nondestructive measurements of the compact strength and the particle-size distribution after milling of roller compacted powders by near-infrared spectroscopy. J Pharm Sci 2004;93(4):1047-1053.

(44) Gupta A, Peck G, Miller R, Morris K. Influence of ambient moisture on the compaction behavior of microcrystalline cellulose powder undergoing uni-axial compression and roller-compaction: a comparative study using near-infrared spectroscopy. J Pharm Sci 2005;94(10):2301-2313.

(45) Gupta A, Peck G, Miller R, Morris K. Real-time near-infrared monitoring of content uniformity, moisture content, compact density, tensile strength, and Young's modulus of roller compacted powder blends. J Pharm Sci 2005;94(7):1589-1597.

(46) Gupta A, Peck G, Miller R, Morris K. Real-time near-infrared monitoring of content uniformity, moisture content, compact density, tensile strength, and Young's modulus of roller compacted powder blends. J Pharm Sci 2005;94(7):1589-1597.

(47) Kirsch JD, Drennen JK. Nondestructive tablet hardness testing by near-infrared spectroscopy: a new and robust spectral best-fit algorithm. J Pharm Biomed Anal 1999;19(3-4):351-362.

(48) Lim H, Dave V, Kidder L, Neil Lewis E, Fahmy R, Hoag S. Assessment of the critical factors affecting the porosity of roller compacted ribbons and the feasibility of using NIR chemical imaging to evaluate the porosity distribution. Int J Pharm 2011;410(1-2):1-8.

(49) Wurster DE. Preparation of compressed tablet granulations by the air-suspension technique. II. J Am Pharm Assoc Am Pharm Assoc 1960;49:82-84.

(50) Wurster DE. Air-suspension technique of coating drug particles a preliminary report. J Am Pharm Assoc Am Pharm Assoc (Baltim) 1959;48(8):451-454.

(51) Scott MW, Lieberman HA, Rankell AS, Battista JV. Continuous Production of Tablet Granulations in a Fluidized Bed. I. Theory and Design Considerations. J Pharm Sci 1964;53:314-320.

(52) Rankell AS, Scott MW, Lieberman HA, Chow FS, Battista JV. Continuous Production of Tablet Granulations in a Fluidized Bed. II. Operation and Performance of Equipment. J Pharm Sci 1964;53:320-324.

(53) Liske T, Mobus W. Drugs made in Germany. 1968;11(4):182-189.

(54) Parikh D, Mogavero M. Batch Fluid Bed Granulation. Handbook of Pharmaceutical Granulation Technology, Third Edition, Informa Healthcare .

(55) Iveson SM, Litster JD, Hapgood K, Ennis BJ. Nucleation, growth and breakage phenomena in agitated wet granulation processes: a review. Powder Technol 2001 6/4;117(1-2):3-39.

(56) Cantor SL, Augsburger LL, Hoag SW, Gerhardt A. Pharmaceutical Granulation Processes, Mechanism, and the Use of Binders. Pharmaceutical Dosage Forms: Tablets. p. 261-302.

(57) Newitt DM, Conway-Jones JM,. A contribution to the theory and practice of granulation. Transactions of the Institution of Chemical Engineers 1958;36:422-441.

(58) Cooper J, Swartz CJ, Suydam Jr., W. Drying of tablet granulations. Powder Tech 1985;50(44):67-75.

(59) Nhale N. Heat Transfer. Available at: http://www.biocab.org/Heat_Transfer.html. Accessed 09/23, 2012.

(60) Augsburger LL, Hoag SW. Pharmaceutical Dosage Forms : Tablets, Volume 1 : Unit Operations and Mechanical Properties (3rd Edition). New York : Informa Healthcare; 2008.

(61) Aulton ME, Banks M. Fluidised bed granulation factors influencing the quality of the product. Int.J.Pharm.Tech.Prod.Manuf.2 1981;2:24-29.

(62) Schaefer T, Worts O. Control of fluidized bed granulation: III. 1978;6:69-82.

(63) Schaefer T, Worts O. Control of fluidized bed granulation: II. 1977;5:178-193.

(64) Davies WL, Gloor Jr., W. T. Batch production of pharmaceutical granulations in a fluidized bed II: Effects of various binders and their concentrations on granulations and compressed tablets. J.Pharm.Sci.61 1972;61:618-622.

(65) Schaefer T, Worts O. Control of fluidized bed granulation: V. 1978;6:1-13.

(66) Ormos Z, Pataki K, Csukas B. Studies on granulation in a fluidized bed II. Hung J Ind Chem 1973;1:307.

(67) Ormos Z, Pataki K, Csukas B. Studies on granulation in a fluidized bed III. calculation of the feed rate of granulating liquid. Hung J Ind Chem 1973;1:463.

(68) Meshali M, El-Banna, HM. Use of fractional factorial design to evaluate granulation's prepared In a fluidized bed. Pharmazie 1983;38:323.

(69) Alkan MH, Yuksel A. Granulation in a fluidized bed II. effect of binder amount on the final granule. Drug Dev Ind Pharm 1986;12:1529.

(70) Alkan H, Ulusoy A. Granulation in a fluidized bed. and Pharm.11 1987;11.

(71) Schaefer T, Worts O. Control of fluidized bed granulation: I. 1977;5:51-60.

(72) Lipsanen T, Antikainen O, Räikkönen H, Airaksinen S, Yliruusi J. Effect of fluidisation activity on end-point detection of a fluid bed drying process. Int J Pharm 2008 6/5;357(1-2):37-43.

(73) Jager K, Bauer K. Acta Pharm Technol 1984;30(1):85-92.

(74) Georgakopoulos PP, Malamataris S, Dolamidis G. The effects of using different grades of PVP and gelatin as binders in the fluidized bed granulation and tabletting of lactose. Pharmazie 1983;38(4):240-243.

(75) Aulton M. Pharmaceutics. Edinburgh: Churchill Livingstone,; 2002.

(76) Sucker H. Test methods for granulates. Pharm Ind 1982;44:312-316.

(77) Davies WL, Gloor WT. Batch production of pharmaceutical granulations in a fluidized bed. I. Effects of process variables on physical properties of final granulation. J Pharm Sci 1971;60(12):1869-1874.

(78) Niskanen T, Yliruusi J, Niskanen M, Kontro O. Granulation of potassium chloride in instrumented fluidized bed granulator—Part I: effect of flow rate. Acta Pharm.Fennica 1990;99:13-22.

(79) Merkku P, Yliruusi J, Hellén L. Testing of an automated laboratory scale fluidised bed granulator using different bed loads. Acta Pharm.Fennica 1992;101:173-180.

(80) Ehrhardt L. Drying granules in the fluid bed drier. Int.Tech.Pharm.3 1977;3:181-190.

(81) Gore AY, McFarland DW, Batuyios NH. Fluid-bed granulation: factors affecting the process in laboratory development and production scale-up. Pharm.Tech.9 1985;9:114-122.

(82) Leuengerber H, Imandis G. Monitoring mass transfer processes to control moist agglomeration. Pharm.Tech. 1986;3:56-73.

(83) Alden M, Torkington P, Strutt ACR. Control and instrumentation of a fluidized-bed drier using the temperature-difference technique. I. Development of a working model. Powder Tech.54 1988;54:15-25.

(84) Alden M, Torkington P, Strutt A. Control and Instrumentation of a Fluidized-Bed Drier Using the Temperature Difference Technique 1. Development of a Working Model. Powder Technol 1988;54(1):15-25.

(85) Leuenberger H. Granulation, new techniques. Pharm Acta Helv 1982;57(3):72-82.

(86) Frake P, Greenhalgh D, Grierson SM, Hempenstall JM, Rudd DR. Process control and endpoint determination of a fluid bed granulation by application of near infra-red spectroscopy. Int.J.Pharm.151 1997;151:75-80.

(87) Rantanen J, Lehtola S, Rämet P, Mannermaa J, Yliruusi J. On-line monitoring of moisture content in an instrumented fluidized bed granulator with a multi-channel NIR moisture sensor. Powder Technol 1998 9/15;99(2):163-170.

(88) Andersson M, Folestad S, Gottfries J, Johansson MO, Josefson M, Wahlund KG. Quantitative analysis of film coating in a fluidized bed process by in-line NIR spectrometry and multivariate batch calibration. Anal Chem 2000;72(9):2099-2108.

(89) Rantanen J, Knskoski M, Suhonen J, Tenhunen J, Lehtonen S, Rajalahti T, et al. Next generation fluidized bed granulator automation. AAPS PharmSciTech 2000;1(2):E10-E10.

(90) Rantanen J, Antikainen O, Mannermaa JP, Yliruusi J. Use of the near-infrared reflectance method for measurement of moisture content during granulation. Pharm Dev Technol 2000;5(2):209-217.

(91) Rantanen J, Jrgensen A, Rsnen E, Luukkonen P, Airaksinen S, Raiman J, et al. Process analysis of fluidized bed granulation. AAPS PharmSciTech 2001;2(4):21-21.

(92) Peinado A, Hammond J, Scott A. Development, validation and transfer of a near infrared method to determine in-line the end point of a fluidised drying process for commercial production batches of an approved oral solid dose pharmaceutical product. J Pharm Biomed Anal 2011;54(1):13-20.

(93) Huang J, Goolcharran C, Utz J, Hernandez Abad P, Ghosh K. A PAT Approach to Enhance Process Understanding of Fluid Bed Granulation Using In-line Particle Size

Characterization and Multivariate Analysis. Journal of pharmaceutical innovation 2010;5(1-2):58-68.

(94) Application of Hazard Analysis and Critical Control Point (HACCP) methodology to pharmaceuticals. WHO Technical Report 2003;Series No. 908(Annex 7).

(95) Daugherity PD, Chu JH. Investigation of Serrated Roll Surface Differences on Ribbon Thickness During Roller Compaction. Pharm Dev Technol 2007 01/01; 2011/12;12(6):603-608.

(96) Cantor S, Hoag S, Ellison C, Khan M, Lyon R. NIR spectroscopy applications in the development of a compacted multiparticulate system for modified release. AAPS PharmSciTech 2011;12(1):262-278.

(97) Tatavarti A, Fahmy R, Wu H, Hussain A, Marnane W, Bensley D, et al. Assessment of NIR spectroscopy for nondestructive analysis of physical and chemical attributes of sulfamethazine bolus dosage forms. AAPS PharmSciTech 2005;6(1):E91-E99.

(98) Fahmy R, Kona R, Dandu R, Xie W, Claycamp G, Hoag SW. Quality-by-Design I: Application of Failure Mode Effect Analysis (FMEA) and Plackett-Burman design of experiments in the identification of "main factors" in the formulation and process design space for roller compacted ciprofloxacin hydrochloride immediate release tablets. 2012, 9, 1-12.

(99) Desai D, Rinaldi F, Kothari S, Paruchuri S, Li D, Lai M, et al. Effect of hydroxypropyl cellulose (HPC) on dissolution rate of hydrochlorothiazide tablets. Int J Pharm 2006;308(1-2):40-45.

(100) Ahmed M, Enever RP. Influence of magnesium stearate on the dissolution and biological availability of sulphadiazine tablet formulations [proceedings]. J Pharm Pharmacol 1976;28 Suppl:5P-5P.

(101) Rao KP, Chawla G, Kaushal A, Bansal A. Impact of solid-state properties on lubrication efficacy of magnesium stearate. Pharm Dev Technol 2005;10(3):423-437.

(102) Olivera ME, Manzo RH, Junginger HE, Midha KK, Shah VP, Stavchansky S, et al. Biowaiver monographs for immediate release solid oral dosage forms: Ciprofloxacin hydrochloride. J Pharm Sci 2011;100(1):22-33.

(103) Okoye P. Lubrication of Direct-Compressible Blends. Pharm Technol 2007;31(9):116.

(104) Dave V, Fahmy R, Bensley D, Hoag S. Eudragit(®) RS PO/RL PO as rate-controlling matrix-formers via roller compaction: Influence of formulation and process variables on functional attributes of granules and tablets. Drug Dev Ind Pharm 2012.

(105) Hyland M, Naunapper D. Continuous control of product moisture content in drying processes. Pharm Ind.48 1986;48:655-660.

(106) Nomikos P, MacGregor J. Multivariate PSC charts for minitoring of batch processes. Technometrics 1995;37:41-59.

(107) Wold S, Kettaneh N, Fridon H, Holmberg A. Modelling and diagnostics of batch processes and analogous kinetic experiments. Chemometr Intell Lab 1998;44:331-340.

(108) Wold S, Sjostorm M, Eriksson L. PLS-regression: a basic tool of chemometrics. Chemometr Intell Lab 2001;58:109-130.

(109) Huang H, Qu H. In-line monitoring of alcohol precipitation by near-infrared spectroscopy in conjunction with multivariate batch modeling. Anal Chim Acta 2011;707(1-2):47-56.

(110) Albazzaz H, Wang XZ. Statistical Process Control Charts for Batch Operations Based on Independent Component Analysis. Ind Eng Chem Res 2004;43(21):6731-6741.